

## Chapter 8

# Meta-Exhalites as Exploration Guides to Ore\*

PAUL G. SPRY,<sup>†</sup>

*Department of Geological and Atmospheric Sciences, 253 Science I, Iowa State University, Ames, Iowa 50011-3212*

JAN M. PETER,

*Mineral Resources Division, Geological Survey of Canada, 601 Booth Street, Ottawa, Ontario K1A 0E8*

AND JOHN F. SLACK

*U.S. Geological Survey, National Center, MS 954, Reston, Virginia 20192*

### Abstract

Meta-exhalites consist of a variety of rock types including iron formation, coticule (garnet-quartz rock), tourmalinite, quartz-gahnite rock, apatite-rich rock, zincian staurolite-bearing rock, and barite-rich rock. Such lithologies may be spatially associated with a diversity of ore deposits, but they are particularly linked to sea floor base metal sulfides that formed in rift settings. Meta-exhalites generally form layers less than 2 m thick, above, below, in, and along strike from stratiform or exhalative ore deposits. Geochemical diagrams for iron formations, coticules, and tourmalinites (chondrite-normalized rare earth element (REE), ternary Al-Fe-Mn, Al/(Al + Fe + Mn) vs. Fe/Ti, TiO<sub>2</sub> vs. Al<sub>2</sub>O<sub>3</sub>) suggest variable contributions of detrital material and hydrothermal components. The detrital component, terrigenous or clastic, is generally less than 30 wt percent for iron formations, whereas for coticules and tourmalinites it is generally 30 to 70 wt percent and greater than 70 wt percent, respectively. Of the major constituents of meta-exhalites, Fe, Mn, B, P, and Zn generally have a hydrothermal source, whereas Al and Ti are from detrital clastic material. Silica can have hydrothermal and/or detrital sources. Hydrogenous contributions are generally small.

The variable setting, mineralogy, primary sedimentary structures, geochemistry, and lithological variants of exhalites show that precursor constituents formed under a variety of physicochemical conditions (e.g., T,  $f_{O_2}$ , pH, ionic strength,  $f_{S_2}$ ,  $f_{CO_2}$ ) and were derived from different sources (clastic and volcanic). Iron formations, coticules, and tourmalinites form by the replacement of permeable aluminous sediments and by exhalation into submarine brine pools. Hydrothermal fluids responsible for the formation of precursors to meta-exhalites range in temperature from approximately 100° to 400°C. Layering in meta-exhalites reflects rapid fluctuations in Eh-pH conditions, metal contents,  $f_{S_2}$ ,  $f_{CO_2}$ , and detrital input. Fractionation of Fe and Mn in the hydrothermal fluids is due to gradual increases in pH or Eh during mixing of ambient seawater with the fluids and may account for differences in proximity of iron formations and coticules to sulfide deposits. The amount of hydrothermal input via venting, fluid/rock ratio, bottom current drift, and the degree of basin isolation from clastic sedimentation also dictate the chemical composition and mineralogy of meta-exhalites.

The presence of a meta-exhalite is indicative of a fossil zone of sea floor hydrothermal activity and, as such, can be utilized as a field guide in the exploration for ore deposits, particularly base metal sulfides. Relative abundance of certain minerals (e.g., iron carbonates, apatite, gahnite, zincian staurolite), bulk compositional variations that record increased ratios of hydrothermal components to detrital material, characteristic elements and elemental ratios, variations in the compositions of mineral phases (e.g., Zn to Fe ratio of staurolite, gahnite, and hōgbomite as well as the Mg to Fe ratio of ferromagnesian silicates due to metamorphic sulfide-silicate reactions), and stable isotope data (S, C, O, and B) provide vectors that are useful in exploration.

### Introduction

THE TERM exhalite was introduced by Ridler (1971) to refer to rocks in an exhalative-sedimentary association of inter-

bedded volcanoclastic and chemical sediments. The volcanoclastic component typically consists of volcanoclastic sediment, siltstone, and shale, whereas the chemical component may include chert, Fe-Mn sediment, and sulfides. Where regionally metamorphosed, exhalites, herein referred to as meta-exhalites, produce a variety of lithologies such as iron formation, coticule, tourmalinite, apatite-rich rock, quartz-

\*Geological Survey of Canada Contribution no. 1997162

<sup>†</sup>Corresponding author; email, pgspry@iastate.edu

gahnite rock, zincian staurolite-bearing rock, barite-rich rock, and metachert. In some localities gradations exist among the different exhalite types.

Meta-exhalites are spatially and temporally associated with some of the largest base metal sulfide deposits in the world. In the paleo-Proterozoic Willyama Complex, Australia, coticles (garnet-quartz rocks) occur in and adjacent to the two largest deposits, Broken Hill (Stanton, 1972; Lottermoser, 1989; Spry and Wonder, 1989) and Pinnacles (Parr, 1992), but they also extend intermittently for over 100 km throughout the complex (Parr and Plimer, 1993). In addition, banded iron formation, tourmalinite, and quartz-gahnite rocks occur in close spatial association with sulfides at Broken Hill (Stanton, 1972, 1976a, b, c, d; Barnes et al., 1983) and are considered by many geologists working in the district to be indicators of paleohydrothermal activity. Volumetrically significant associations of meta-exhalites with world-class base metal ores occur at the meso-Proterozoic Gamsberg and Aggeneys, South Africa (Rozendaal and Stumpfl, 1984; Hoffman, 1993) deposits, and at Sullivan, British Columbia (e.g., Slack et al., 2000). Iron formation is host to sulfides in the Aggeneys and Gamsberg deposits; coticles exist in the vicinity of sulfides in both mining camps. Although iron formation is not present at Sullivan, spectacular occurrences of tourmalinite, and to a lesser extent coticle, occur above, below, and along strike from the deposit (Slack et al., 2000).

There are several Paleozoic (e.g., Buchans, Newfoundland; Rosebery, Tasmania; Mount Chalmers, Queensland; Hellyer, Tasmania) and Archean (e.g., Big Stubby and North Pole, Western Australia) volcanogenic massive sulfide deposits that contain barite that has been metamorphosed at or below lower greenschist facies (e.g., Green et al., 1981; Barley, 1992; Large, 1992). Barite-bearing ore deposits metamorphosed to the amphibolite facies include those at Gamsberg, South Africa (Rozendaal and Stumpfl, 1984) and Aberfeldy, Scotland (Coats et al., 1980). Lottermoser and Ashley (1996) have noted the exploration potential of barite-rich rocks for strata-bound Cu-Au mineralization in the Proterozoic Olary block, South Australia. Although we briefly mention these barite-bearing meta-exhalites, they are not discussed further since they are relatively uncommon in settings distal from ore deposits.

We describe herein the geological setting, petrography, mineralogy, geochemistry, and genesis of meta-exhalites that are spatially and temporally associated with metamorphosed ores. Particular emphasis is placed on iron formations, coticles, and tourmalinites that are related to sea floor massive sulfide deposits. The spatial and temporal association of meta-exhalites with sea floor hydrothermal deposits makes their recognition and characterization potentially valuable in the search for concealed mineralization; hence, we also discuss these rocks in terms of their utility as exploration guides.

### Iron Formations

There are many variants of iron formations which have been referred to variously as banded iron formation, fer-

ruginous chert, jasper, jasperoid, tetsusekiei (literally translated "iron-quartz" from Japanese), vasskis (Norwegian term for sulfidic black chert, but thought to derive from the German term "weiss-kies" meaning white sulfide), graphitic chert, cherty tuff, tuffaceous exhalite, chloritic iron formation, sulfide iron formation, or simply hydrothermal sediment. These rocks are commonly referred to as Algoma-type iron formation (Gross, 1980). They are not to be confused with Superior-type iron formation (e.g., Cloud, 1973; Holland, 1984; Beukes and Klein, 1992; Morris, 1993), consisting of chemical sediment deposited from iron-rich waters that continuously upwelled from suboxic marine basins and encountered more oxygen-rich waters on continental shelves.

With few exceptions, iron formations associated with massive sulfide ores are considered to be chemical sediments deposited from hydrothermal fluids that vented into submarine basins (e.g., Stanton, 1972; Morris, 1993; Isley, 1995). In his classic paper, James (1954) characterized iron formation as a thin-bedded or laminated chemical sediment having a minimum of 15 wt percent Fe; herein we adopt a more liberal interpretation and include rocks with somewhat lower Fe content (as low as 10 wt % Fe). Table 1 provides an overview of selected localities of iron formation associated with massive sulfide mineralization mentioned in the text. Photographs of iron formation from some classic localities are shown in Figure 1 and reflect differences in composition, metamorphic grade, and deformational factors.

### Geology and petrography

Iron formations are associated with various types of volcanogenic and sedimentary exhalative base metal sulfide deposits, including those of Cyprus- (Franklin et al., 1981), Besshi- (Slack, 1993a), Kuroko- (Kalogeropoulos and Scott, 1983), and Broken Hill-type (Beeson, 1990). Iron formation generally caps massive sulfides and forms the immediate hanging wall of a deposit. In many Cyprus- and Besshi-type deposits, iron formations cover an area about twice that of the massive sulfides. Less commonly, they are lateral facies equivalents of massive sulfides and may extend for many kilometers along strike from the mineralization. For example, the iron formations and massive sulfide deposits that define the Brunswick and Heath Steele belts in the Bathurst district, New Brunswick, are traceable for over 12 km of strike length. In other deposits, such as those at Manitouwadge, Ontario, massive sulfides grade into iron formation. Iron formation is also known to form discontinuous horizons above and below massive sulfides with no clear temporal equivalence to the massive sulfides; such is the case for the many different exhalite types and lode rocks (e.g., massive sulfides) in the Broken Hill area of Australia (Stanton, 1972; Barnes et al., 1983; Plimer, 1988a).

In general, iron formations consist of layers less than 2 m thick, although some can be tens of meters thick. The best developed and most laterally extensive massive sulfide-associated iron formations are those in volcanosedimen-

TABLE 1. Geology of Selected Iron Formation Localities

Deposit, district	Age	Geologic setting	Metals	Iron formation type	Associated exhalites	References
Bathurst, New Brunswick	Ordovician	Mrhy, Cmsd	Pb, Zn, Cu	Carbonate, oxide, Silicate	Coticule	1, 2, 3
Millenbach, Quebec	Archean	Mrhy, Mbas	Cu, Zn, Au	Main Contact tuff (quartz, sulfides)		4
Lake Dufault, Quebec	Archean	Mhry, Mbas	Cu, Zn, Au	Chert tuff		5
Matagami, Quebec	Archean	Mrhy, Mbas	Cu, Zn, Au	Chert, carbonate, sulfide		6, 7, 8
Soucy, Quebec	Proterozoic	Mgab, Cmsd	Cu	Silicate		9
Manitouwadge, Ontario	Archean	Cmsd, Mrhy, Mbas, Gran	Cu, Zn, Au	Oxide, silicate, sulfide		10, 11
Windy Craggy, British Columbia	Triassic	Mbas, Cmsd	Cu, Zn	Chert, carbonate		12
Prescott-Jerome, Arizona	Proterozoic	Mhry	Cu, Zn, Au	Oxide, carbonate, sulfide		13, 14
Broken Hill, Australia	Proterozoic	Cmsd, Mrhy, Mbas	Pb, Zn, Ag	Oxide, silicate	Coticule, tourmalinite, quartz-gahnite rock	15, 16, 17, 18, 19, 20, 21, 22, 23
Olary block, Australia	Proterozoic	Cmsd, Mrhy	Cu, Au	Oxide, carbonate	Barite-rich rock, coticule	24, 25
Mt. Isa block, Australia	Proterozoic	Cmsd, Mbas	Pb, Zn, Ag	Silicate	Coticule	26, 27, 28
Thalanga, Australia	Cambro-Ordovician	Mrhy, Cmsd	Zn, Pb, Cu, Ag	Silicate		29, 30
Aggeneys, South Africa	Proterozoic	Cmsd, Mrhy	Pb, Zn, Cu	Carbonate, silicate, oxide	Coticule, tourmalinite	31, 32
Gamsberg, South Africa	Proterozoic	Cmsd	Pb, Zn	Oxide, silicate	Coticule	33, 34
Otjihase-Matchless belt, Namibia	Proterozoic	Mbas, Cmsd	Cu	Oxide		35, 36, 37
Iimori, Japan	Jurassic-Cretaceous	Mbas, Cmsd	Cu	Oxide		38
Okuki, Japan	Jurassic	Mbas, Cmsd, Mgab	Cu	Oxide		39
Boquira, Brazil	Archean	Cmsd, Mbas, Mrhy	Pb-Zn	Oxide, carbonate, sulfide, silicate		28, 40
Trondheim, Norway	Ordovician	Mbas, Cmsd, Mrhy	Cu	Vasskis, jaspers		41, 42, 43
Bergslagen, Sweden	Proterozoic	Mrhy, Mbas, Cmsd, Mcar	Zn, Pb, Ag	Silicate, oxide, carbonate	Coticule, tourmalinite	28, 44, 45
Skellefte, Sweden	Proterozoic	Mbas, Mrhy, Cmsd	Cu, Zn, Pb, Au, Ag	Oxide		46

Abbreviations: Cmsd = clastic metasediments (e.g., pelitic schist), Gran = granite or felsic porphyry, Mbas = metabasalt (greenstone, amphibolite), Mcar = metacarbonate, Mgab = metagabbro and metadiorite, Mrhy = metarhyolite

References: 1, Graf (1975); 2, Troop (1984); 3, Peter and Goodfellow (1996b); 4, Kalogeropoulos and Scott (1989); 5, Sakrison (1967); 6, Davidson (1977); 7, Costa et al. (1983); 8, Liaghat and MacLean (1992); 9, Barrett et al. (1988); 10, Friesen et al. (1982); 11, Zaleski and Peterson (1995); 12, Peter and Scott (1998); 13, Brook (1974); 14, Anderson and Guilbert (1979); 15, Richards (1966a); 16, Richards (1966b); 17, Stanton (1976a); 18, Stanton (1976b); 19, Stanton (1976c); 20, Stanton (1976d); 21, Stanton (1976e); 22, Lottermoser (1989); 23, Parr (1992); 24, Lottermoser and Ashley (1995); 25, Lottermoser and Ashley (1996); 26, Stanton and Vaughan (1979); 27, Vaughan and Stanton (1986); 28, Beeson (1990); 29, Gregory et al. (1990); 30, Duhig et al. (1992); 31, Hoffman (1993); 32, Hoffman (1994); 33, Rozendaal (1980); 34, Rozendaal (1986); 35, Killick (1982); 36, Killick (1983); 37, Adamson and Teichmann (1986); 38, Kanehira and Tatsumi (1970); 39, Imai (1978); 40, Carvalho et al. (1982); 41, Nilsen (1978); 42, Grenne and Vokes (1990); 43, Grenne and Slack (1997); 44, Hedström et al. (1989); 45, Parr and Plimer (1993); 46, Parák (1991)

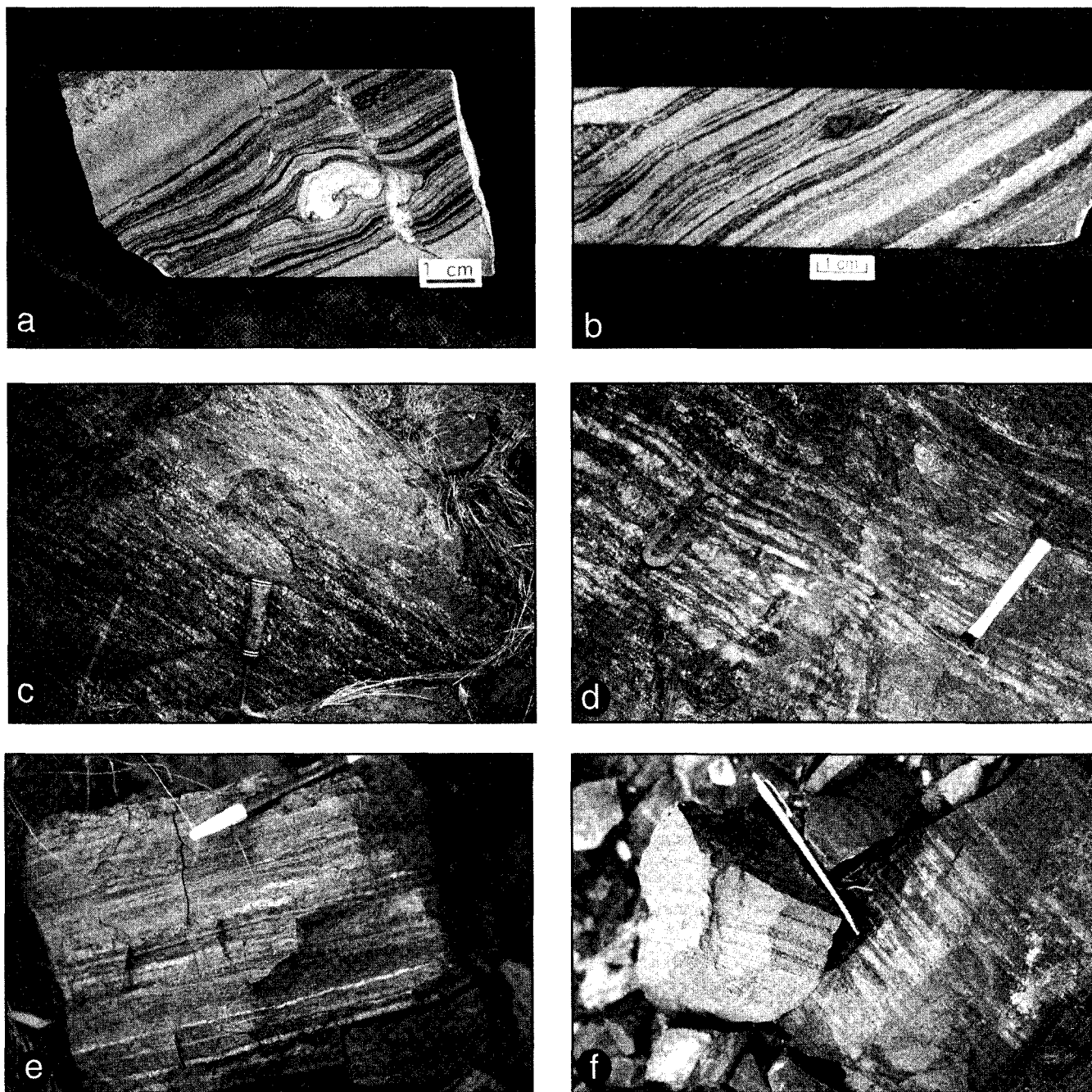


FIG. 1. Photographs of iron formation associated with metamorphosed massive sulfide deposits. a. Siderite-chert iron formation from drill hole DDH-284, Bathurst district, New Brunswick. b. Banded-quartz-magnetite iron formation (POA 172), Bathurst district, New Brunswick. c. Quartz-magnetite rock from Razorback ridge, Broken Hill area, Australia. d. Quartz-magnetite iron formation, Willecho mine, Manitouwadge, Canada. e. Quartz-magnetite lode rock, Pegmont deposit, Australia. f. Magnetite-quartz-garnet layers in banded iron formation, Broken Hill mine area, Australia.

tary sequences that formed in rift settings (e.g., Broken Hill, Australia; Bathurst, New Brunswick). The tectonic setting at the time of massive sulfide formation in the Bathurst area is thought to have been a back arc that formed on continental crust (e.g., van Staal, 1992), whereas that for Broken Hill was an ensialic intraconti-

ental rift (e.g., Cook and Ashley, 1992). Such rift sequences typically are composed of clastic sedimentary rocks (metamorphosed shale and lesser sandstone or graywacke) and metarhyolites or related felsic metamorphosed igneous rocks; mafic volcanic rocks, if present, generally do not occur within the ore horizon.

A popular classification scheme for iron formations (James, 1954) distinguishes among sulfide, carbonate, oxide, and silicate facies, or predominant varieties, all of which may grade into each other. The underlying tenet is that the occurrence and distribution of the different types of iron formation are controlled by redox conditions (discussed below). Sulfide-predominant iron formation consists of one or more Fe, Cu, Zn, and Pb sulfides (e.g., pyrite, pyrrhotite, chalcopyrite, galena, sphalerite). In many localities, this type forms the lode rocks of the deposit, such as at Gamsberg, South Africa (Rozendaal, 1986), Boquira, Brazil (Carvalho et al., 1982), and Soucy, Canada (Barrett et al., 1988). Anderson and Guilbert (1979) interpreted the chalcopyrite-rich, banded massive sulfide deposits of the Jerome-Prescott district, Arizona, as sulfide-facies iron formation that is capped by oxide-facies iron formation. Various sulfides are interlaminated with chert in the immediate hanging wall to the massive sulfides, with pyrite being the most common at a variety of deposits including Matagami, Quebec (Davidson, 1977), Delbridge, Quebec (Boldy, 1968), and Høydal, Norway (Grenne and Vokes, 1990).

Carbonate-predominant iron formation contains a variety of carbonates including siderite, ankerite, dolomite, and kutnahorite. Districts where carbonate-predominant iron formation is especially well developed include Bathurst, New Brunswick (Peter and Goodfellow, 1996a) and Boquira, Brazil (Carvalho et al., 1982).

Oxide-predominant iron formation consists of magnetite and/or hematite interbedded with chert at, for example, Broken Hill, South Africa (Moore, 1989; Hoffmann, 1993, 1994), Boquira, Brazil (Carvalho et al., 1982), and Bergslagen, Sweden (Plimer, 1988a). In many localities, jasper is the most common type of oxide-predominant iron formation, and forms the immediate hanging wall to many massive sulfide deposits including Okuki, Japan, (Imai, 1978), Løkken, Norway (Grenne, 1986; Grenne and Slack, 1997), and Windy Craggy, Canada (Peter and Scott, 1998), although it may also occur within the footwall or higher in the hanging wall. Magnetite-quartz  $\pm$  garnet  $\pm$  Fe-bearing silicate iron formation is prevalent in other deposits or districts including Fairmile, Australia (Beeson, 1990; Taylor and Scott, 1982), Otjihase, Namibia (Killick, 1982, 1983; Adamson and Teichmann, 1986), Geco, Ontario (Friesen et al., 1982), and Besshi, Japan (Kanehira and Tatsumi, 1970). Silicate-predominant iron formation consists mainly of Fe-, Mg-, and Mn-bearing silicates. In greenschist-facies rocks the dominant mineral is chlorite, however, at higher metamorphic grades silicates such as grunerite, actinolite, cummingtonite, spessartine garnet, and clinopyroxene prevail (Table 2).

Sulfide-, carbonate-, oxide-, and silicate-predominant iron formation may be complexly interbedded as, for example, in the Brunswick belt, Bathurst (Peter and Goodfellow, 1996a, fig. 5). This is consistent with fluctuating physicochemical conditions (e.g.,  $T$ ,  $f_{O_2}$ , pH, ionic strength,  $f_{S_2}$ ,  $f_{CO_2}$ ) of the mineralizing fluid or at the depositional site.

Iron formation may contain interbedded detrital clastic sediment or limestone. Iron formation typically is well laminated, with individual laminae consisting of one or several oxides, silicates, sulfides, or carbonates that are different from those of adjacent laminae; in many localities quartz is the most common interbedded mineral. In undeformed and weakly metamorphosed terranes, primary framboids, colloform structures, spheroidal cracks, and siliceous filaments may be present, but these are generally obliterated at amphibolite facies conditions or higher. Primary structures, such as crossbedding and graded bedding, have been observed in rocks metamorphosed even to granulite facies (e.g., Stanton, 1976a), but there is generally a direct relationship between grain size of constituent minerals and metamorphic grade. Iron formations in undeformed and weakly metamorphosed terranes (lower greenschist and below) are commonly very fine grained, whereas in upper greenschist, amphibolite, and granulite facies rocks, iron formations typically are coarser grained due to the effects of recrystallization (Duhig et al., 1992).

#### Geochemistry

Bulk compositions of iron formations are dominated by  $Fe_2O_3$ ,  $SiO_2$ ,  $CO_2$  (if carbonate is present), CaO (if carbonate and/or apatite are present), and MnO. In some iron formations, however, Mn is virtually absent (e.g., Løkken jaspers—Grenne and Slack, 1997). Concentrations of MgO,  $Al_2O_3$ ,  $TiO_2$ ,  $P_2O_5$ , and  $SO_2$  are generally minor, but the first three can be major if there is a significant contribution from detrital sediment. Space considerations preclude listing representative bulk-rock compositions of iron formations spatially associated with ore deposits; however, such compositions are available elsewhere (e.g., Richards, 1966a; Stanton, 1976c; Kalogeropoulos and Scott, 1983; Moore, 1989; Peter and Goodfellow, 1996a).

Due to their coherent geochemical behavior, the rare earth elements (REE) are particularly useful in tracing hydrothermal, sedimentary, and igneous processes. The behavior of the REE in modern sea-floor hydrothermal environments is sufficiently well known to make comparisons with ancient samples and therefore deduce past processes and/or sources that controlled their distribution. Rare earth elements in iron formation and coticles (discussed below) can originate from hydrothermal, hydrogenous, and detrital sources. Rare earth element patterns of several iron formations are shown in Figures 2a to f.

Chondrite-normalized REE patterns for iron formations associated with massive sulfide mineralization typically show positive Eu anomalies (e.g., Graf, 1975, 1977, 1978) and negative Ce anomalies (e.g., Lottermoser, 1989; Liaghat and MacLean, 1992; Peter and Goodfellow, 1996a; Grenne and Slack, 1997; Peter and Scott, 1998; Fig. 2a, d). Positive Eu anomalies indicate significant contributions from high-temperature ( $>250^\circ C$ ), reduced hydrothermal fluids (Sverjensky, 1984). Negative chondrite-normalized Ce anomalies are characteristic of seawater (Fig. 2g; Hogdahl et al., 1968). Authigenic sediments are thought to accurately reflect the relative Ce abundances of the waters

TABLE 2. Relative Stabilities of Predominant Constituent Minerals in Metamorphosed Iron Formations<sup>1</sup>

General mineral type	Specific mineral type	Precursor mineral	Low-grade metamorphism (200°–350°C)	Intermediate-grade metamorphism (350°–550°C)	High-grade metamorphism (>550°C)
Sulfides	Fe sulfides	Py, Po, Apy	Py, Po, Apy	Py, Po, Apy	Py, Po, Apy
	Pb sulfide	Gn	Gn	Gn	Gn
	Zn sulfide	Sp, Wtz	Sp, Wtz	Sp	Sp
	Cu-Fe sulfides	Ccp, Cb	Ccp, Cb	Ccp, Cb	Ccp, Cb
Carbonates	Fe carbonate	Sd	Sd, Ank	Sd, Ank	Sd, Ank
	Mg carbonate			Mgs	
	Ca-Mg carbonate	Dol	Dol	Dol	Dol
	Mn carbonate		Rds, Kut	Rds, Kut	
	Ca carbonate	Cal	Cal	Cal	(Cal)
Oxides	Hydrated Fe oxides	Hydrated Fe oxides	Hem, Mag	Hem, Mag	Hem, Mag
	Gahnite		(Gah)	Gah	Gah
Silicates	7Å serpentine-like	Amorphous Gnl, Brt	Gnl, Brt	Gnl, Brt	
	Talc-like structure	Nn, amorphous Fe oxide	Stp, Fe-Ann, Bt	(Stp), Fe-Ann, Bt	
	Fe-talc	Nn	Mn, Tlc	(Mn)	
	Fe-Mg chlorite	Chm, Cln	Chm, Cln	(Chm, Cln)	
	Na-rich amphibole		Rbk	Rbk	
	Mg-Fe amphiboles		Gru	Gru-Cum, Ath, Ged	Gru-Cum, Ath, Ged
	Ca-Mg-Fe amphiboles		Act-Tr, Hbl		
	Mn-Fe-Al rich	Chm?	(Sps)	Alm, Sps	Alm, Sps
	Orthopyroxene			(Fs)	Fs
	Clinopyroxenes		(Agt)	Agt, (Hd)	Agt, Hd
	Quartz	Amorphous silica	Qtz	Qtz	Qtz
	Fe olivine			(Fa)	Fa
	Ba feldspar	Ba-Al-Si gel?		Hy	
	Ba mica	Ba-Al-Si gel?		Kn	Kn
Zircon	Zrn	Zrn	Zrn	Zrn	
Phosphates	Apatite		Ap	Ap	Ap

<sup>1</sup> Based on data from French (1968, 1973), Immege and Klein (1976), Frost (1979), Haase (1982), Klein (1983), and Miyano and Klein (1986)

Abbreviations after Kretz (1983) or otherwise indicated: Act = actinolite, Agt = aegerine-augite, Alm = almandine, Ank = ankerite, Ann = annite, Ath = anthophyllite, Apy = arsenopyrite, Brt = berthierine, Bt = biotite, Cal = calcite, Cb = cubanite, Ccp = chalcopyrite, Chm = chamosite, Cln = clinocllore, Cum = cummingtonite, Dol = dolomite, Fa = fayalite, Fe-Ann = ferroannite, Ged = gedrite, Gn = galena, Gru = grunerite, Hbl = hornblende, Hem = hematite, Hy = hyalophane, Hd = hedenbergite, Kn = kinoshitalite, Kut = kutnahorite, Mag = magnetite, Mgs = magnesite, Mn = minnesotaite, Nn = nontronite, Po = pyrrhotite, Py = pyrite, Qtz = quartz, Rbk = riebeckite, Rds = rhodochrosite, Sd = siderite, Sp = sphalerite, Sps = spessartine, Tlc = talc, Tr = tremolite, Wtz = wurtzite, Zrn = zircon; minerals in brackets denote possible presence or presence in lesser amounts

from which they formed (Shimizu and Masuda, 1977), and marine carbonate, foram tests, modern pelagic clays, and modern metalliferous sediments all have negative anomalies (Piper and Graef, 1974; Palmer, 1985; Shaw and Wasserburg, 1985). Chondrite-normalized REE patterns for some iron formations show positive Ce anomalies (e.g., hematitic chert from the Iberian pyrite belt (Leistel et al., 1998), Main Contact tuff (Kalogeropoulos and Scott, 1989; Fig. 2b); however, while such a feature is atypical of iron formations, it commonly characterizes modern Fe-Mn crusts (Elderfield et al., 1981), which are the largest known Ce repository in modern oceans.

On chondrite-normalized REE plots, average continentally derived sediments and intermediate and felsic volcanic rocks are light REE enriched and show negative Eu anomalies. Therefore, if an iron formation contains an appreciable proportion (> ca. 30 wt %) of such detritus, the REE patterns will display light REE enrichment and have nil to negative Eu anomalies (compared to that of, for example, hydrothermal Fe oxides and carbonates). This seems to be the best explanation of nil to negative Eu

anomalies in some iron formations (Fig. 2b, c, f; see also Barriga, 1983; Lottermoser and Ashley, 1995).

Rare earth element patterns of iron formations are commonly similar to those of intermixed sea-floor hydrothermal fluids and seawater (Fig. 2g). As pointed out by Mills and Elderfield (1995) for modern sea-floor hydrothermal systems, negative Ce anomalies (and strong REE enrichments) on chondrite-normalized plots are only found in mixtures of greater than 90 percent seawater and end-member hydrothermal vent fluid. For this reason, REE are of limited use as tracers of fluid-seawater mixing, although they place a lower limit on the seawater contribution to samples.

Few studies exist on the sulfur isotope composition of iron formation-hosted sulfides.  $\delta^{34}\text{S}$  values for pyrite in tetsekiei from the Hokoroku district (Japan) range from -0.6 and 6.1 per mil and indicate an igneous sulfur source, together with a small possible contribution from reduced seawater sulfate (Kalogeropoulos and Scott, 1983). Brunswick belt iron formation  $\delta^{34}\text{S}$  values for sulfides vary from -15.6 to 22.4 per mil (Peter and Goodfellow, 1993); this range is similar to that for the ore sulfides

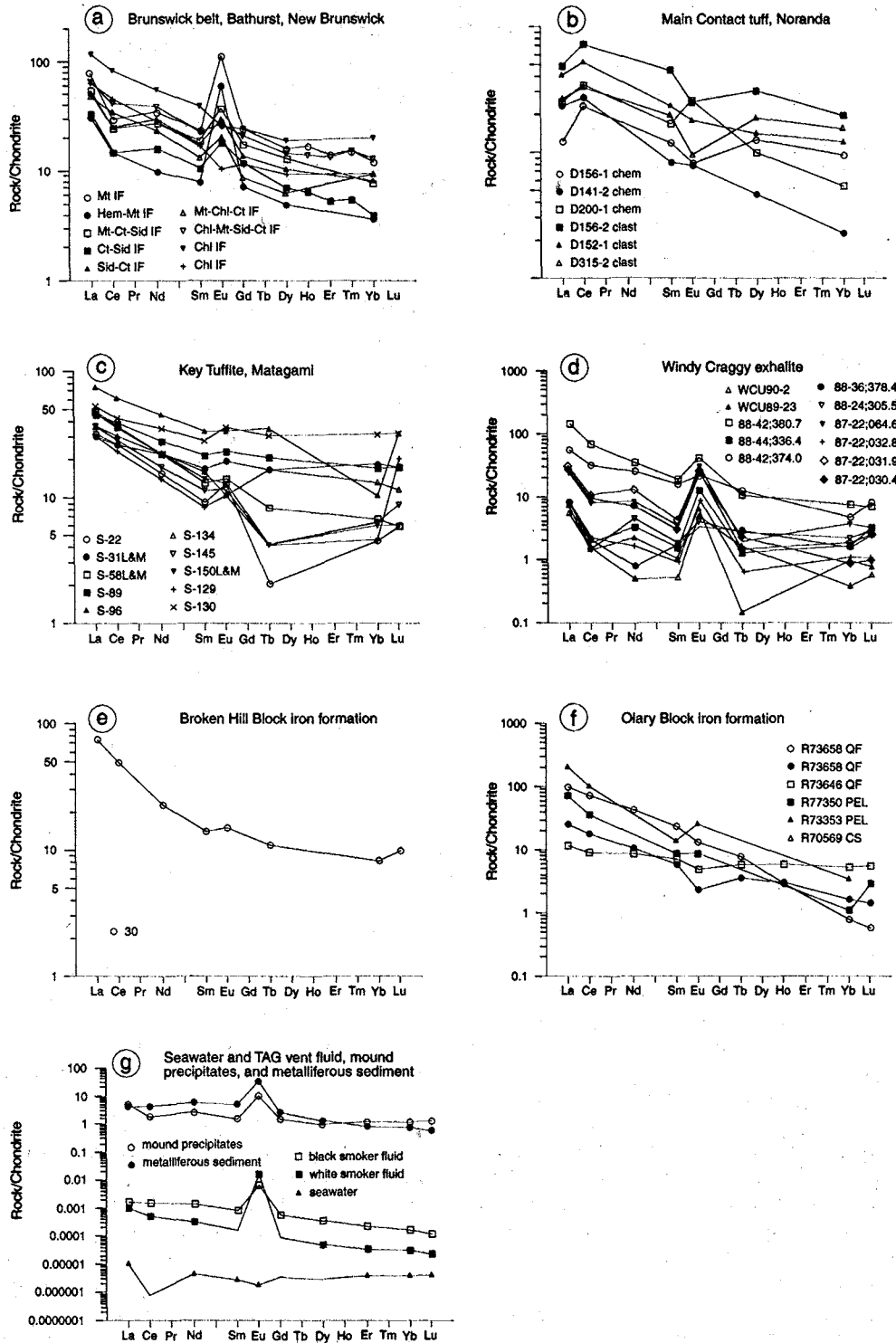


FIG. 2. Chondrite-normalized (Rock, 1988) rare earth element plots of iron formation samples from selected deposits and areas. a. Brunswick horizon iron formation, Bathurst mining camp, New Brunswick (Peter and Goodfellow, 1996a). b. Chemical- and clastic-predominant samples of the Main Contact tuff, Noranda, Quebec (Kalogeropoulos, 1982). c. Key tuffite, Mattagami area, Quebec (Liaghat and MacLean, 1992). d. Chert-carbonate-sulfide exhalite, Windy Craggy deposit, British Columbia (Peter and Scott, 1998). e. Iron formation, Broken Hill block, Australia (Lottermoser, 1989). f. Iron formation from the Olary block, Australia (Lottermoser and Ashley, 1995). g. Seawater (Mitra et al., 1994), metalliferous sediment on mound, mound material, and white and black smoker hydrothermal fluid from the modern TAG sea-floor sulfide site (Mills and Elderfield, 1995).

and thereby indicates common sulfur sources from reduced seawater sulfate and bacteriogenic sulfur. Sulfide minerals in vasskis units in Norway have  $\delta^{34}\text{S}$  values between  $-20$  and  $-25$  per mil (Sand, 1986), which imply sulfur derivation from biogenic sources or formation under oxidized conditions. Minor pyrite in ironstones distal from the Thalanga deposit in Australia have  $\delta^{34}\text{S}$  values between  $-14.4$  and  $5.7$  per mil (average  $-8.1\%$ ); these values are unlike those for the massive sulfides ( $\delta^{34}\text{S} = 10\text{--}18\%$ ). They suggest open-system bacterial (biological) reduction of seawater sulfate for the ironstones, versus inorganic reduction of seawater sulfate for the massive sulfides (Duhig et al., 1992).

Carbon and oxygen isotope studies of hydrothermal iron formation are even more limited in number than those for sulfur. The paucity of studies is due, in part, to the difficulties in interpreting the isotopic data, particularly for carbon, given the sensitivity of carbon isotopic compositions to a variety of physicochemical conditions (e.g.,  $T$ ,  $f_{\text{O}_2}$ , pH, ionic strength,  $\delta^{13}\text{C}_{\Sigma\text{C}}$ ) and the rate of isotopic exchange between various carbon species (e.g., Ohmoto, 1972). Despite these difficulties, various studies have utilized C or O isotopes in interpreting the origin of carbonates in iron formations associated with metamorphosed ore deposits. For example, carbonates in carbonate-facies iron formation from Boquira, Brazil, have  $\delta^{13}\text{C}_{\text{PDB}}$  values between  $-5.5$  and  $3.3$  per mil (Carvalho et al., 1982) and are consistent with a predominantly marine carbon source. Carbon isotope analyses of siderite and calcite in Brunswick belt iron formation range between  $-16.2$  and  $-7.2$  per mil and suggest a mixed carbon source consisting of organic matter, seawater, and marine carbonate (Peter and Goodfellow, 1993). Barriga (1983) reported oxygen isotope compositions of quartz in jasper overlying the Aljustrel deposit in the Iberian pyrite belt as being between  $17.9$  and  $20.1$  per mil. Whole-rock  $\delta^{18}\text{O}_{\text{SMOW}}$  analyses of jaspers from the area of the Løkken and Høydal deposits, Norway, range from  $13.0$  to  $15.5$  per mil (Grenne and Slack, 1997). Carbonates in carbonate facies iron formation from Boquira, Brazil, have  $\delta^{18}\text{O}$  values between  $8.6$  and  $21.5$  per mil (Carvalho et al., 1982). Values of  $\delta^{18}\text{O}_{\text{SMOW}}$  for siderite, calcite, and rhodochrosite in iron formation from the Brunswick belt vary from  $9.6$  to  $15.6$  per mil, whereas those for quartz in Key tuffite samples from the Mattagami Lake deposit are between  $8.7$  and  $12.3$  per mil (Costa et al., 1983).

Published strontium and lead isotope data for iron formations are rare. Siderite from the Brunswick belt has  $^{87}\text{Sr}/^{86}\text{Sr}$  values between  $0.71189$  and  $0.71508$  (W.D. Goodfellow, unpub. data) that are intermediate between those of Middle Ordovician seawater ( $0.7082$ ; Burke et al., 1982) and continental crust ( $0.713$  to  $0.720$ ), thus suggesting Sr input from both sources. Lead isotope ratios for chert facies iron formation that locally cap massive sulfides in the Iberian pyrite belt range between  $18.20$  and  $18.44$  for  $^{206}\text{Pb}/^{204}\text{Pb}$  and are more radiogenic than the associated massive sulfides ( $^{206}\text{Pb}/^{204}\text{Pb} = 18.13\text{--}18.23$ ); sulfide facies pyritic chert is also more radiogenic ( $^{206}\text{Pb}/^{204}\text{Pb} = 18.24$  to  $18.45$ ; Leistel et al., 1998; Marcoux, 1998). Differences in Pb isotope signatures and lead contents between

cherts and sulfide-rich rocks were considered (Leistel et al., 1998) to show that there is no genetic link between the cherts and the massive sulfides and that their leads have different sources.

### Origin

*Style of mineralization:* Given the multiple sources possible for constituent elements within iron formations, there is considerable debate as to whether certain elements were introduced directly from the hydrothermal fluid or were scavenged from the water column onto iron oxyhydroxide particles. However, despite this debate, it is widely accepted that Algoma-type iron formations are ancient metalliferous sediments that were deposited on the sea floor like those on modern midocean ridges and back-arc basins (e.g., Isley, 1995; Peter and Goodfellow, 1996a). Recent REE and Nd isotope evidence indicates that the iron in some Algoma-type iron formations also originated from hydrothermal sources (e.g., Jacobsen and Pimentel-Klose, 1988). Iron formations associated with Cu-Au mineralization of the Selwyn Range, Australia, are excluded from this review, as they are considered to be (Williams, 1994) epigenetic, structurally-controlled replacements.

The following three models have been proposed for the origin of Algoma-type iron formations:

1. Precipitation from buoyant, high-temperature ( $350^\circ\text{--}400^\circ\text{C}$ ) hydrothermal fluids (Fig. 3a): particulates are carried upward in a buoyant hydrothermal plume until they reach a neutral density, disperse laterally from the vent site, and are influenced by bottom currents. The plume particulates are sedimented largely due to gravitational settling and are dispersed on a scale of kilometers to tens and even hundreds of kilometers. Particulates are deposited as sulfides, carbonates, sulfates, silicates, or oxyhydroxides. The redox conditions of the ambient water column play an important role in the nature of the particles deposited, as well as their preservation. Restricted basins are conducive to reducing conditions and better preservation, whereas oxygenated conditions give rise to precipitates similar to modern metalliferous Fe-Si-Mn oxyhydroxides, such as those at modern ridge crests along the East Pacific Rise, Bauer Deep, and Galapagos rift (e.g., Boström and Peterson, 1966; Dymond, 1981; Barrett, 1987). In the Bathurst mining camp, the distribution of iron formation over several kilometers suggests that the hydrothermal fluids formed buoyant plumes from which minerals precipitated, settled on the sea floor, and produced the sulfide ores and associated iron formations. It is possible that megaplumes, tied to magmatic and tectonic evolution of a ridge crest (Embley et al., 1991), have contributed to the widespread occurrence of interlaminated or interbedded sulfides, carbonates, oxides, and silicates in ancient iron formations.

2. Precipitation from highly saline, high-temperature hydrothermal fluids (Fig. 3b): particulates are carried to the sea floor in a buoyant hydrothermal plume where they hug the bottom or rise until they reach a pycnocline and spread out

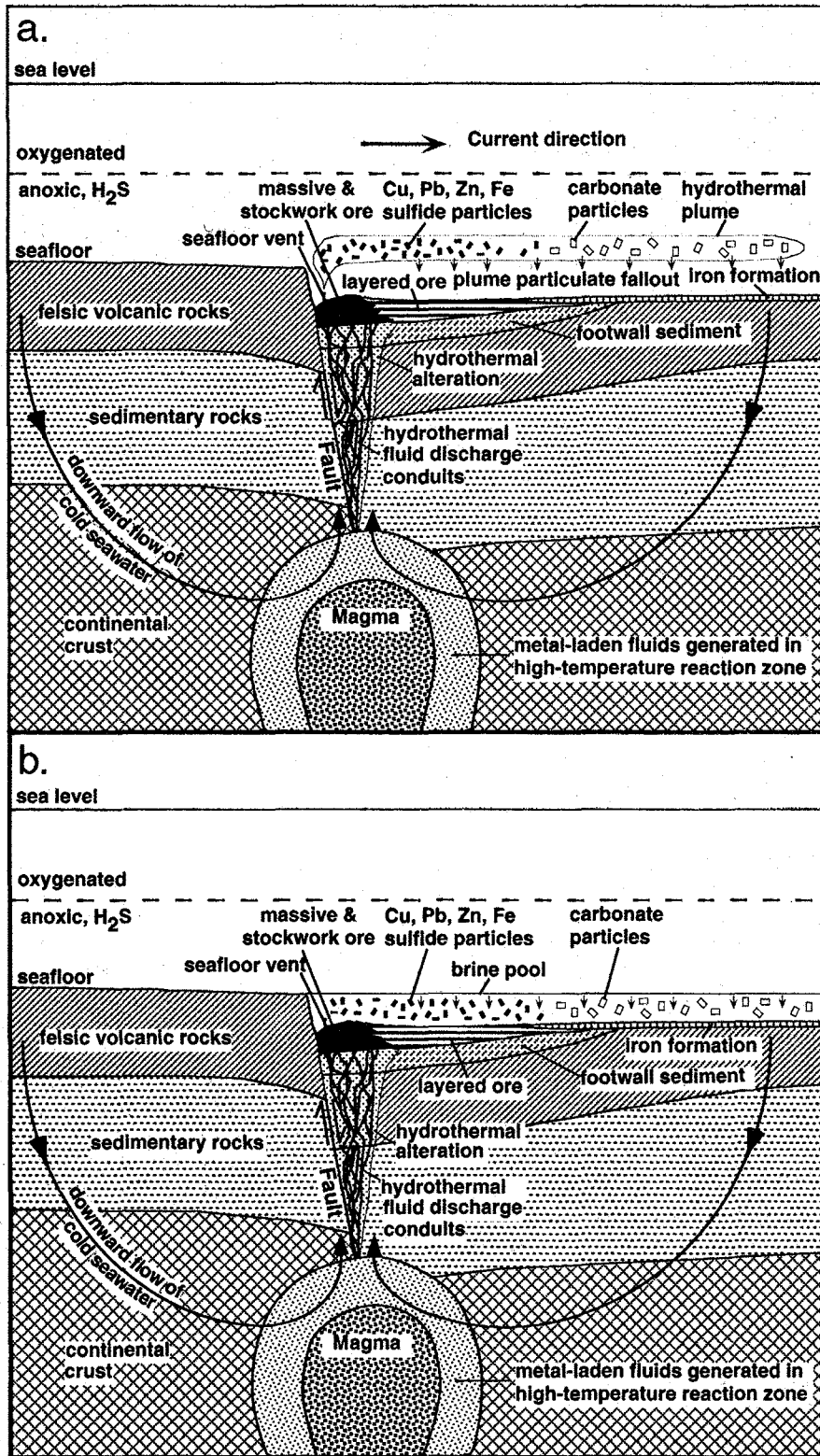


FIG. 3. Schematic cross sections depicting two possible end-member models: a. hydrothermal plume, and b. brine pool, for the formation of iron formations temporally and spatially associated with massive sulfide mineralization.

laterally from the vent. An example of the latter case is in the Atlantis II Deep of the Red Sea, where hydrothermal fluids leach Miocene evaporites in the subsurface and give rise to dense, saline brines that pond in smaller, restricted basins (e.g., Degens and Ross, 1969). Sediments are finely layered (typically 1–5 mm), containing oxides as well as laminae and beds of sulfides. Sulfides are precipitated from this dense fluid under anoxic conditions, whereas interlaminated oxides are precipitated from overlying, more oxidized fluids. These two fluids are separated at a density interface.

3. Precipitation from low-temperature (<250°C), diffusely venting hydrothermal fluids rather than high-temperature, highly focused fluids: several studies provide evidence for low-temperature formation. Tetsusekiei is thought to have formed at temperatures less than 150°C (Kalogeropoulos and Scott, 1983). The REE patterns of modern ochers from the TAG site on the Mid-Atlantic Ridge (Fig. 2g) indicate that they cannot have formed from black smoker fluid-seawater mixtures or by oxidation of chimney sulfides (Mitra et al., 1994). Instead, these ochers probably formed from low-temperature, diffusely flowing fluids, or from a late-stage, silica-rich fluid during waning hydrothermal activity (Lalou et al., 1990). Low temperatures of formation have been determined for some ancient iron formations. Based on oxygen isotope data, jaspers from the area of the Iøkken and Høydal deposits give formational temperatures between 150° and 220°C (Grenne and Slack, 1997); calculated temperatures for the cherts and jaspers overlying the sulfide deposits at Aljustrel, Iberian pyrite belt, are around 120°C (Munha et al., 1986).

In the above models, the iron formation minerals (or their precursors) are precipitated directly from the vent fluid and the hydrothermal plume. Individual laminae are therefore ascribed to discrete pulses of hydrothermal fluid. This contrasts with the ochers on Cyprus, which formed by oxidative sea-floor weathering of preexisting sulfide minerals (Herzig et al., 1991). Debate still exists about the syngenetic nature of certain oxide-facies iron formations such as those associated with the Irish-type deposits (e.g., Hitzman et al., 1995; Cruise, 1996). High Fe and Mn within the Irish iron formations is attributed (Cruise, 1996) to the presence of late ferroan dolomite; however, this observation does not a priori rule out a stratiform origin by precipitation on the sea floor.

*Hydrothermal, detrital, and hydrogenous sources:* By analogy with modern sea-floor hydrothermal vent fluids (e.g., Von Damm, 1990), elements such as Fe, Mn, Cu, and Zn in iron formations are generally assigned a hydrothermal origin. In many instances, the detrital component can be readily identified, and largely attributed to enclosing host rocks (whether sedimentary, mafic volcanic, or felsic volcanic). Strong correlations involving a major component ( $Al_2O_3$ ), and minor and trace elements such as Ti, Cr, Zr, Nb, Th, and REE can be explained by the presence of clay-rich detrital clastic material of sedimentary or volcanic origin (e.g., Peter and Goodfellow, 1996a).

Boström (1973a) used a ternary Al-Fe-Mn plot to distinguish between hydrothermal, detrital (e.g., eolian, turbiditic, epiclastic, pyroclastic), and hydrogenous inputs to metalliferous sediments. The rationale behind the distinction is that Al is essentially of detrital origin, whereas Fe and Mn are predominantly hydrothermal (Fig. 4). Another commonly used plot is  $Al/(Al + Fe + Mn)$  versus  $Fe/Ti$  (Boström, 1973a), which strictly assumes that Ti, like Al, is detrital. Such plots show that data for iron formations from a variety of sites span a continuous trend between hydrothermal sediment and terrigenous and pelagic sediment (Fig. 5).

Techniques such as interelement correlations and Q-mode factor analysis (e.g., Gross, 1993) have also been used for differentiating hydrothermal, detrital, and seawater sources for iron formation. Pearson interelement correlations for Brunswick belt iron formations between  $SiO_2$  and  $TiO_2$ ,  $Al_2O_3$ ,  $MgO$ ,  $Na_2O$ ,  $K_2O$ , Be, Ce, Co, Cr, Ga, Hf, La, I.u, Nb, Ni, Rb, Sc, Ta, Th, U, V, Y, Yb, and Zr are attributed to detrital silicate and aluminosilicate minerals; between Be and Ce, Cr, Ga, Hf, La, I.u, Nb, Ni, Sc, Ta, Th, U, Yb, and Zr to mafic aluminosilicates; between Ba and

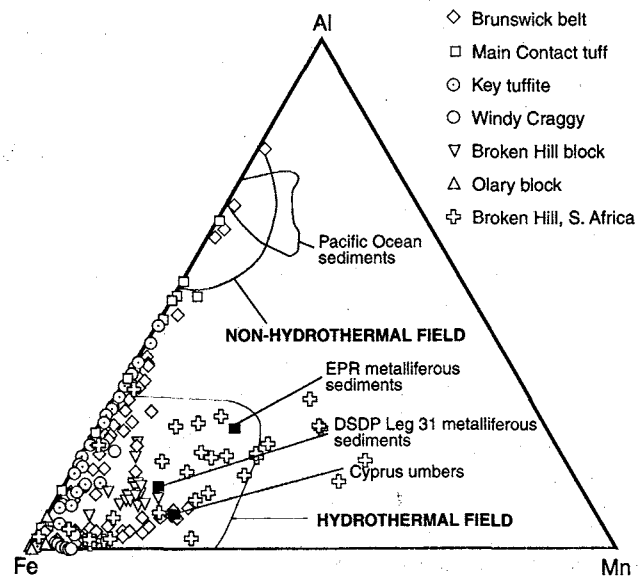


FIG. 4. Al-Fe-Mn ternary plot (mole %) of iron formation samples from selected deposits and areas: Brunswick horizon iron formation, Bathurst mining camp, New Brunswick (Peter and Goodfellow, 1996a); Main Contact tuff, Noranda, Quebec (Kalogeropoulos, 1982); Key tuffite, Mattagami area, Quebec (Davidson, 1977; Liaghat and MacLean, 1992); Windy Craggy deposit, British Columbia (Peter and Scott, 1998); iron formation, Broken Hill block, Australia (Eeson, 1971; Stanton, 1976a); Olary block, Australia (Lottermoser and Ashley, 1996); Broken Hill, South Africa (Moore, 1989; Hoffmann, 1993, 1994). Shown for reference are the compositional fields of metalliferous sediments from the East Pacific Rise and the Afar Depression (hydrothermal field), and basalts, shales, and granites (nonhydrothermal field) utilizing data from Boström (1973a). The compositions of Deep Sea Drilling Project Leg 31 (Bonatti et al., 1979), umbers associated with Cyprus massive sulfide deposits (Robertson and Hudson, 1973), and Pacific Ocean sediments (Dymond et al., 1973) are also indicated.

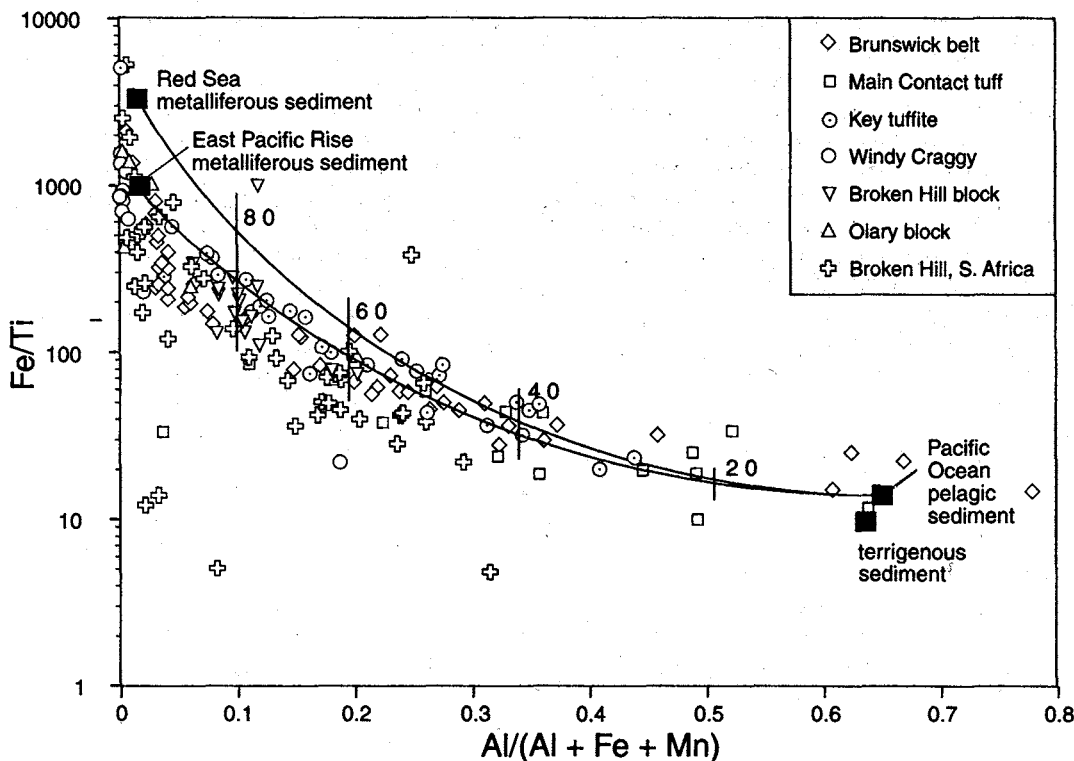


FIG. 5. Fe/Ti vs. Al/(Al + Fe + Mn) plot of iron formation samples from the same selected deposits and areas shown in Figure 4. Also shown for reference are average compositions for metalliferous sediment from the East Pacific Rise (Boström, 1973a), pelagic sediment from the Pacific Ocean, and terrigenous sediment.

Be, Cs, Ga, Nb, Rb, and Tl to feldspar; and between  $Fe_2O_3^T$  and CaO,  $CO_2$ ,  $P_2O_5$ , Sr, S, Ag, As, Au, Bi, Cd, Cu, Eu, Eu/Eu\*, Hg, In, Mo, Pb, Sb, Se, Tl, and Zn to hydrothermal iron oxides, carbonates, apatite, and sulfides (Peter and Goodfellow, 1996a). Strong correlations among the relatively immobile elements Al, Sc, V, Y, and heavy REE indicate a small component (mostly <5%) of detrital, probably basaltic, material within the jaspers of the Løkken-Høydal area, Norway (Grenne and Slack, 1997). Lottermoser and Ashley (1995) noted that Olary block (Australia) iron formations display correlations between Al and Ti, K, Hf, Rb, and Zr, which reflect clastic or volcanic detritus. At Broken Hill, South Africa, the amphibole-rich iron formations ( $Fe/Ti = 100-7,000$ ;  $Al/(Al + Mn + Fe) = 0.01-0.05$ ;  $n = 10$ ) are interpreted to have a greater hydrothermal component, whereas the garnet-rich varieties ( $Fe/Ti = 40-100$ ;  $Al/(Al + Mn + Fe) = 0.11-0.21$ ;  $n = 8$ ) contain a greater detrital component (Hoffmann, 1994, fig. 7.8).

Factor analysis has also been used to identify contributions from hydrothermal, hydrogenous, and detrital components in iron formation. Factors commonly include geochemically coherent elements that relate to sample type or processes that have affected the rocks. Factor analysis by Davidson (1977) on samples of Key tuffite from Matagami, Quebec, identified four major groupings: (1) Zn, Cu, Cd, Pb, Ag, P, and Na (30% of total variability) attributed to hydrothermal component; (2) Fe, Cr, and Co

(15% of variability) attributed to hydrothermal pyrite and pyrrhotite; (3) Al, Ba, Ti, Mg, and V (27% of total variability) due to detrital aluminosilicates; and (4) Ca, Mn, Sr, K, and Be attributed to detrital aluminosilicates of volcanic origin. Factor analysis of iron formation from the Soucy deposit, Labrador, indicates that  $SiO_2$ ,  $Na_2O$ , and  $TiO_2$  reside in detrital material, whereas Fe is hydrothermal (Barrett et al., 1988).

Stanton (1972) noted the coincidence between high P and sulfides in Broken Hill (Australia) iron formation, and on this basis argued that P was derived from the hydrothermal fluid rather than from seawater. Work on modern hydrothermal plumes (Mottl and McConachy, 1990) has shown that P, Si, Ca, V, and As in hydrothermal particles originate by these species being chemically scavenged from the water column by iron oxyhydroxide particles. The degree of enrichment thus depends on the residence time of the particles in the water column and the ambient element concentrations in seawater. Caution must be noted here that the P budget is likely to be very different in modern seawater than in the Proterozoic, since most P in modern deep-sea sediment occurs as skeletal biogenous remnants in the form of apatite (e.g., Marchig, 1978).

In the Bathurst area, As values in iron formation are highest overlying (or close to) known massive sulfide deposits. This indicates that As is not hydrogenous; any plume particles over the massive sulfide deposits would have settled out more quickly than those transported

away from the vent site, and thus would have had shorter residence times in the water column (and reduced potential to scavenge elements from seawater). The hydrogenous component in iron formations is generally very small and, therefore, is not discernible in Al-Fe-Mn and Al/(Al + Fe + Mn) -Fe/Ti plots. Lottermoser and Ashley (1995) suggested that the high Th content of Olary block (Australia) iron formation is due to a large hydrogenous component that was scavenged from the water column, although high Th contents could also reflect clastic detritus derived from A-type granites and/or rhyolites (cf. Ashley et al., 1996). The best indicator of a hydrogenous origin is a distinct negative Ce anomaly on a chondrite-normalized REE plot (Fig. 2a-g), as is found with modern oxygenated seawater.

*Precursor mineralogy:* The oxide, silicate, carbonate, and sulfide mineralogy of metamorphosed iron formations is dependent on bulk composition and a variety of physicochemical conditions (e.g., P, T,  $f_{O_2}$ , pH, I,  $f_{S_2}$ , and  $f_{CO_2}$ ). Although the mineralogy of iron formations at various metamorphic grades (Table 2) is well documented, there is much debate in the literature as to their precursors. Duhig et al. (1992) suggested, on the basis of textural considerations, that iron formation in the Mount Windsor volcanic belt, Australia, was derived from silica gels. Grenne and Slack (1997), in their study of jaspers from the Trondheim district, Norway, reached a similar conclusion. They proposed that the jaspers formed by crystallization from siliceous colloids or gels that were genetically related to the hydrothermal system(s) responsible for deposition of the nearby Løkken and Høydal massive sulfide deposits.

Magnetite is commonly thought to be a dehydration product of a precursor mixture of  $Fe(OH)_2$  and  $Fe(OH)_3$ . Stanton (1976c) argued that chamosite was a primary precursor phase of iron formation associated with the Broken Hill deposit, Australia. Modern metalliferous sediments contain a high proportion of nontronite, an Fe-rich smectite clay (e.g., Dymond et al., 1973). The hydrothermal deposits of the FAMOUS area on the Mid-Atlantic Ridge are composed, in large part, of nontronite, and have bulk compositions remarkably similar to those of iron formations. Minnesotaite in iron formations is thought to form during diagenesis or low-grade metamorphism from precursor septechlorites and chamositic iron minerals. Stülpnomelane bands may have formed from precursor ash-fall tuff beds (e.g., Beukes and Klein, 1992).

*Physicochemical constraints:* A strong influence on the nature of the hydrothermal precipitates is the redox conditions at the depositional site. Water depth and circulation influence redox conditions (Eh). The different facies of iron formation (sulfide, carbonate, oxide, silicate; James, 1954) are thought to have formed under differing conditions of Eh or pH in the local depositional environment. Garrels and Christ (1965) determined the stability relationships in the system Fe-O-H-S-CO<sub>2</sub> at 25°C. Sulfide-facies iron formation forms in the deepest water under

strongly reducing and strongly negative Eh conditions. Carbonate- and silicate-facies iron formation require intermediate Eh conditions, such as those favored in deep water under moderately reducing conditions, albeit in slightly shallower waters than sulfide-facies iron formation. Siderite precipitation is favored over magnetite precipitation at relatively neutral pH and under the same Eh conditions (but ranging to lower values). Oxide-facies iron formation is precipitated under high Eh, oxidizing conditions, such as in shallow waters where iron is deposited as amorphous  $Fe^{3+}$  hydroxides [ $Fe(OH)_3$ ]. Under more reducing conditions, fine-grained magnetite ( $Fe_3O_4$ ) forms. Hydroxides of divalent iron [ $Fe(OH)_2$ ] are deposited only in highly reducing environments in a narrow field near the limit of stability of water at atmospheric pressure.  $Fe(OH)_3$  converts to  $Fe_3O_4$  in the presence of a reducing agent such as organic matter, or it could convert to siderite or greenalite. Magnetite also forms as a result of a reaction between hematite and carbonate during burial metamorphism. Thus, fluctuations in T, Eh, or pH and in  $P_{CO_2}$ , coupled with variations in the amount of reduced sulfur available, determine whether hematite, magnetite, siderite, pyrite, or pyrrhotite are precursor minerals. Stanton (1976b) suggested that the mineralizing fluids at Broken Hill, Australia, were warm and acidic, and that the ambient basin waters were cool and neutral. Distinct mineralogical layers in iron formation at Broken Hill led Stanton (1976c) to propose oscillations of pH and Eh conditions in the depositional basin.

The observation that iron formations are typically associated with Broken Hill-type deposits and not, for example, with most sedimentary-exhalative (sedex) deposits is because conditions for the former were more oxidized (e.g., Large et al., 1996) than the reducing conditions invoked for the latter (Goodfellow et al., 1993). In Broken Hill-type deposits, magnetite is abundant, whereas graphite is abundant in the sedex-type deposits. Where graphite is present, such as in the lower parts of the Gamsberg orebody, South Africa, locally reducing conditions were likely, whereas the barite-hematite-magnetite layers in the same orebody were deposited under more oxidizing conditions (Rozendaal and Stumpfl, 1984).

Redox conditions also control the distribution of Fe and Mn in hydrothermal precipitates (e.g., Crerar et al., 1980; Spry and Wonder, 1989). Mn is more mobile with increased pH and Eh, whereas  $Fe^{2+}$  is oxidized to  $Fe^{3+}$  where hydrothermal fluid and seawater mix. Higher pH and Eh conditions are required to oxidize  $Mn^{2+}$  to insoluble  $Mn^{4+}$ . The study of Mn distribution in modern marine basins shows it to be soluble in anoxic waters, precipitating as Mn oxides or carbonates in the zone of mixing with oxic waters. Thus, Fe and Mn are fractionated in solution due to gradual pH increase or gradual oxidation during mixing of hydrothermal fluid with ambient seawater. The presence at Tynagh, Ireland, of iron formation and a syngenetic manganese aureole around the deposit, as well as the presence of fossil worms (Banks, 1985), indicate that fluids vented into an oxidizing water column. Broken Hill-

type and sedex deposits typically also have Mn enrichment haloes in the wall rocks that may be used in the search for concealed mineralization (see below).

Implicit reference to proximal versus distal settings (i.e., distance from the site of focused hydrothermal discharge) is made in many studies of iron formation genesis (e.g., Scott et al., 1983). The reasoning is that sulfides are deposited close to the fluid discharge site in the deepest (most reduced) parts of the basin, whereas oxides and silicates are transported to shallower, more oxidized waters farther from the vent. The lateral zonation of iron formation at Pegmont, Australia, has been ascribed to an increase in Eh from center to edge of a paleobasin (Vaughan and Stanton, 1986).

Complex hydrologic conditions, such as those in the modern Red Sea, can give rise to a density-stratified basin with surface waters that are more oxic and deeper waters that are anoxic and enriched in dissolved ferrous iron (due to hydrothermal input). Interaction between these two water masses, together with the rates of supply of oxygen and carbon to the interface between the surface and the deep waters, can produce complex interbedding of sulfide- and oxide-predominant precursor minerals to iron formation. Plimer (1988a) favored a brine pool spillover model for the origin of the sulfides, iron formations, and cotiules at Broken Hill, Australia. He suggested that paleotopographic variations due to horsts and grabens controlled the distribution of sulfides and iron formations, with the sulfides and reduced iron formation assemblages restricted to grabens and the more oxidized assemblages to horsts. Such a scenario would be similar to that in the Red Sea.

A change from highly acid to moderately acid pH leads to the total removal of iron from solution. End-member, high-temperature, sea-floor vent fluids are reduced and acidic (e.g., Von Damm, 1990). Vent fluids, on mixing with cooler seawater in the subsurface or on the sea floor, precipitate sulfides and thereby lower the Fe/H<sub>2</sub>S ratio of the fluid mixture. If the fluids were 200°C or cooler, inorganic sulfate reduction in the feeding aquifer would be sluggish (Ohmoto and Lasaga, 1982) and high Fe/H<sub>2</sub>S ratios result. Continued cooling and mixing would yield precipitation of Fe and Mn oxides rather than sulfides. As discussed by Duhig et al. (1992), fluids with Fe/H<sub>2</sub>S less than 1 would potentially precipitate Fe sulfides in and around the vent site and Mn oxide distally; fluids with Fe/H<sub>2</sub>S greater than 1 would precipitate Fe and Fe-Mn oxide deposits.

In summary, the chemical composition and mineralogy of iron formation in a given area depends on the physicochemical conditions of the venting hydrothermal fluid (e.g., pH, T, ionic strength,  $f_{s_2}$ ), the redox conditions of the basin or water column into which venting occurs (water depth may partly control this also), the degree of basin isolation from clastic sedimentation, the amount of hydrothermal fluid input via venting, and bottom current drift. Predominantly gradational boundaries between iron formation facies and between iron formation and underlying host rocks could reflect waxing and waning hydrothermal activity against steady-state sedimentation, whereas

complex facies changes could be due to fluctuating physicochemical conditions of mineral precipitation. Detrital sedimentary interbeds in iron formation result from periodic turbiditic sedimentation.

### Cotiules

Renard (1878) coined the term cotiule and referred to it as a rock containing essential spessartine garnet in a matrix of sericite and/or quartz. A quartz-garnet rock, in which the garnet exhibits a dominance of the almandine, grossular, andradite, or pyrope compositional end-members, should strictly be referred to as quartz garnetite. The terms garnet quartzite and quartz garnetite were used by Richards (1966a, b) and Spry and Wonder (1989), respectively, to describe garnet-quartz rocks at Broken Hill, Australia. Nevertheless, the term cotiule is herein applied to garnet-quartz rocks, regardless of garnet composition, since intimate spatial relationships among spessartine-quartz-rich rocks, almandine-rich rocks, and grossular-quartz-rich rocks occur in various localities (e.g., Broken Hill, Australia—Spry and Wonder, 1989; Aggeneys, South Africa—Spry, 1990). The andradite and calderite components of garnet in cotiules are negligible. Cotiules are not to be confused with fine-grained, essentially unmetamorphosed ferromanganiferous sediments, called umbers, which occur stratigraphically above Cyprus-type massive sulfide deposits (Constantinou and Govett, 1972).

Although found in a variety of geological settings, cotiules are commonly spatially associated with metamorphosed base metal, scheelite, and gold deposits (Table 3). As is the situation for tourmalinites (below), most recent studies of cotiules associated with metamorphosed massive sulfide deposits suggest formation either by exhalative processes or subsea-floor replacement (e.g., Cook and Halls, 1990; Spry, 1990; Slack et al., 2000). However, earlier genetic interpretations of cotiules associated with these metamorphosed massive sulfide deposits are diverse. For example, cotiule at Broken Hill, Australia, has been variously interpreted as a metamorphosed chemical sediment (Segnit, 1961; Richards, 1966a, b; Stanton, 1976c; Stanton and Williams, 1978; Spry and Wonder, 1989; Slack et al., 1993b), a variant of metamorphosed detrital sands (Haydon and McConachy, 1987), and as metasomatized sediment (Stillwell, 1959).

### Geology and petrography

In ore-forming environments, cotiules are typically associated with rift-hosted volcanosedimentary base metal sulfide deposits, particularly those of the Broken Hill (Beeson, 1990) and Besshi (Slack, 1993a) types. They occur within sulfide deposits or as discontinuous units above, below, or along strike from massive sulfides, in some localities extending intermittently over several kilometers (e.g., Willyama Complex, Aggeneys). Cotiules generally form layers less than 2 m thick, but in some locations, such as the Broken Hill area, Australia, they may be greater than 10 m thick. Cotiules are most common in siliciclastic sedimentary rocks (graywackes and shales) that have experienced

TABLE 3. Geological Setting of Selected Coticule Localities

Deposit, district	Age	Geological setting	Metals	Garnet-bearing rock type	Associated exhalites	References
Glendalouh, Ireland	Cambro-Ordovician	Cmsd, Gran	Pb, Zn	Coticule	Tourmalinite	1
Tinahely, Ireland	Cambro-Ordovician	Cmsd, Gran	W	Coticule	Tourmalinite	2
Sultjelma, Norway	Early Paleozoic	Mbas	Cu	Coticule		3
Skorovass, Norway	Early Paleozoic	Mbas	Cu	Coticule		4
Bleikvassli, Norway	Early Paleozoic	Cmsd, Mbas	Pb, Zn, Ag, Cu, Au	Coticule		5, 6
Karnten, Austria	Siluro-Devonian	Cmsd	Zn, Cu	Coticule	Quartz-spinel rock	7
Angas, Australia	Cambrian	Cmsd	Pb, Zn	Coticule	Gahnite-staurolite rock	8
Western Georgia	Early Paleozoic	Cmsd, Mbas	Cu, Zn	Coticule	Tourmalinite, iron formation	9
Sullivan, Canada	Proterozoic	Cmsd, Mbas	Pb, Zn	Coticule	Tourmalinite	10
Willyama Complex (Broken Hill, Pinnacles) Australia	Proterozoic	Cmsd, Mrhy, Mbas	Pb, Zn, Ag	Coticule, garnetite, quartz garnetites	Tourmalinite, iron formation, quartz-gahnite rock	11, 12, 13, 14, 15, 16
Elizabeth, Vermont	Ordovician	Cmsd, Mbas	Cu, Zn	Coticule	Tourmalinite	6, 17
Aggeneys, South Africa	Proterozoic	Cmsd, Mrhy	Pb, Zn, Cu	Coticule	Iron formation, tourmalinite	6, 18, 19
Gamsberg, South Africa	Proterozoic	Cmsd	Pb, Zn	Coticule	Iron formation	20, 21
Quha River, South Africa	Proterozoic	Cmsd, Mbas	Disseminated sulfides	Coticule	Tourmalinite	22
Pegmont, Australia	Proterozoic	Cmsd	Pb, Zn	Coticule	Iron formation, tourmalinite	23
New Brunswick, Canada	Ordovician	Mrhy, Cmsd	Pb, Zn, Cu, Sn, W, Mo	Coticule	Iron formation	24
Sierras Pampeanas Orientales, Argentina	Proterozoic	Cmsd	W	Coticule	Tourmalinite	25
Cannington, Australia	Proterozoic	Cmsd	Pb, Zn, Ag	Coticule		26
Gossan Lead, Virginia	Proterozoic	Cmsd, Mbas	Cu, Zn	Coticule		27

Notes: Abbreviations: Cmsd = clastic metasediments (e.g., pelitic schist), Gran = granite or felsic porphyry, Mbas = metabasalt (greenstone, amphibolite), Mcar = metacarbonate, Mgab = metagabbro and metadiorite, Mrhy = metarhyolite

References: 1, Williams and Kennan (1983); 2, McArdle and Kennan (1988); 3, Cook and Halls (1990); 4, Halls et al. (1977); 5, Skauli (1990); 6, this study; 7, Williams and Manby (1987); 8, Both et al. (1995); 9, Wonder et al. (1988); 10, Slack et al. (2000); 11, Barnes et al. (1983); 12, Lottermoser (1989); 13, Lottermoser (1988); 14, Spry and Wonder (1989); 15, Parr (1992); 16, Wiggins (1990); 17, Annis et al. (1983); 18, Spry (1988); 19, Lipson (1990); 20, Stumpfl (1979); 21, Rozendaal and Stumpfl (1984); 22, Cornell et al. (1996); 23, Vaughan and Stanton (1986); 24, Gardiner and Venugopal (1992); 25, de Brodtkorb et al. (1995); 26, Bodon (1996); 27, Gair and Slack (1984)

anything from greenschist to granulite facies metamorphism. They are typically intercalated with other meta-exhalites, particularly iron formations and tourmalinites.

Garnets in cotiules vary in grain size from a few hundred microns to greater than 1 cm in diameter (Fig. 6a-c). Garnets in cotiules metamorphosed to upper amphibolite and granulite facies tend to be coarser, due to the effects of recrystallization. In undeformed to weakly deformed rocks at the Bleikvassli Zn-Pb-(Cu) deposit, Norway, fine-grained garnets (<1 mm diam) can form laminations in quartz horizons of varying thickness (up to 1 m). Primary structures, such as crossbedding and graded bedding, have been observed in rocks metamorphosed even to the granulite facies (e.g., Broken Hill, Australia).

The mineralogy of cotiules associated with metamorphosed ore deposits consists primarily of quartz and garnet,

with or without accompanying muscovite, biotite, chlorite, amphibole, gahnite, feldspar, carbonate, aluminosilicates, pyroxenoids, apatite, scheelite, tourmaline, and sulfides. Accessory minerals include cordierite, epidote, staurolite, titanite, zircon, fluorite, and ilmenite. Graphite is absent from cotiules, unlike tourmalinites where it is relatively common, suggesting deposition of the cotiules under relatively oxidizing conditions. Mineral inclusions in garnet vary but consist predominantly of quartz. Rare carbonate inclusions have also been documented in garnet (e.g., the Sullivan deposit), thereby suggesting a Mn carbonate or rhodochrosite precursor for the Mn component (Slack et al., 2000).

Garnets in cotiules consist predominantly of spessartine-almandine solid solutions. However, extensive solid solutions with the pyrope and grossular molecules have also been documented (e.g., from the Broken Hill deposit,

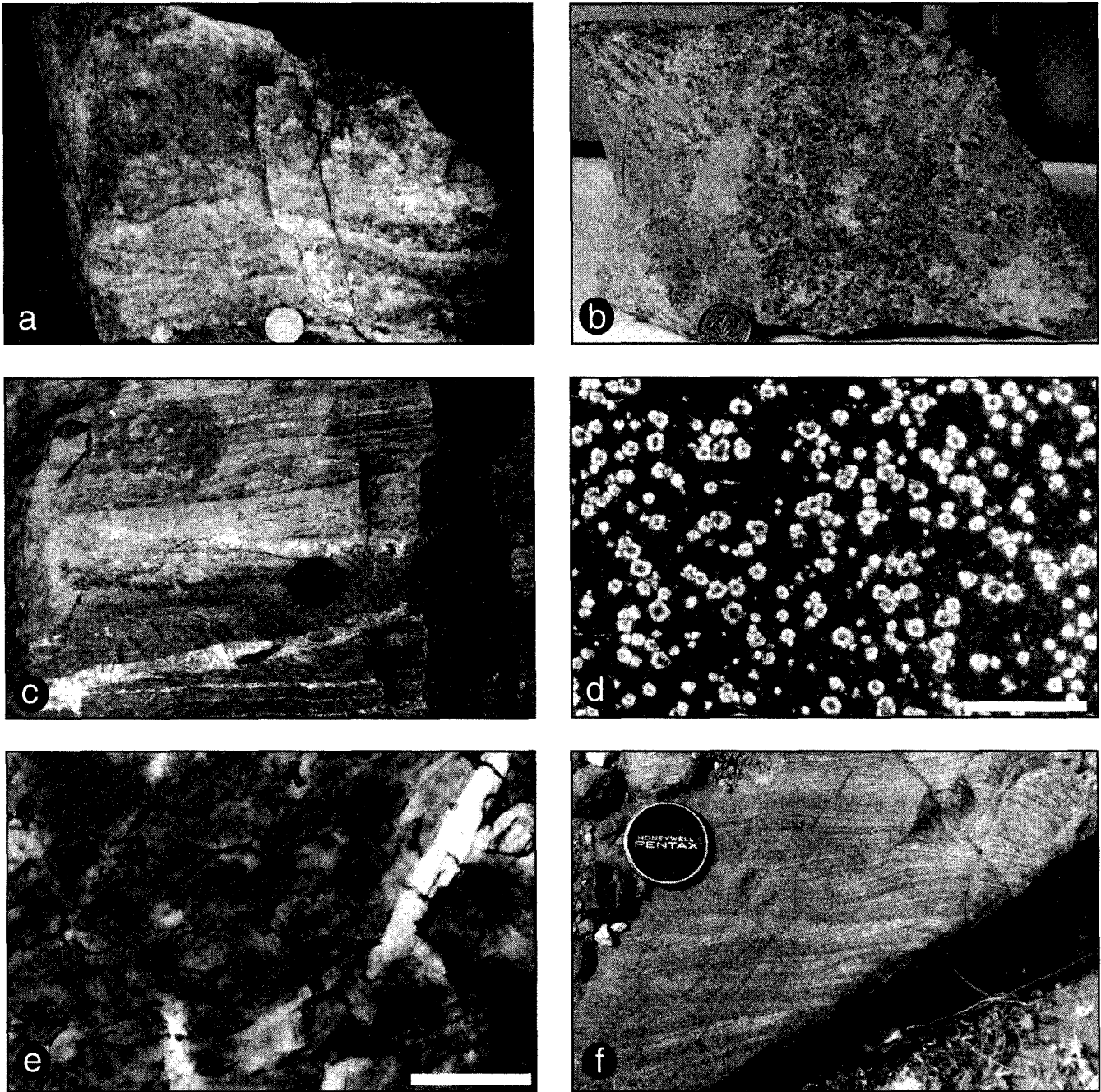


FIG. 6. Photographs of coticules and tourmalinites. a. Coticule (quartz-garnetite) along strike from the northern end of the Bleikvassli deposit, Norway. b. Garnetite crosscut by coarse-grained coticule (quartz-garnetite) from 3 lens, Broken Hill deposit, Australia. c. Coticule (quartz-garnetite) in contact with magnetite iron formation (bottom) from the Big Syncline deposit, Aggeney, South Africa. The lens cap is sitting on the iron formation near the contact. d. Photomicrograph (plane-polarized light) of garnet grains in tourmalinite from the footwall of the Sullivan deposit, Canada. Note that the cores of garnet grains consist of tourmaline. Scale bar = 2.3 mm. e. Photomicrograph (plane-polarized light) of interlocking grains of tourmaline in tourmalinite in the Villa Rica area, western Georgia. Scale bar = 1 mm. f. Crossbeds in tourmalinite from the Silver King East mine, Broken Hill, Australia.

Australia—Spry and Wonder, 1989; and Spry, 1990; and from the Aggeneys area, South Africa—Spry, 1988). The compositional variations in garnet in these deposits reflect changes in Eh, pH,  $f_{\text{CO}_2}$ , fluid/rock ratios, and metal contents during the precipitation of precursor minerals, such as rhodochrosite, carpholite, todorokite, birnessite, nontronite,  $\text{Fe}(\text{OH})_2$ , and  $\text{Fe}(\text{OH})_3$ .

The garnets locally show compositional zoning but are less well zoned than garnets in spatially associated schists and gneisses. Some garnet overgrowths at Broken Hill are the result of a late metasomatic overgrowth on an early-formed metamorphic garnet (Spry and Wonder, 1989). Bodon (1998) described a similar textural relationship for garnet in the Cannington deposit, Queensland.

### Geochemistry

Geochemical studies of cotiules have, in large part, been restricted to acquisition of major and trace (including rare earth) element compositions. A limited review of major and trace element studies of cotiules spatially associated with base metal sulfide occurrences was made by Spry (1990); however, several substantial geochemical studies of cotiules have been completed since that review (e.g., Parr, 1992; Slack et al., 2000). Representative bulk-rock compositions are given by Wonder et al. (1988), Lottermoser (1989), Spry and Wonder (1989), Parr (1992), Bjerkgård and Bjørlykke (1996), and Slack et al. (2000).

The few stable isotope data obtained on cotiules are sulfur isotope analyses collected as part of larger studies of spatially related massive sulfide deposits. The sulfur isotope compositions fall within the range of values reported for the associated massive sulfides and suggest a common origin (e.g., Spry, 1988; Parr, 1992).

**Major elements:** Cotiules show variable contents of  $\text{SiO}_2$  (31.3–94.3 wt %),  $\text{Al}_2\text{O}_3$  (1.3–21.1 wt %),  $\text{Fe}_2\text{O}_3$  (0.8–37.4 wt %),  $\text{MnO}$  (0.2–18.2 wt %),  $\text{FeO}$  (2.1–27.2 wt %),  $\text{CaO}$  (0.2–17.3 wt %),  $\text{MgO}$  (0.1–4.0 wt %), and  $\text{TiO}_2$  (0.0–1.3 wt %). Concentrations of alkalis, halogens,  $\text{H}_2\text{O}$ , and  $\text{CO}_2$  are generally less than 2 wt percent.

Various discrimination diagrams have been used to assist interpretation of source environments and evaluate hydrothermal, hydrogenous, and pelagic contributions to cotiule-forming precursors (e.g., Wonder et al., 1988; Spry, 1990; Cornell et al., 1996). However, many such diagrams involve silica versus alumina and should be avoided. This is because coupled data for oxides constituting a major proportion of the rock, as is the case with  $\text{SiO}_2$  and  $\text{Al}_2\text{O}_3$ , are strongly affected by statistical closure and can be misleading (Slack et al., 1993b, 2000). Furthermore,  $\text{SiO}_2$ -based discrimination diagrams do not distinguish between detrital and hydrothermal sources of silica.

A plot of  $\text{TiO}_2$  versus  $\text{Al}_2\text{O}_3$  by Slack et al. (2000) shows strong correlations among tourmalinites, cotiules, and unaltered metasedimentary host rocks at the Sullivan and nearby North Star deposits, British Columbia (Fig. 7).

These correlations were believed (Slack et al., 2000) to reflect similar processes of detrital sedimentation for clays, ilmenite, and rutile for the three lithologies, and therefore support a major detrital contribution to the tourmalinites and cotiules. A comparable scenario was envisioned (Slack et al., 1993b) for protoliths of cotiules, tourmalinites, and pelitic schists in the Broken Hill district, where a strong correlation between  $\text{TiO}_2$  and  $\text{Al}_2\text{O}_3$  occurs for each of these rock types. A plot of  $\text{TiO}_2$  versus  $\text{Al}_2\text{O}_3$  for metasedimentary rocks and cotiules at Broken Hill is shown in Figure 8a. A much weaker correlation is observed between  $\text{TiO}_2$  and  $\text{Al}_2\text{O}_3$  for cotiules from the Aggeneys district (Fig. 8b), primarily due to  $\text{TiO}_2$  contents close to detection limits (0.02 wt %  $\text{TiO}_2$ ). These  $\text{TiO}_2$ - $\text{Al}_2\text{O}_3$  plots demonstrate that cotiules and tourmalinites contain a substantial detrital component, and that previous models that relied only on exhalative processes are invalid.

Molar element ratios normalized to molar Al can also be useful in identifying the origin of cotiule. Slack et al. (1993b) used this approach for Broken Hill cotiules and found them to be enriched in Si, Fe, Mn, and Ca relative to unaltered clastic metasediments of the district (cf. Slack and Stevens, 1994). In a similar way, Slack et al. (2000) evaluated protoliths of cotiules at the Sullivan and North Star deposits, British Columbia, and found enrichments of these same elements (except Si), together with B and several metals. These results were interpreted (Slack et al., 1993b, 2000) in terms of a hydrothermal source for the Fe and Mn, while the Ca and Mn data were considered to support abundant carbonate in precursors to the cotiules.

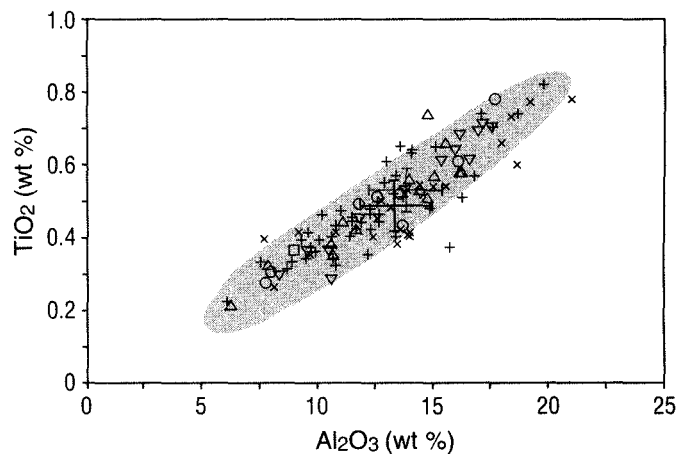


FIG. 7. Variation in  $\text{Al}_2\text{O}_3$  versus  $\text{TiO}_2$  for tourmalinites and cotiules from the Sullivan, North Star, and Stemwinder deposits, Canada. The large black cross shows mean compositions and one standard deviation for all analyzed tourmalinites exclusive of cotiules ( $\text{Al}_2\text{O}_3 = 13.30 \pm 3.06$  wt %;  $\text{TiO}_2 = 0.50 \pm 0.14$  wt %;  $n = 72$ ); the large gray cross shows mean and one standard deviation for unaltered clastic metasedimentary rocks of the lower and middle Aldridge Formation ( $\text{Al}_2\text{O}_3 = 13.82 \pm 3.24$  wt %;  $\text{TiO}_2 = 0.54 \pm 0.12$  wt %;  $n = 92$ ); + = Sullivan shallow footwall tourmalinites; x = Sullivan deep footwall tourmalinites;  $\Delta$  = Sullivan hangingwall tourmalinites;  $\square$  = Stemwinder tourmalinites;  $\nabla$  = North Star tourmalinites;  $\circ$  = Sullivan and North Star cotiules (from Slack et al., 2000, fig. 10).

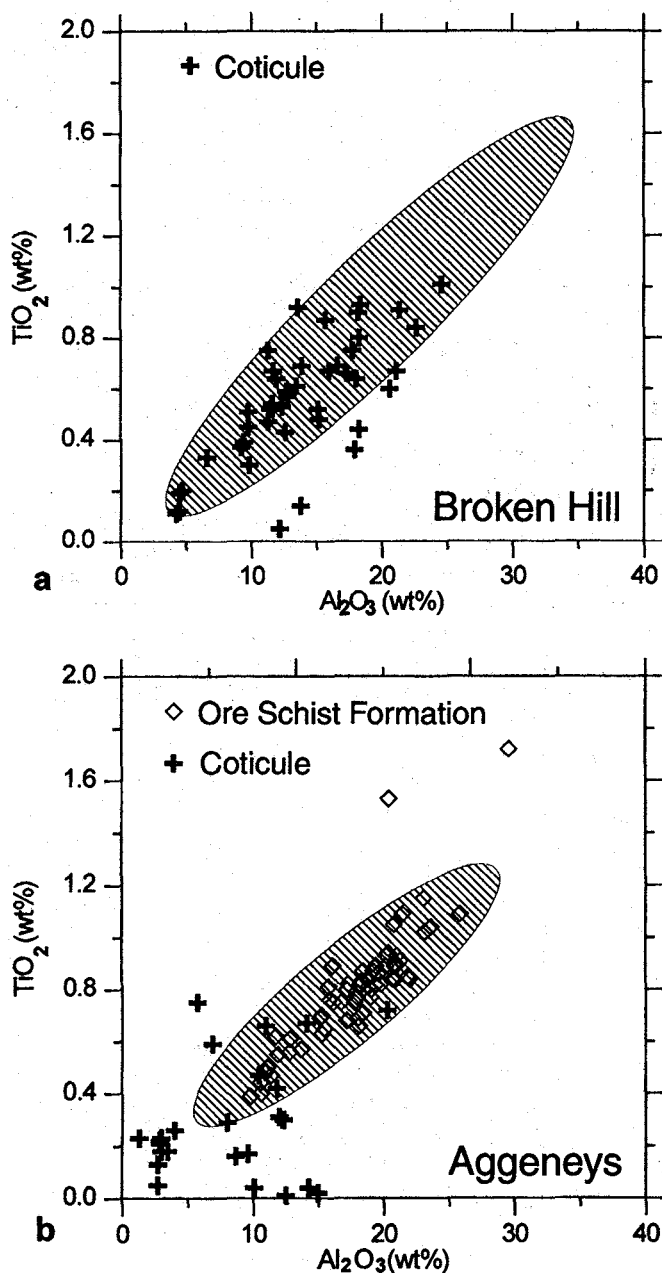


FIG. 8.  $\text{Al}_2\text{O}_3$  versus  $\text{TiO}_2$  plot for metasedimentary rocks and coticles from a. Broken Hill, Australia, and b. Aggeneys, South Africa. The compositions of coticles from Broken Hill, Australia, are from Spry (1978), Elliot (1979), Wiggins (1990), and Slack (1993b), whereas the shaded field outlining the compositions of clastic metasediments derived from the Broken Hill area was compiled by CRA Exploration Pty. Ltd (Main et al., 1983). The compositions of coticles from the Aggeneys area are from this study, Lipson (1990), and Hoffman (1993). The shaded area outlines the compositions of clastic metasediments in the Ore Schist Formation hosting the Aggeneys deposits that were determined by Lipson (1990). The poor correlation between the Ore Schist Formation and coticles likely suggests contributions of clastic components from schist horizons in the immediate stratigraphic footwall (e.g., Namies schist and Shaft schist) and the hanging wall (e.g., Hanging-wall schist).

Iron and Mn in marine sediments are derived predominantly from hydrothermal sources, whereas Al is of detrital origin and is added to the sediment by clay minerals (Boström, 1973b; Peter and Goodfellow, 1996a). Figure 9 is a ternary Fe-Al-Mn plot of coticle compositions showing a broad scatter of data that suggests mixtures of hydrothermal and nonhydrothermal components to coticle protoliths.

These same data are plotted as a function of Fe/Ti versus  $\text{Al}/(\text{Al} + \text{Mn} + \text{Fe})$  to indicate the relative contributions of terrigenous clastic and/or pelagic sediment and hydrothermal components (Fig. 10). Most of the data have Fe/Ti less than 200 and  $\text{Al}/(\text{Al} + \text{Fe} + \text{Mn})$  greater than 0.2, suggesting an input of up to 70 percent hydrothermal component in metalliferous sediment, with the remainder being detrital terrigenous and/or pelagic sediment. Some samples from Broken Hill (Australia) appear to have little or no component of metalliferous hydrothermal sediment, based on values of Fe/Ti less than 20 and  $\text{Al}/(\text{Al} + \text{Fe} + \text{Mn})$  greater than 0.6. Although plots of this type have not previously been used to evaluate the compositions of clay minerals, it is possible that nine of the Bleikvassli data points fall above the hydrothermal component-terrigenous clastic and/or pelagic sediment mixing curve because the precursor clay mineral in the nonhydrothermal component was predominantly montmorillonite.

Theye et al. (1996) showed that the precursor to spessartine in the Lienne syncline, Venn-Stavelot massif, Belgium, was a carpholite  $((\text{Fe}^{2+}, \text{Mn}^{2+}, \text{Mg})(\text{Al}, \text{Fe}^{3+})_2[\text{Si}_2\text{O}_6](\text{OH}, \text{F})_4)$  group mineral. Utilizing compositional data of carpholite from Theye et al.'s (1998, Table 2) study, average values of  $\text{Fe}/\text{Ti} = 8.22$  and  $\text{Al}/(\text{Al} + \text{Mn} + \text{Fe}) = 0.68$  are obtained. These values are very similar to those shown for the average composition of terrigenous sediment at the end of the mixing curve in Figure 10. Whether carpholite is a common precursor to spessartine remains uncertain; however, the field and experimental evidence of Theye et al. (1998) support the concept that it may be important in the formation of coticles. It should be stressed herein that carpholite is just one of several possible precursor minerals. Other such minerals include, for example, rhodochrosite and manganosiderite, which have been proposed as possible Mn-bearing precursor minerals to coticles elsewhere in the Venn-Stavelot massif and the Sullivan deposit by Schreyer et al. (1992) and Slack et al. (2000), respectively.

**Rare earth elements:** Chondrite-normalized REE patterns for coticles (Figs. 11 and 12) are very similar to those for iron formations (Fig. 2) in that both types of meta-exhalites are generally enriched in light REE and depleted in heavy REE. Coticles, like iron formations, may also display small negative Ce anomalies as well as positive or negative Eu anomalies. Rare earth element data for the Sullivan and North Star deposits, British Columbia, show light REE enrichment, heavy REE depletion, and negative Eu anomalies relative to chondrites (Fig. 11a; Slack et al., 2000). Sample JS-81-72B, a pyrrhotite- and biotite-rich coticle from the footwall of the Sullivan deposit, exhibits a positive Eu anomaly. The fact that REE patterns for the

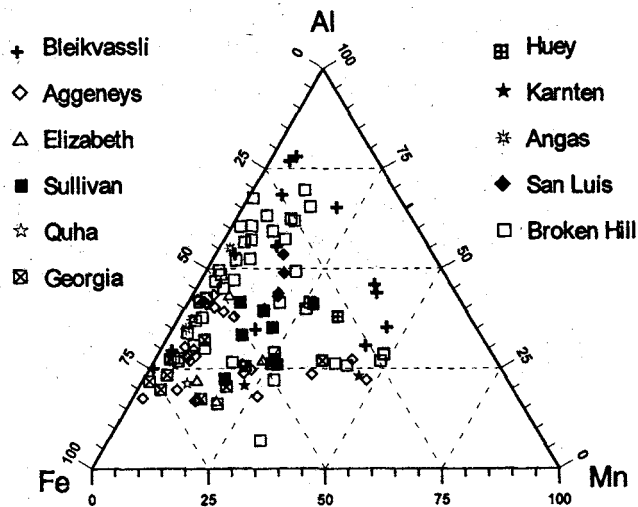


FIG. 9. Al-Fe-Mn ternary plot for coticules: Broken Hill, Australia (Spry, 1978; Elliot, 1979; Spry and Wonder, 1989; Wiggins, 1990); Aggeneys, South Africa (Lipson, 1990; Hoffman, 1993; this study); Elizabeth, Vermont (this study); Sullivan, Canada (Slack et al., 2000); San Luis, Argentina (Fernández et al., 1994); Bleikvassli (Skauli, 1990; this study); Quha River prospect, South Africa (Cornell et al., 1996); western Georgia (Wonder et al., 1988); Huey deposit, Virginia (Gair and Slack, 1984); Karnten deposit, Austria (Williams and Manby, 1987); and Angas deposit, Australia (McElhinney, 1994).

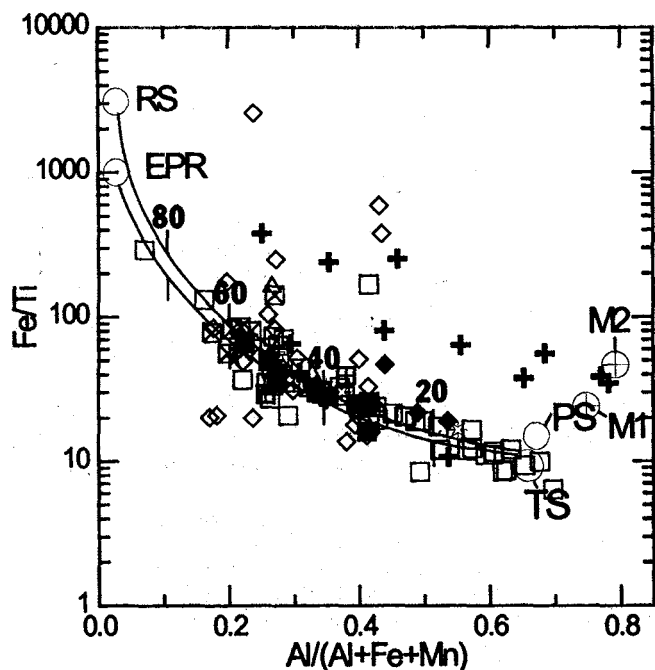


FIG. 10. Al/(Al + Fe + Mn) versus Fe/Ti plot of coticules. Symbols and locations are as in Figure 9. Curves are theoretical mixing lines between metalliferous sediment from the East Pacific Rise (EPR) and Red Sea (RS), with terrigenous sediment (TS) and pelagic sediment (PS). Numbers along curves represent approximate amount of metalliferous sediment within the mixtures. Modified from Barrett (1981) and Spry (1990). The composition of two montmorillonites (M1 and M2) taken from Grim and Kulbricki (1961) are also included (circle over a cross).

coticules are essentially the same as those of unaltered Aldridge metasedimentary rocks (hachured), that host the Sullivan and North Star deposits, suggests a detrital input to the coticules. Based on their geochemical data, and on the occurrence of carbonate inclusions in some of the coticule garnets, Slack et al. (2000) postulated that the protolith to the Sullivan and North Star coticules included a significant proportion of manganosiderite.

As noted by Peter and Goodfellow (1996a) and in the above discussion of iron formations, greater than ca. 30 wt percent detritus in the depositional environment of the coticules should produce enriched light REE and depleted heavy REE patterns and a negative Eu anomaly. Such negative Eu anomalies are common in coticules and suggest a large detrital component. The Fe/Ti versus Al/(Al + Mn + Fe) data shown in Figure 10 support a minimum of 30 wt percent detritus in the source environment. The possibility that a significant contribution of detritus is present in the precursors to coticules is also supported by plots of  $TiO_2$  versus  $Al_2O_3$  for the Broken Hill (Australia) and Aggeneys areas (Figs. 8a and b), as well as by similarity in the REE patterns of coticules and associated metasedimentary rocks in the Pinnacles area (Fig. 12a).

Assuming that metamorphism does not alter the REE pattern of coticules (e.g., Lottermoser, 1988, 1989; Parr, 1992), the presence of small, negative Ce anomalies in some samples from the Elizabeth (Fig. 11b), San Luis (Fig. 11d), and Pinnacles (12a) deposits shows varying inputs of seawater to the fluids responsible for the formation of the coticules. Positive Eu anomalies occur in coticules from the Sullivan, Pinnacles, Broken Hill, and Aggeneys deposits, suggesting contributions from high-temperature, reduced hydrothermal fluids (Sverjensky, 1984; Peter and Goodfellow, 1996a). Lottermoser (1988, 1989) showed that exhalites (e.g., iron formation, coticules, quartz-gahnite rocks), are enriched in  $Eu^{2+}$  with proximity to sulfide zones in the Broken Hill area, Australia (see coticule sample 5, Fig. 12c), and depleted in  $Eu^{2+}$  from distal localities. This relationship was interpreted (Lottermoser, 1989) as reflecting higher temperatures in the hydrothermal fluid and lower detrital input to the protolith of proximal coticules, compared with distal coticules where the hydrothermal fluid had a lower temperature and the detrital input was higher.

#### Tourmalinites

Tourmalinites are volumetrically minor rocks that occur in close association with many types of exhalative mineral deposits. Following Nicholson (1980) and Slack et al. (1984), tourmalinites are defined as strata-bound rocks that contain in excess of 15 to 20 percent tourmaline by volume. Many workers in Europe, and others elsewhere, have used the term tourmalinite to refer to discordant tourmaline-rich veins (i.e., postprimary) and breccias, but this usage is not adopted here. In the following sections, descriptions and interpretations of tourmalinites are restricted to occurrences that are closely associated with clearly exhalative deposits and/or chemical sediments (Table 4). We have also included in our discussion tour-

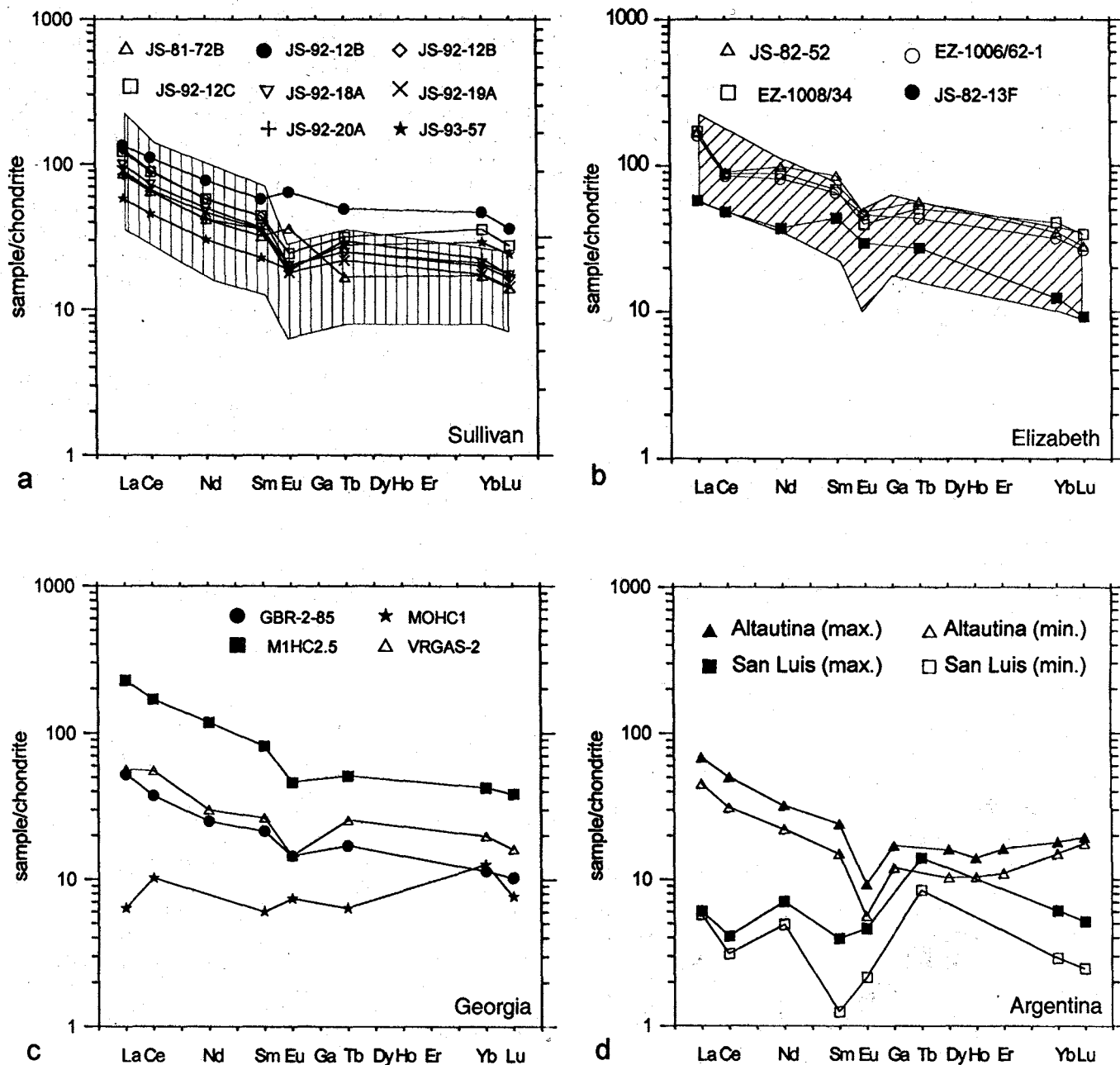


FIG. 11. Chondrite-normalized (Rock, 1988) rare earth element plots for cotiules. a. Sullivan, British Columbia; shaded field outlines abundances for typical unaltered clastic metasediments of the lower and middle Aldridge Formation (Slack et al., 2000). b. Elizabeth deposit, Vermont (Slack, unpub. data); shaded area represents the compositional field of Gile Mountain metasedimentary rocks (45 samples) that enclose the deposit (Slack, 1994). c. Western Georgia (Wonder et al., 1988). d. Altautina and San Luis, Argentina (Fernández et al., 1994); the maximum and minimum compositions of cotiules in both localities are indicated.

malinites that occur as discordant zones in the footwall of the vent complex of the Sullivan deposit. Tourmalinites related to strata-bound and/or stratiform rocks, unrelated to ore-forming processes, that formed by syn- or postmetamorphic replacement processes were discussed in detail by Slack (1996) and are not repeated herein.

Studies of tourmalinites associated with massive sulfide deposits suggest that boron-rich rocks form both by exhalative activity and subsea-floor replacement (e.g., Slack et al., 1993b; Slack, 1996). Tourmalinites that originated through each process are described below, since both types may be associated with exhalative mineral deposits.

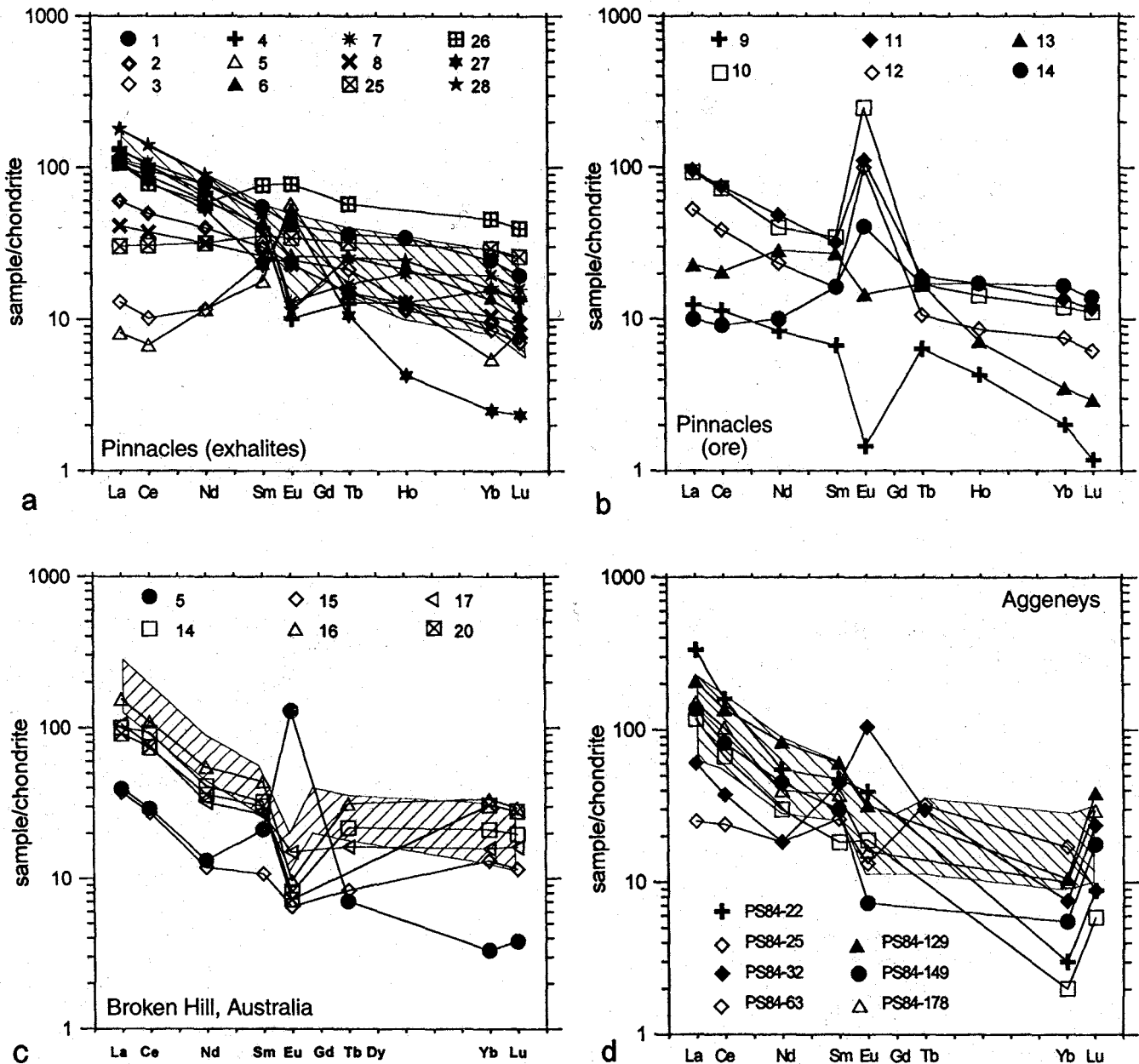


FIG. 12. Chondrite-normalized (Rock, 1988) rare earth element plots. a. Coticules from Pinnacles, Australia (Parr, 1992); shaded area represents the compositional field of metapelites from the Pinnacles mine stratigraphy from Parr (1992). b. Ore from Pinnacles (Lottermoser, 1989). c. Coticules from Broken Hill, Australia (Lottermoser, 1989); shaded area represents Broken Hill clastic metasedimentary rocks (Slack and Stevens, 1994). d. Coticules from Aggeneys, South Africa.

Because it is advantageous in exploration to distinguish exhalative tourmalinites from those formed by replacement (Slack, 1993b, 1996), various discriminating criteria are presented.

*Geology and petrography*

Tourmalinites are most common in siliciclastic meta-sedimentary sequences (Slack et al., 1984). These sequences typically comprise metamorphosed shale, schist, gneiss,

and lesser sandstone or graywacke, with variable amounts of interbedded metabasalt; rhyolites or related felsic metamorphosed igneous rocks generally are not abundant. Tourmalinites may be interbedded with chert, coticule, iron formation, and carbonates or calc-silicate rocks. Rift-type tectonic settings are common. In such settings, clastic sediments and evaporites serve as the chief sources of the boron through convective leaching by circulating hydrothermal fluids (Slack, 1982; Palmer and Slack, 1989).

TABLE 4. Geologic Setting of Selected Tourmalinite Localities

Deposit-district	Age	Geologic setting	Metals	Associated exhalites	References
Bergslagen, Sweden	Proterozoic	Mrhy, Mbas, Cmsd, Mcar	Pb, Zn, Ag	Iron formation, coticule	1
Sierras Pampeanas Orientales, Argentina	Proterozoic	Cmsd	W	Coticule	2
Western Georgia	Early Paleozoic	Cmsd, Mbas	Cu, Zn	Coticule, iron formation	3
Pegmont, Australia	Proterozoic	Cmsd	Pb, Zn	Iron formation, coticule	4
Sullivan, Canada	Proterozoic	Cmsd, Mbas	Pb, Zn	Coticule	5, 6
Broken Hill, Australia	Proterozoic	Cmsd, Mrhy, Mbas	Pb, Zn, Ag, W	Coticule, iron formation, quartz-gahnite rock	7, 8
Elizabeth, Vermont	Ordovician	Cmsd, Mbas	Cu, Zn	Coticule	9
Aggeneys, South Africa	Proterozoic	Cmsd, Mrhy	Pb, Zn, Cu	Iron formation, coticule	10
Western Greenland	Archean	Mbas	W	Iron formation	11
Leinster, Ireland	Siluro-Devonian	Cmsd, Gran	Au	Coticule	12
Eastern Alps, Austria	Ordovician-Carboniferous	Cmsd, Mbas	W		13
Nagpur, India	Proterozoic	Cmsd, Mbas	Cu, Zn		14
Bagdad, Arizona	Proterozoic	Mrhy, Mbas	Cu, Zn		15
Bottino, Italy	Siluro-Ordovician	Cmsd, Mrhy	Pb, Zn, Ag		16

Notes: Abbreviations: Cmsd = clastic metasediments (e.g., pelitic schist), Gran = granite or felsic porphyry, Mbas = metabasalt (greenstone, amphibolite), Mcar = metacarbonate, Mgab = metagabbro and metadiorite, Mrhy = metarhyolite

References: 1, Hellingwerf et al. (1994); 2, de Brodtkorb et al. (1995); 3, Wonder et al. (1988); 4, Plimer (1988b); 5, Hamilton et al. (1982); 6, Slack et al. (2000); 7, Slack et al. (1993b); 8, Plimer (1987); 9, Slack et al. (1993a); 10, Wilner (1992); 11, Appel and Garde (1987); 12, McArdle et al. (1989); 13, Raith (1988); 14, Bandyopadhyay et al. (1993); 15, Conway (1986); 16, Benvenuti et al. (1989)

Textural features of tourmalinites vary widely as a function of setting and superimposed metamorphism. In undeformed and weakly metamorphosed terranes (lower greenschist facies and below), tourmalinites are extremely fine grained and may resemble dark chert (Ethier and Campbell, 1977; Zhang et al., 1994), whereas in upper greenschist facies through to granulite facies, tourmalinites are coarse grained and display prominent layering defined by alternating quartz and tourmaline bands (Fig. 6d and e). Primary sedimentary structures are preserved within some tourmalinites, including those in high-grade metamorphic terranes (Fig. 6f), as well as multiple generations of folds (see Slack et al., 1984, 1993b).

Quartz and subequal tourmaline, with or without accompanying feldspar, mica, chlorite, garnet, apatite, graphite, and sulfides dominate the mineralogy of tourmalinites. Accessories may include zircon, titanite, rutile, ilmenite, allanite, monazite, and epidote. Oxidized species such as hematite and barite are unknown. The occurrence of graphite in many tourmalinites, and the uniform lack of highly oxidized minerals, imply deposition under reducing conditions in an anoxic basin or in subsurface pore waters.

#### Origin

Recent geologic and geochemical studies suggest that tourmalinites form both by replacement of aluminous sediments or volcanic rocks and by exhalation in brine pools (Slack, 1993b; Slack et al., 1993b). Tourmalinites form by

replacement in submarine-hydrothermal systems beneath the sediment- (or volcanic-) water interface, and in primary feeder zones of proximal deposits such as at the Sullivan Pb-Zn-Ag mine, British Columbia, where tourmalinites occur in a discordant, funnel-shaped pipe that extends more than 450 m below the stratiform ores (Hamilton et al., 1982; Turner et al., 1993; Slack et al., 2000). Some tourmalinites result from replacement of aluminous rocks during contact and regional boron metasomatism (e.g., Slack, 1996), but these occurrences will not be discussed.

Recent models for the formation of stratiform tourmalinites require the interaction of B-rich fluids with permeable aluminous sediments or volcanic rocks. These models involve a local (internal) source of Al in the spatially associated sediments, due to the limited solubility of Al in aqueous solutions at low to moderate temperature (200–400°C) and moderate pH (6–8; Slack, 1993b). In many cases, the major element composition of the tourmalinites simply requires the introduction of B, but in other cases Si, Fe, Mg, Mn, and/or P may also be introduced; Ca, K, Na, and trace elements such as Ba, Rb, and Cs are commonly depleted (e.g., Slack, 1996; Slack et al., 2000). Relative enrichment in Fe (excluding Fe in sulfides), Mn, and/or P appears to be characteristic of exhalative tourmalinites (Slack et al., 1993b), these elements being added to sea-floor sediments or felsic volcanic rocks through syngenetic precipitation, typically in a saline brine pool. However, if this type of exhalative transformation of aluminous sediments or volcanic rocks is to form

tourmalinites, it requires diagenetic replacement of detrital clay, feldspar, and/or chlorite by reaction with hot B-rich brines on or near the sea floor (Slack, 1996). Recent studies by Slack et al. (1998) suggest that boron-rich mud volcanoes of the Black Sea south of the Crimean Peninsula may be modern analogues to tourmalinites associated with Sullivan-type deposits.

### *Geochemistry*

For space reasons, whole-rock compositions of tourmalinites associated with hydrothermal ore deposits are not given here. However, representative compositions are available in, for example, Annis et al. (1983), Plimer (1987), Slack et al. (1993b, 2000), and Slack (1996). Whole-rock geochemical analyses show that the contents of many minor, trace, and rare earth elements in tourmalinites largely match those of their respective host rocks. In most cases, tourmalinites are contained within clastic metasediments, the latter displaying broad correlations of compositional data for selected major elements, and strong correlations for relatively immobile minor and trace elements such as Ti, Cr, Zr, Nb, Th, and REE (e.g., Sawyer, 1986; Slack and Stevens, 1994). Such correlations for clastic metasediments are widely accepted as mixing lines between primary quartz-rich and clay-rich end-members, due to sorting and other sedimentary processes that occurred during transport and deposition of the sediments. Similarity in correlations between relatively immobile trace elements in the metasediments and tourmalinites reflects a detrital component in the latter, presumably inherited from the clastic sedimentary protoliths of the tourmalinites (Bandyopadhyay et al., 1993; Slack et al., 1993b; Slack, 1996). Rhyolitic volcanic rocks also may be protoliths to tourmalinites in some cases, such as those associated with massive sulfide deposits of the Bagdad district in Arizona (Conway, 1986), the Bieluwutu prospect in China (Nie, 1993), and the Bergslagen district in Sweden (Hellingwerf et al., 1994); some tourmalinites in the Broken Hill district of Australia, particularly those in contact with the felsic metavolcanic Hores Gneiss, may have a rhyolitic volcanic precursor (Slack et al., 1993b; Fig. 6). One of the few known basaltic protoliths to tourmalinites is found at the Elizabeth massive sulfide deposit in Vermont, where a strata-bound quartz-albite-tourmaline gneiss has a geochemical signature that matches that of associated tholeiitic amphibolites, but not that of surrounding clastic metasediments (Slack et al., 1993a).

The formation of tourmalinites generally involves some net mass change. Mass losses are most common, due to the characteristic removal of substantial Ca, K, and Na from precursor sediments or volcanic rocks during tourmalinization. A small to moderate volume loss may be associated with the mass loss. Evaluation of mass and volume changes during the formation of tourmalinites requires whole-rock geochemical data for relatively immobile elements (e.g., Slack, 1996; Slack et al., 1996, 2000). Evaluation is complicated, however, by the typically clastic sedimentary protoliths of many tourmalinites.

Such protoliths inherently have large statistical uncertainties in their mean compositions, due to variation in primary sand/clay ratios. Calculations of absolute mass change in the formation of tourmalinites therefore are not meaningful, but calculations of relative change are acceptable. This can be achieved by determining gains or losses of elements by normalizing data for individual elements to the average Al content of each tourmalinite, and in turn to the Al-normalized average for the inferred unaltered protolith (Slack, 1996). The nature and degree of the mass change depend on factors such as fluid composition, pH, and the time-integrated fluid/rock ratio. Large mass losses are characteristic of the high fluid/rock environment of tourmalinized feeder zones, in contrast to the formation of exhalative tourmalinites that tend to show little or no mass loss (Slack, 1996; Slack et al., 2000).

Slack et al. (1993b) proposed that elevated contents of Fe (nonsulfide), Mn, and/or P in tourmalinites are indicative of an exhalative origin. This hypothesis rests on the concentrations of these elements measured in modern sea-floor deposits such as the metalliferous sediments of the Pacific Ocean and the Red Sea deeps, and in ancient banded iron formations. Figure 13 shows the compositions of selected stratiform tourmalinites, on a whole-rock (weight) basis, compared to those of modern oceanic sediments and metalliferous deposits. Most of the tourmalinites have Fe/Ti less than 15 and Al/(Al + Fe + Mn) greater than 0.6, indicating little or no component of metalliferous hydrothermal sediment. However, such tourmalinites are not necessarily excluded from having an exhalative origin; field relationships, including the spatial association of tourmalinites to sulfides and other meta-exhalites, are critical. Tourmalinites that have Fe/Ti greater than 15 and Al/(Al + Fe + Mn) less than 0.6 include three each from the Broken Hill district in New South Wales and the Sullivan deposit in British Columbia (Slack et al., 1993b; 2000), and one each from the Bottino district in Italy (Benvenuti et al., 1989), the Nagpur district in India (Bandyopadhyay et al., 1993), the Bieluwutu deposit in China (Nie, 1993), the Tisová deposit in the Czech Republic (Pertold et al., 1994), and the Morning Glory prospect in Montana (Slack, 1996). Four of these tourmalinites (Broken Hill, Sullivan, Morning Glory, Tisová) have 22 to 30 percent metalliferous sediment component, with the remainder being detrital terrigenous and/or pelagic sediment. Note that the estimates of the relative input of metalliferous sediment component and detrital terrigenous and/or pelagic sediment component are maintained notwithstanding the possibility of a small amount (<5%) of detrital Fe and Mn.

The compositions of tourmalines in relatively unmetamorphosed and metamorphosed exhalative mineral deposits and tourmalinites are a function of several parameters including (Slack and Coad, 1989; Slack 1996) the chemistry of their host rocks and hydrothermal fluids and the time-integrated fluid/rock ratio. In more strongly metamorphosed mineral deposits (amphibolite facies and higher), the compositions of tourmaline may also reflect

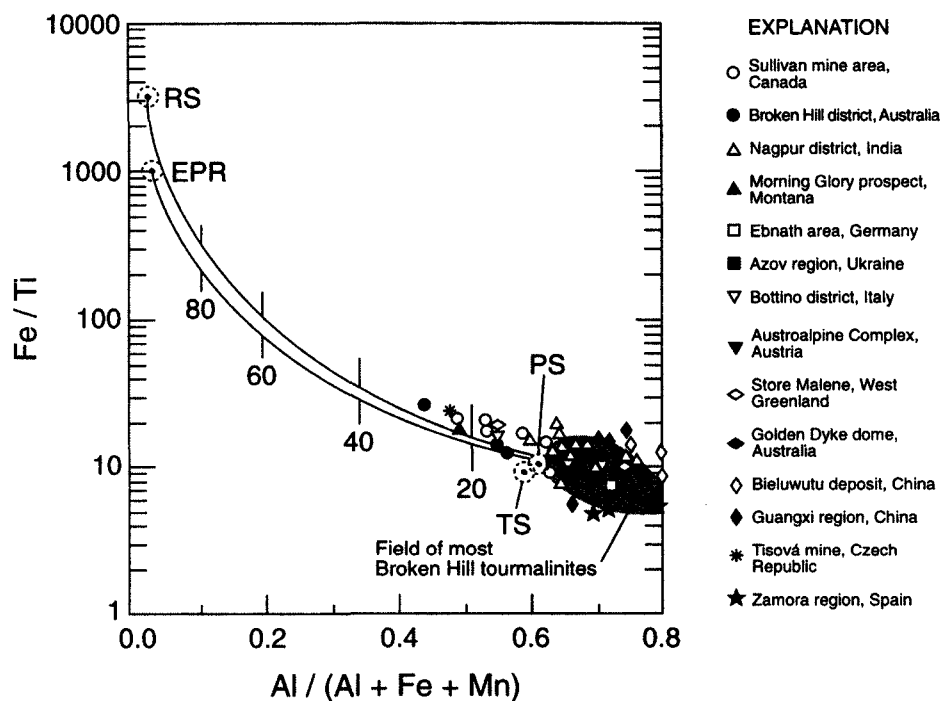


FIG. 13. Bulk compositions of stratiform tourmalinites of potential exhalative origin, shown in terms of Fe/Ti versus Al/(Al + Fe + Mn), on a weight percent basis (see Figure 10 caption). Data sources: Sullivan mine area, British Columbia (Slack et al., 2000); Broken Hill district, Australia (Slack et al., 1993b); Nagpur district, India (Bandyopadhyay et al., 1993); Morning Glory prospect, Montana (Slack, 1996); Ebnath area, Germany (Abraham et al., 1972); Azov region, Ukraine (Serdyuchenko, 1977); Bottino district, Italy (Benvenuti et al., 1989); Austroalpine complex, Austria (Raith, 1988); Store Malene area, west Greenland (Appel and Garde, 1987); Golden Dyke dome, Northern Territory, Australia (Plimer, 1986); Bieliwutu deposit, China (Nie, 1993); Guangxi region, China (Mao, 1995); Tisová mine, Czech Republic (Pertold et al., 1994); Zamora region, Spain (Fernández Fernández and Moro Benito, 1992). Note that the compositional field for most Broken Hill tourmalinites (from Slack et al., 1993b) excludes data points for three samples that are shown separately.

sulfide-silicate reactions in which tourmaline, in equilibrium with pyrite and/or pyrrhotite, has formed Mg-rich discordant rims or individual grains (Taylor and Slack, 1984; Slack and Coad, 1989), or developed recrystallized, compositionally homogeneous grains (Slack et al., 1993b). If the fluid/rock ratio is low, the bulk composition of the host rock is most important, such as in the Broken Hill district (Australia) where tourmalines have high Fe contents inherited from their clastic metasedimentary country rocks (Slack et al., 1993b; Slack and Stevens, 1994). However, in high fluid/rock settings, such as the feeder zones of the Kidd Creek (Ontario) and Sullivan deposits, compositions of tourmalines are controlled largely by the chemistry of the hydrothermal fluids (Slack and Coad, 1989; Slack et al., 2000). Magnesian tourmalines nevertheless clearly form in submarine-hydrothermal settings, independent of regional metamorphism (Slack, 1996), by entrainment of Mg-rich seawater into the tops and margins of sea-floor hydrothermal systems. Examples include the Sullivan deposit (Ethier and Campbell, 1977; Jiang et al., 1998) and the Yingdongzi and Tongmugou Pb-Zn-Ag deposits, China (Jiang et al., 1995).

#### Isotope data

Isotopic studies of tourmalinites (and tourmalines) from stratiform deposits have focused on the stable isotopes of oxygen, hydrogen, and boron (e.g., Slack, 1996; Jiang, 1998). The first oxygen isotope analyses of tourmalinites were reported by Nesbitt et al. (1984) for samples from the Sullivan Pb-Zn-Ag deposit. They found whole-rock  $\delta^{18}\text{O}_{\text{SMOW}}$  values of 10.7 to 13.1 per mil for six tourmalinites, similar to the range of values obtained for unaltered metasedimentary rocks of the surrounding Aldridge Formation. The data were interpreted by Nesbitt et al. (1984) as indicating a relatively low temperature (<100°C) of formation for the tourmalinites. A more detailed oxygen isotope study of 34 Sullivan area tourmalinites by Seal et al. (2000) reveals a slightly larger range of  $\delta^{18}\text{O}$  values (10.3–14.2‰), but much higher temperatures (250°–300°C) of tourmalinization (see also Beatty et al., 1988). The difference in tourmalinite-forming temperatures results from Nesbitt et al. (1984) not considering the effect of detrital quartz (ca. 40–80 vol %) on the whole-rock  $\delta^{18}\text{O}$  values (quartz preferentially incorporates  $^{18}\text{O}$  relative to tourmaline). Data for tourmaline separates

are preferable, but pure separates are difficult to obtain for very fine-grained tourmalinites like those in the Sullivan area (Ethier and Campbell, 1977; Slack et al., 2000) and other greenschist facies terranes (e.g., Slack, 1996). Hydrogen isotope compositions of tourmalinites are only affected by minerals that contain OH<sup>-</sup> and/or H<sub>2</sub>O other than tourmaline (e.g., micas, amphiboles, chlorites, and clays). Seal et al. (2000) interpreted a large range of whole-rock  $\delta D_{SMOW}$  values of -65 to -27 per mil for Sullivan area tourmalinites, in terms of precipitation mainly from evolved seawater.

Other oxygen and hydrogen isotope analyses for tourmalines related to stratiform mineralization are from tourmaline separates. However, the data were derived from a variety of sample types that were not restricted to exhalative massive sulfide occurrences. Taylor and Slack (1984) reported  $\delta^{18}O_{SMOW}$  and  $\delta D_{SMOW}$  values of 8.5 to 15.5 and -67 to -43 per mil, respectively, for tourmalines from volcanogenic massive sulfide deposits in the Appalachian-Caledonian orogen; they interpreted these data in terms of evolved seawater that had reacted extensively with high-<sup>18</sup>O footwall sedimentary rocks. Tourmaline from the Kidd Creek deposit has somewhat lower values of  $\delta^{18}O_{SMOW}$  (8.2 to 11.2 per mil) and much higher values of  $\delta D_{SMOW}$  (-48 to -13 per mil) that are believed to record early boiling and reaction with <sup>18</sup>O-rich footwall sediments (Taylor et al., 1999). The lower  $\delta D$  values of the Appalachian-Caledonian tourmalines probably are due, at least in part, to incorporation of metamorphic fluids in the tourmaline crystal structure during recrystallization associated with postore deformation and regional metamorphism (Slack, 1996).

Boron isotope studies of tourmalines associated with stratiform mineral deposits have focused on volcanogenic massive sulfide and sedimentary-exhalative deposits. Palmer and Slack (1989) analyzed tourmalines from 60 volcanogenic massive sulfide and sedimentary-exhalative deposits and tourmalinites worldwide, and reported a range of  $\delta^{11}B$  values from -22.8 to 18.3 per mil. They interpreted these data as reflecting the combined influences of boron isotopic compositions of the boron source (e.g., footwall rocks), water/rock ratios, temperatures of tourmaline formation, and metamorphic recrystallization. Detailed studies of tourmalines from the Broken Hill district of Australia (Slack et al. 1989, 1993b) suggest that, despite significant boron isotope fractionation during regional metamorphism, a primary nonmarine evaporite signature is preserved in the  $\delta^{11}B$  values. This interpretation was, in part, constrained by the correlation of  $\delta^{11}B$  with metamorphic textures and grade in the district. Boron isotope data for tourmalines from the Kidd Creek deposit show a  $\delta^{11}B$  range from -13.6 to -7.8 per mil, which probably reflects derivation of the boron from footwall basalts and/or ultramafic rocks (Taylor et al., 1999; see also Slack and Coad, 1989). Although based in part on indirect evidence, this interpretation rests on the known boron isotopic compositions of altered basalts and ultramafic rocks, experimentally determined tourmaline-fluid fractionations, and a calculated temperature of formation for the tourmaline from oxygen isotope data (Taylor et al., 1999). The boron isotope analyses of tourmaline from

volcanogenic massive sulfide and sedimentary-exhalative deposits in the Nagpur district, and Rampura-Agucha and Deri deposits, India, are -13.8 to -13.1 per mil (Bandyopadhyay et al., 1993) and -16.4 to -15.5 per mil (Deb et al., 1997), respectively. These isotope compositions largely record control by their respective footwall lithologies; secondary effects are related to metamorphic recrystallization.

In summary, stable isotope studies of tourmaline in stratiform mineral deposits suggest that the boron is from various footwall lithologies and that the hydrothermal fluids were derived mainly from seawater. With the exception of Broken Hill, which appears to have a nonmarine evaporite component in the district tourmalines, tourmalines from nearly all other massive sulfide deposits seem to have been deposited from evolved seawater. No magmatic water component has been unequivocally documented in any sulfide-related tourmalines studied to date.

### Apatite-Rich Rocks

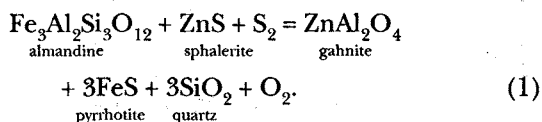
Concentrations of apatite occur in some meta-exhalites. The apatite is either a major component of apatite-rich stratiform units, or a minor component of other types of meta-exhalites, such as iron formations and tourmalinites. Major stratiform Pb-Zn deposits that possess apatite or fluorapatite concentrations include Broken Hill, Australia, and Howards Pass, Yukon Territory. At Broken Hill, fluorapatite occurs in banded magnetite iron formation and accounts for 3.4 to 5.4 wt percent P<sub>2</sub>O<sub>5</sub> on a whole-rock basis (Eeson, 1971). Abundant fluorapatite is also present locally within the Broken Hill deposit, where P<sub>2</sub>O<sub>5</sub> contents reach up to 7.5 wt percent in some samples (Stanton, 1972); the Zn-rich B lode has ca. 2 percent fluorapatite and averages 0.9 wt percent P<sub>2</sub>O<sub>5</sub> (Plimer, 1984). However, the concentration of apatite in other meta-exhalites (i.e., tourmalinite, coticule, iron formation, gahnite-bearing rocks) at Broken Hill is variable. For example, quartz-tourmaline-gahnite-garnet (Slack et al., 1993b) and quartz-tourmaline-apatite tourmalinites (Slack et al., 1996, table 6) contain 0.18 and 3.25 wt percent P<sub>2</sub>O<sub>5</sub>, respectively. In the Howards Pass Pb-Zn deposit, Goodfellow (1984) reported multiple monomineralic fluorapatite laminae (ca. 0.3 cm thick) within a carbonaceous chert unit (up to 50 m thick) that directly overlies the deposit; fluorapatite also occurs interbedded with sphalerite and galena in the upper part of the Pb-Zn zone (W.D. Goodfellow, pers. commun., 1997). The volcanic-hosted massive sulfide deposit at Vihanti, Finland, similarly has an apatite-rich hanging wall unit that contains elevated uranium in uraninite and apatite (Rehtjärvi et al., 1979).

The abundant apatite and fluorapatite associated with some exhalative ores probably records either chemical precipitation in a submarine brine pool or plume fallout. Evidence in support of this hypothesis comes mainly from the Howards Pass deposit, where the P<sub>2</sub>O<sub>5</sub> content of the hanging wall unit decreases laterally away from the deposit and the fluorapatite forms distinctive spherical structures (Goodfellow, 1984) of apparent primary origin. Support for chemical precipitation is also provided

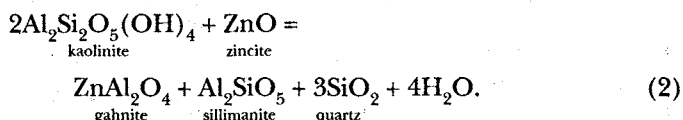
by the local occurrence of elevated  $P_2O_5$  values (ca. 1.0 wt %) in some Fe-rich sediments of the Red Sea (Hendricks et al., 1969). In both areas, the apatite or fluorapatite has apparently precipitated from anoxic waters due to a lack of coeval carbonate deposition (i.e., availability of  $Ca^{2+}$ ) and possibly to a decrease in pH (Goodfellow, 1984).

### Quartz-Gahnite Horizons

Gahnite ( $ZnAl_2O_4$ ), or zincian spinel ( $Zn,Fe,Mg(Al_2O_4)$ ), occurs in quartz-gahnite-almandine-sphalerite-pyrrhotite rocks that envelope B and C lodes of the Broken Hill deposit, Australia. It is believed to have formed by desulfidation of sphalerite by reactions of the type (Spry and Scott, 1986a; Zaleski et al., 1991; Spry, 2000):



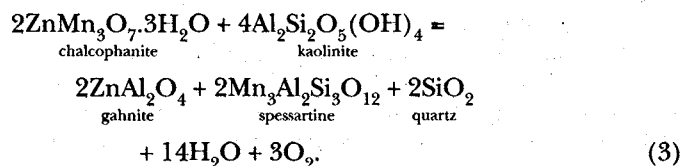
Such reactions are considered to be responsible for the formation of gahnite in metamorphosed massive sulfide deposits in general, and have led to the suggestion that gahnite can be used as an exploration guide (Sheridan and Raymond, 1984; Sandhaus and Craig, 1986; Spry and Scott, 1986a, b). Despite the spatial relationship between sulfide and gahnite at Broken Hill, sulfide-free quartz-gahnite rocks occur intermittently over 100 km throughout the Willyama Complex. This widespread gahnite probably did not form by desulfidation of sphalerite, but the quartz-gahnite rocks are nevertheless regarded as having an exhalative hydrothermal (premetamorphic) component (Spry and Scott, 1986a), an interpretation partly based on the spatial association of quartz-gahnite rocks enveloping B and C lodes in the stratigraphic footwall of the Broken Hill lode. Segnit (1961) suggested the following gahnite-forming reaction for these rocks:



Segnit proposed that the ZnO originally was adsorbed on kaolinite but this relationship has not been recognized in natural settings. Riviere et al. (1985) reported a spatial association between aluminous clays and Zn-hydroxide. Alternatively, Zn derived from exhalative processes may have subsequently been linked to organic or phosphatic material. Zinc can be incorporated in Zn-Fe (Al-poor) spinels that formed near active hydrothermal vents (Jedwab and Boulègue, 1986). The high quartz to gahnite ratios in most of the quartz-gahnite rocks of the Willyama Complex, and elsewhere, suggests that the exhaled Zn was swamped by hydrothermal silica.

To account for the common spatial relationship between gahnite and spessartine in the Willyama Complex

(e.g., Angus mine) and Namaqualand complex, South Africa, an alternative reaction should be considered. The following is a modification of that proposed by Bernier et al. (1986) for the formation of gahnite at Montauban-Les Mines, Québec:



### Staurolite-Bearing Rocks

Zincian staurolite has been documented in metamorphosed massive sulfide deposits, exhalites, alteration zones, and pelites and is considered to be a potential exploration guide for massive sulfides (e.g., Sandhaus and Craig, 1986; Spry and Scott, 1986b; Huston and Patterson, 1995). In sulfide-free rocks, Zn stabilizes staurolite to upper amphibolite facies where it may contain as much as 13 wt percent ZnO (Soto and Azañón, 1993). In massive sulfide deposits, meta-exhalites, and related alteration zones staurolite typically contains between 5 and 9 wt percent Zn, generally in the presence of quartz, (e.g., Sandhaus and Craig, 1986; Spry and Scott, 1986b; Huston and Patterson, 1995). Utilizing AFM plots, Froese and Moore (1980) and Zaleski et al. (1991) showed that, in quartz-bearing rocks in contact with sphalerite and/or gahnite, the elevated Zn stabilizes staurolite and prevents its breakdown during metamorphism. These AFM plots may be seen elsewhere in this volume (Spry, 2000; figs. 9a, b).

For some zincian staurolite occurrences, it is difficult to identify the protolith of the host rock because of the gradational nature of the staurolite-bearing lithologies. For example, zincian staurolite occurs along the margins of the massive sulfides at Dry River South, Queensland, in rocks that were regarded by Huston and Patterson (1995) to be altered metavolcanic rocks. Although more common in alteration zones than in meta-exhalites, zincian staurolite has been reported in a banded garnet-chlorite-gahnite rock that surrounds and is along strike from the small Angus Pb-Zn deposit, South Australia, and was interpreted by Both et al. (1995) as a meta-exhalite. Zincian staurolite also occurs as a prograde mineral in iron formation hosting the Gamsberg deposit, South Africa (Spry and Scott, 1986b), and as a product of the retrograde breakdown of gahnite in meta-exhalative quartz-gahnite rocks at Kraaifontein, South Africa (Moore and Reid, 1989).

In evaluating reasons for the elevated zinc content of staurolite associated with metamorphosed massive sulfide ores, Spry and Scott (1986b) proposed that, similar to gahnite, Zn-rich staurolite forms through desulfidation of sphalerite.

### Exploration Guides

Iron formations have been used in exploration for concealed massive sulfide deposits in several ways: (1) spatial

distribution (presence/absence) with respect to sulfide deposits; (2) abundances of minerals (e.g., Peter and Goodfellow, 1996b); (3) bulk geochemical variations (e.g., Peter and Goodfellow, 1994); (4) variations in the composition of mineral phases; and (5) variations in stable isotope compositions (e.g., Peter and Goodfellow, 1993). Similar approaches have been proposed for coticules (Spry, 1990) and tourmalinites (Slack, 1982, 1996).

#### Iron formations

**Spatial distribution:** Stanton (1972) was the first to make the observation that iron formations are spatially related to massive sulfide mineralization. Later, Stanton (1976a, p. B46) suggested that the association of certain iron formations with stratiform lead-zinc deposits "may provide a powerful tool in exploration for deposits of this kind." Although many iron formations are discontinuous and only cover an area slightly greater than that of the massive sulfides, some examples exist where the metamorphosed iron formations are much more extensive (e.g., Bathurst-Peter and Goodfellow, 1996b; Broken Hill-Plimer, 1988a; Mattagami-Davidson, 1977).

**Mineral abundance variations:** Variations in the presence and/or abundance of certain minerals in iron formation may reflect proximity to massive sulfide mineralization. The rationale for this hypothesis is that the mineralogy is controlled by the so-called facies of iron formation, which is in turn controlled by redox conditions at the site of precipitation (James and Howland, 1955). Figure 14 is a proportional symbol map of siderite abundance (determined by X-ray diffraction; XRD) in iron formation samples from the Brunswick belt; it shows that this mineral is most abundant in and around known deposits (as well as several other areas). Utilizing this approach, Peter and Goodfellow (1996b) showed that the localized abundance of siderite, ankerite, calcite, dolomite, magnetite, stilpnomelane, apatite, and pyrite was an aid in the exploration for concealed mineralization in the Brunswick belt.

At Broken Hill, Australia, the apatite-bearing iron formations generally occur closer to mineralization than the quartz-magnetite rocks (Stanton, 1976a). At the Broken Hill-type Pegmont Pb-Zn deposit, Queensland, there is an increase in the abundance of garnet in iron formation as the deposit is approached (Vaughan and Stanton, 1986).

In the Cues Formation (Thackaringa Group), stratigraphically hundreds of meters below the main Broken Hill Pb-Zn-Ag lodes, a lateral facies change over 700 m strike length is observed (Plimer, 1988a). An inner sulfide-facies sequentially gives way to a Mn fayalite Mn-Ca-Fe garnet-sphalerite-galena assemblage (carbonate-sulfide facies), a Mn hedenbergite-Fe-Mn-Ca garnet-cummingtonite-sphalerite assemblage (silicate-sulfide facies), and an outer Mn hedenbergite-Fe-Mn-Ca garnet-magnetite assemblage (silicate-oxide facies).

**Bulk geochemical variations:** The aim is to search for favorable geochemical patterns in iron formation that are indica-

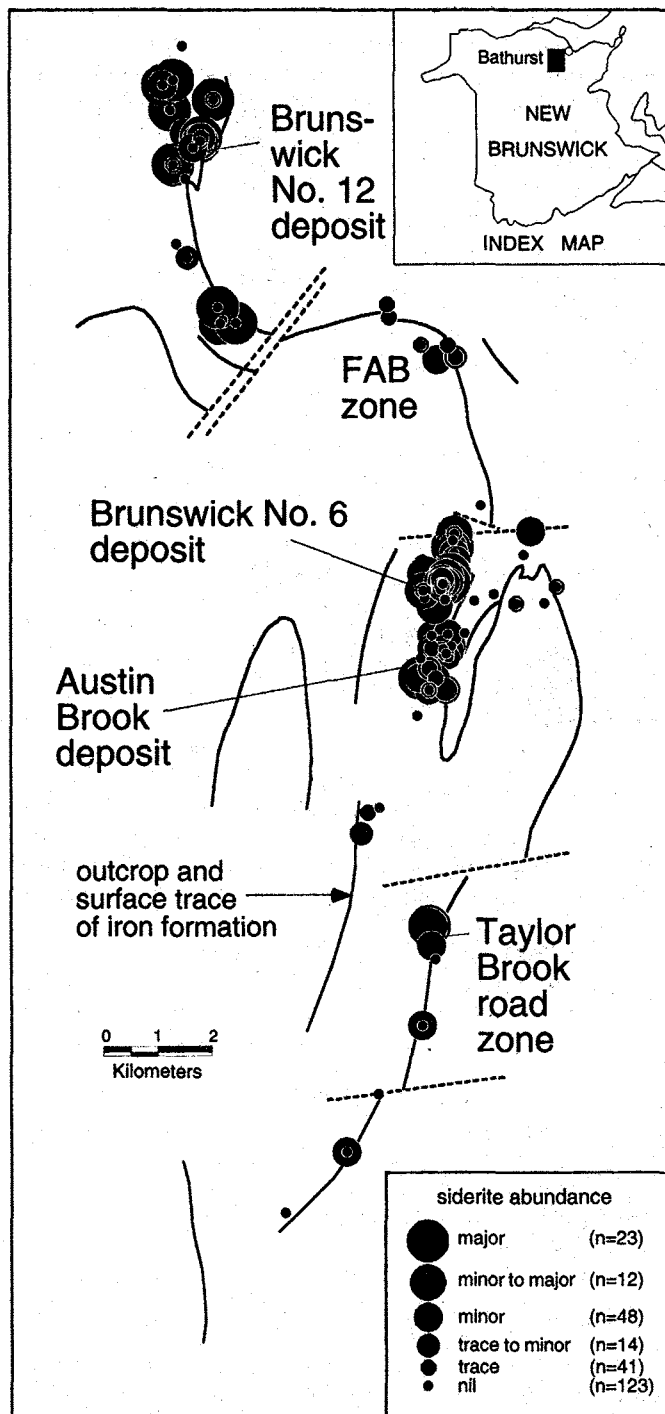


FIG. 14. Proportional symbol map of siderite abundance (as determined by X-ray diffractometry) in iron formation along the Brunswick belt, Bathurst. Solid lines are the surface trace of the iron formations; the dashed lines are major faults. Also shown are major deposits. Note anomalous abundances near known deposits. An inset map of New Brunswick showing the location of the enlarged map is included.

tive of spatially associated sulfide mineralization. Difficulties include the selection of background values and the possible presence of nonhydrothermal (predominantly detrital clastic) material that can weaken or dilute the hydrothermal component (i.e., potential anomaly). This effect can be lessened by using a ratio of the concentration of a hydrothermal element (e.g., Fe or Mn) over that of a detrital element (e.g., Al or Ti). Simple geochemical patterns, typified by a bullseye pattern, could be complicated if the iron formation formed from plume fallout in the presence of strong bottom currents. Furthermore, folding can make the interpretation of anomalies difficult and distort resultant vectors.

In the Bathurst camp, elements and element ratios that serve as useful indicators of known sulfide deposits, and which could be employed in the search for concealed mineralization, include:  $Fe^T + Mn/Al$ ,  $Fe^T/Ti$ ,  $Fe^T/Mn$ ,  $Fe^T + Mn$ ,  $Ba/Ti$ ,  $Ba/Al$ ,  $P/Ti$ ,  $Sr/Ti$ ,  $Pb$ ,  $Cu$ ,  $Cu/(Cu + Pb + Zn)$ ,  $Pb/Zn$ ,  $Pb/(Cu + Pb + Zn)$ ,  $S$ ,  $Ag$ ,  $As$ ,  $Au$ ,  $Ag/Cu$ ,  $Bi$ ,  $Cd$ ,  $Hg$  (Fig. 15),  $In$ ,  $Sb$ ,  $Te$ ,  $Tl$ ,  $Mo$ ,  $Eu/Eu^*$ ,  $1/(Ce/Ce^*)$ ,  $Se$ ,  $Co$ ,  $Ni$ ,  $F$ , and  $Cl$ . Increases in these values occur with proximity to sulfides over distances of up to 2 km (Peter and Goodfellow, 1994, 1995).

Numerous other studies have applied iron formation geochemistry to the exploration for sulfide deposits. At Matagami, Quebec, Davidson (1977) noted increases in  $Cu$ ,  $Zn$ , and other metals in Key tuffite as the massive sulfides were approached. Sakrison (1967) found that only  $Zn$ ,  $Pb$ , and  $Cd$  were significantly higher in the cherty tuff around the Lake Dufault deposit at Noranda, Quebec. At the Willroy no. 4 deposit, Manitouwadge, anomalous trace element contents in iron formation only occur a few meters from ore, but  $Ag$  and  $As$  are anomalous up to approximately 200 m away (Siriunas, 1979). Kalogeropoulos and Scott (1983) determined that trace element distribution patterns in Kuroko tetsusekiei were not useful mineralization vectors; the irregular patterns are believed to reflect multiple hydrothermal vent sources situated along linear structures. In the vicinity of the Løkken and Høydal massive sulfides in Norway, concentrations of  $Zn$ ,  $As$ ,  $Sb$ ,  $Hg$ , and  $Ge$  in jasper-type iron formation are highest near the deposits, suggesting a proximal hydrothermal origin (Grenne and Slack, 1997). At Gairloch, Scotland, quartz-magnetite schist immediately above the sulfides contains higher levels of  $Cu$  and  $Zn$  than that distant from the ore horizon (Jones et al., 1987).

Stanton (1976a) stated that there was no discernible, regular, along-strike variation for any element (whole-rock basis) within the banded iron formations at Broken Hill, Australia. However, Lottermoser (1991) demonstrated that proximal exhalites have elevated  $Ag$ ,  $Au$ ,  $Sb$ ,  $As$ , and  $W$  concentrations. At Fairmile, in the Mt. Isa region of Australia, Taylor and Scott (1982) found that maximum base metal and  $Ba$  contents occur within the thickest portion of the iron formations, whereas the bulk  $Ca$  contents increase along strike away from this portion.

*Mineral composition variations:* Variations in the chemical composition of mineral phases in iron formation may assist

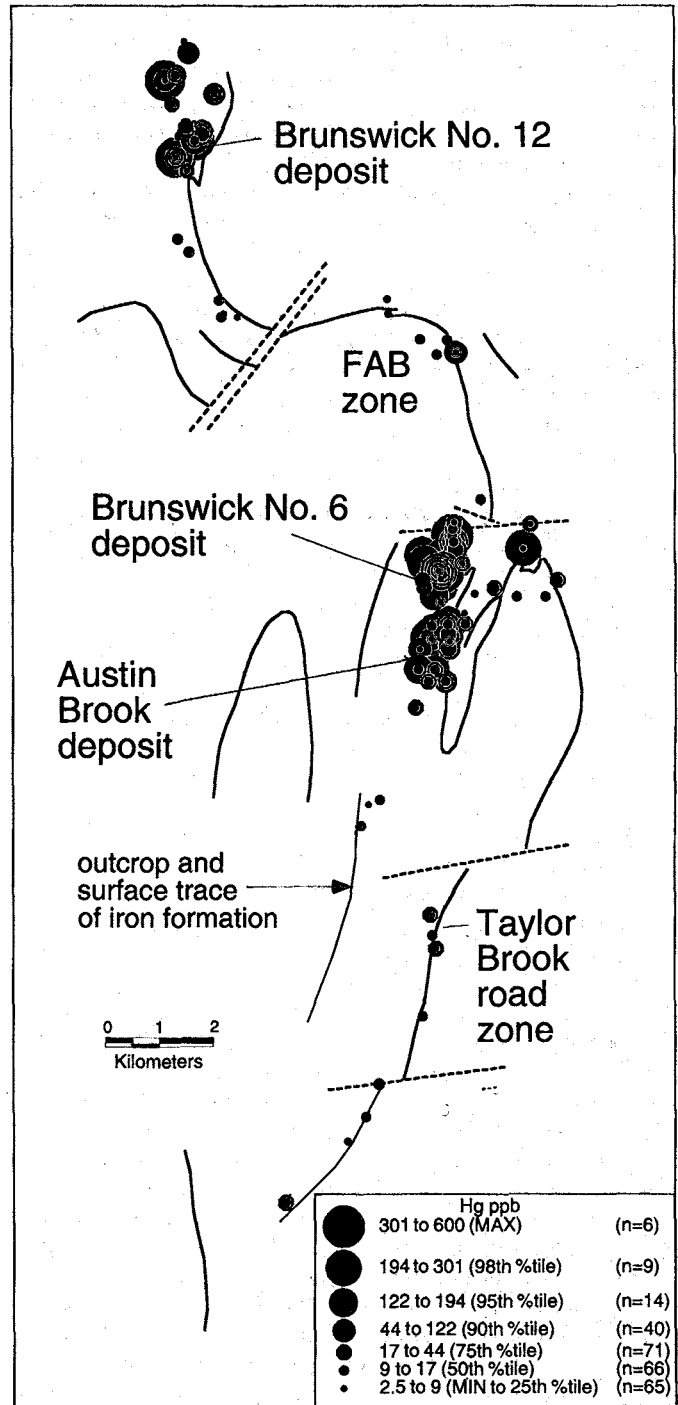


FIG. 15. Proportional symbol map of Hg content in bulk samples of iron formation from along the Brunswick belt, Bathurst. See caption and inset map of Figure 14.

exploration for massive sulfide deposits. For example, at the Millenbach mine, Noranda,  $Fe/(Fe + Mg)$  ratios of chlorite and whole-rock  $FeO/(FeO + MgO)$  ratios in the Main Contact tuff decrease with proximity to massive sulfides; also, ilmenite is replaced in massive sulfide by rutile and/or titanite, with the most manganiferous ilmenite oc-

curing closest to the sulfides (Kalogeropoulos and Scott, 1989). At Broken Hill, Australia, Stanton (1976a) noted an increase in the MnO, MgO, and CaO (with a concomitant decrease in FeO) contents of garnets in, above, and along strike from the main lode banded iron formation as the ore is approached. Stanton and Vaughan (1979) found a variation in the Mn content of garnet and fayalite in iron formation at the Pegmont Pb-Zn deposit; samples distal from ore are Fe-rich (and Mn-poor) compared to those proximal to ore (Mn-rich and Fe-poor). They also identified systematic variations in the chemistry of hornblende, characterized by increases in Ca + Na + K and Fe (and corresponding decreases in Mg), as ore is approached. Similarly, the highest Mn contents of clinopyroxene occur nearest to the ore, whereas more Fe-rich compositions are farther away (Vaughan and Stanton, 1986). Stumpfl (1979) noted that Mn contents of sphalerite at the Gamsberg and Broken Hill deposits in South Africa are highest in the upper parts of the mineralized horizon and in the vicinity of magnetite-garnet rock. Lipson and McCarthy (1977) found that the Mn content of garnets increases with decreasing stratigraphic distance from the Broken Hill (South Africa) ore-bodies (both from the hanging wall and footwall).

A detailed study of the compositions of minerals in iron formation along the Heath Steele belt, New Brunswick (Peter and Goodfellow, 1996b, 1997; Peter, unpub. data) shows the following minerals, elements, and/or element ratios to be of exploration interest: chlorite (Fe, Mn, Sr, and Na contents, Fe/Mn ratio, Fig. 16); stilpnomelane (Fe and Mn contents, Fe/Mn ratio); magnetite (Fe<sup>2+</sup>, Fe<sup>3+</sup>, Si contents); siderite (Mn content, Fe/Mn ratio); and sphalerite (Mn content, Fe/Mn ratio).

*Stable isotope variations:* Few studies have investigated variations in stable isotope ratios of constituent minerals and bulk samples of iron formation in the exploration for concealed mineralization. Whole-rock  $\delta^{18}\text{O}_{\text{SMOW}}$  values decrease from 9 per mil for ore horizon tuff to 5.1 per mil for tetsusekiei in the Japanese Kuroko deposits over a distance of 0.5 km from ore (Scott et al., 1983);  $\delta^{18}\text{O}$  values also decrease with proximity to the massive sulfides (range 4.0 to 18.7‰; Kalogeropoulos and Scott, 1983). A reconnaissance study of sulfides and carbonates within iron formation in and around the Brunswick no. 12 deposit (Peter and Goodfellow, 1993; Peter, unpub. data) shows that sulfides immediately overlying the deposit have higher  $\delta^{34}\text{S}$  values than those from distal iron formations. This is probably due to incorporation of greater amounts of reduced seawater sulfate (28‰) in the immediate vicinity of the deposit. Lower  $\delta^{34}\text{S}$  values farther from the deposit reflect mixed sources of sulfur from reduced seawater sulfate and bacteriogenic sulfur. Carbonate minerals in iron formations immediately overlying the Brunswick no. 12 deposit also have higher  $\delta^{13}\text{C}$  values than those from distal iron formations.

#### Coticules

The Fe and Mn (and in some localities, Si) components of coticules almost undoubtedly derive from hydrothermal

sources, therefore these elements are indicators of fossil zones of hydrothermal activity. This suggests that coticules warrant attention in the search for various economic commodities such as base metal sulfides, gold, and tungsten, with which they are spatially associated. However, Spry (1990) pointed out that coticules do not always directly indicate ore because they are found in a variety of geological settings. Even in the Broken Hill district where coticule units (specifically garnetites and varieties of quartz garnetites) are abundant, distinguishing coticules spatially related to ore from those lacking an applicable spatial relationship is a daunting task. However, it should be noted that garnet-rich rocks possessing a variety of minerals (i.e., apatite, gahnite, biotite, feldspar, cordierite, feldspar, or sillimanite, in addition to quartz and garnet) are spatially related to the largest deposit in the Willyama Complex, Broken Hill, whereas minor sulfide occurrences are spatially associated with coticules dominated by quartz and garnet. In this context, garnet-rich rocks from the Pinnacles deposit in the Broken Hill area are predominantly garnetite and quartz garnetite (coticule), but garnet-quartz-magnetite and garnet-hematite rocks also occur in the near vicinity of ore (Parr, 1992). Similarly, coticules associated with the Aggeneyns deposits are mineralogically variable and contain such minerals as magnetite, biotite, feldspar, grunerite, sulfides, apatite, gahnite, and muscovite (Spry, 1990).

The composition of garnet in coticules is not a particularly good indicator of ore because spessartine-, almandine-, and grossular-rich varieties are found in the same ore deposit (e.g., Broken Hill, Pinnacles, and Aggeneyns), in places within alternating bands.

Apart from bulk and trace element studies of coticules, other geochemical data are fairly limited. Unlike iron formations and tourmalinites, which have been the subjects of stable isotope studies (e.g., S, B, C, and O), there is a paucity of such work on coticules. Of all the geochemical parameters that have been utilized in the study of coticules, perhaps the most useful parameter from an exploration standpoint is the presence of positive Eu anomalies. Where not negated by clastic material, such anomalies may record a component of high-temperature (>250°C), end-member hydrothermal fluids that is indicative of close proximity to a fossil vent site (e.g., Lottermoser, 1989, at Broken Hill, Australia).

The depositional environment must also be carefully thought about when utilizing coticules as an exploration guide to ore. Like iron formations and tourmalinites, coticules may be considered in terms of a brine pool model versus a plume fallout model. Those coticules spatially associated with volcanogenic massive sulfide or sedimentary exhalative deposits are likely to have formed in brine pools, whereas coticules unrelated to such deposits perhaps formed by plume fallout since metalliferous sediment on the modern sea floor contains abundant Fe and Mn. Detrital clays are the likely source of Si and Al.

#### Tourmalinites

Tourmalinites may be useful exploration guides for a variety of exhalative mineral deposits. Most tourmalinites

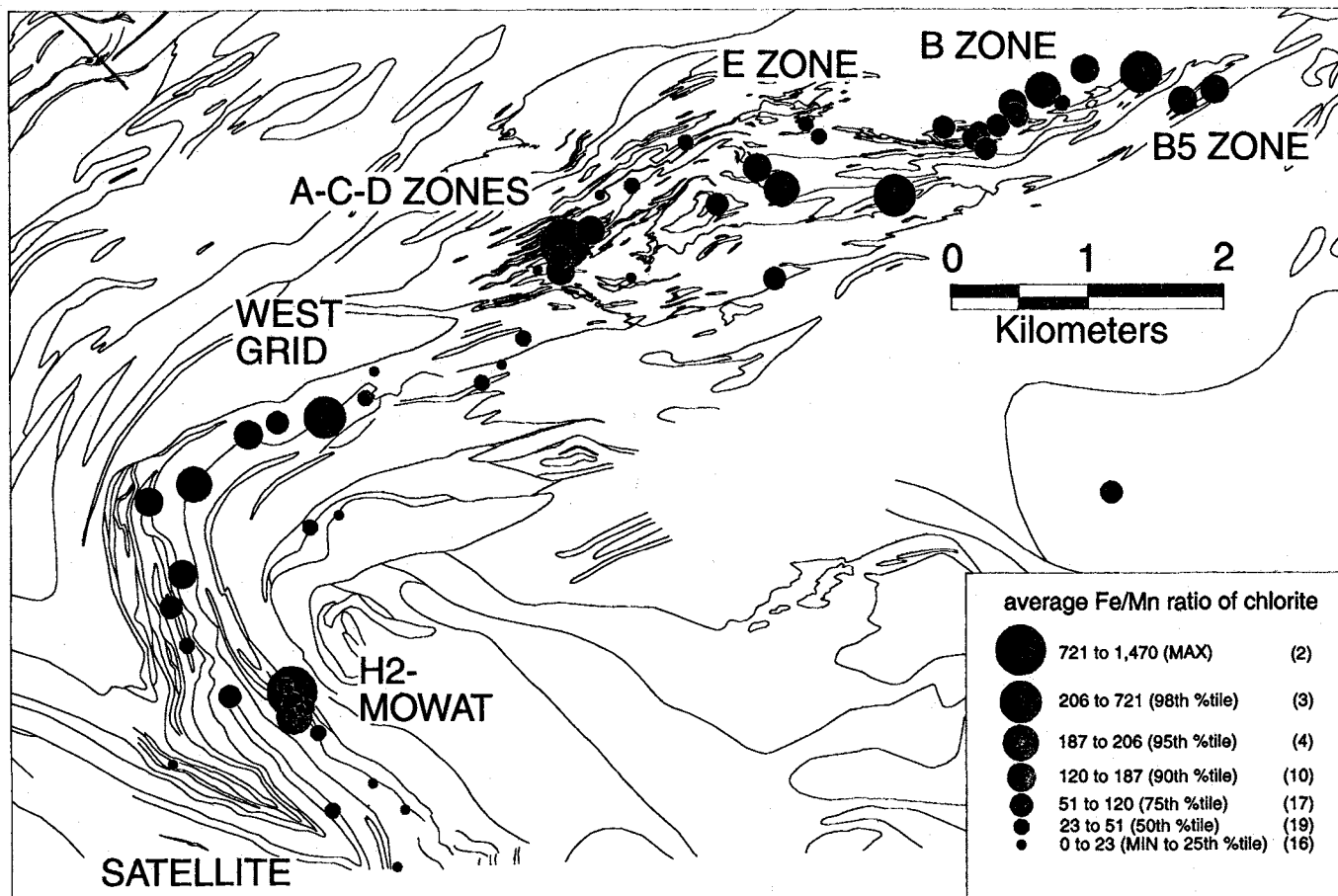


FIG. 16. Proportional symbol map of Fe/Mn of chlorite in iron formation along the Brunswick belt, Bathurst. Note anomalously high values in and around the B and B5 zones, and in several other areas along the belt. Note outline geology shown for reference; each dot represents a sample of iron formation. The location of the map is indicated approximately by the index map shown in Figure 14.

are unrelated to mineralization, but some show a close association with deposits of base metals, silver, gold, tungsten, cobalt, and/or uranium (e.g., Slack, 1996). Tourmalinites associated with base metal mineralization may be stratiform, or strata-bound but not stratiform. The distinction is critical, because the latter type develops by sub-sea-floor replacement without a preferred stratigraphic position, whereas the former type includes exhalative tourmalinites that constitute time-stratigraphic markers (Slack, 1993b; Slack et al., 1993b). Thus, in the exploration for sedex-type Pb-Zn ores, exhalative tourmalinites can be considered better prospecting guides because they may occur at the same stratigraphic level as the deposit. Nevertheless, stratiform tourmalinites can also form by sub-sea-floor replacement of favorable beds, particularly near feeder zones and growth faults that serve as channelways for hydrothermal fluids. Determining the origin of stratiform tourmalinites is, therefore, fundamental to evaluating their exploration potential. In this context, the case should be noted of tourmalinite associated with the strata-bound Sullivan deposit, the tourmalinite form-

ing as discordant to concordant (bedded) units in the footwall, ore zone, and hanging wall. Formation of the tourmalinites and spatially associated coti-cules involved replacement and exhalative processes contemporaneous with deposition of the sulfides and the enclosing sediments (Slack et al., 2000). The discordant variety of tourmalinite formed where B-rich hydrothermal fluids reacted with aluminous sediments beneath the sediment-seawater interface. Exhalative processes formed most of the concordant tourmalinites and coti-cules.

Criteria for the identification of exhalative tourmalinites are based mainly on empirical mineralogical and chemical data. Favorable mineralogical data include the presence of abundant Mn-rich garnet (or closely associated coti-cules) and/or apatite. The premise is that these minerals primarily record exhalative (rather than inhalative) contributions of Mn and P, respectively, from hydrothermal plume-type precipitates (e.g., Spry, 1990). The presence of abundant sulfide minerals can also be favorable, but care must be taken (utilizing field and petrographic observations) to determine whether the sulfides were introduced

synchronously with, or later than, the tourmaline.

Geochemical studies may aid in the identification of some exhalative tourmalinites. Such tourmalinites are locally characterized by elevated Fe (nonsulfide), Mn, and/or P on a whole-rock basis (Slack et al., 1993b). In addition to the Mn and P, high Fe contents (in tourmaline) are believed to derive from exhalative sources. Anomalous concentrations of these elements can be identified on Harker-type diagrams (e.g.,  $\text{Fe}_2\text{O}_3^1$  vs.  $\text{SiO}_2$ ), in which compositions of the tourmalinites are compared with those of unaltered precursor sediments (or volcanic rocks) of the study area (Slack et al., 1993b). An alternative approach is through the use of diagrams (e.g., Fig. 13) that evaluate relative contributions of metalliferous, terrigenous, and pelagic sediments in tourmalinites. Such diagrams readily identify exhalative components not necessarily discernible on Harker-type plots and tourmalinites that are potentially useful as exploration guides. An important caveat, however, is that Fe-rich tourmalinites can also form through metasomatic processes in the contact aureoles of granitic intrusions, including pegmatite bodies (e.g., London et al., 1996). A second caveat is that, in clastic metasedimentary terranes having an anorogenic (A-type) granite and/or rhyolite provenance, tourmalinites that formed under low fluid/rock conditions may be Fe-rich due to high Fe/Mg ratios inherited from the primary sediments (cf. Slack and Stevens, 1994).

Mineral chemistry can be useful but is not a panacea in evaluating the exploration favorability of tourmalinites. This is because the compositions of tourmalines in tourmalinites may reflect one or more parameters including: (1) the bulk composition of the host rock prior to tourmalinization; (2) the nature and amount of exhalative metalliferous sediment (if any); (3) the relative contribution of Fe-rich end-member hydrothermal fluid and entrained Mg-rich seawater; (4) the fluid/rock ratio of the hydrothermal system; and (5) the extent of Mg enrichment induced by sulfide-silicate reactions during regional metamorphism. Although the occurrence of relatively Fe-rich tourmaline is associated with some strata-bound sulfide mineralization (e.g., Plimer, 1988b), several studies have shown that, in general, Mg-rich tourmalines are characteristic of volcanogenic and sedimentary exhalative sulfide deposits (Taylor and Slack, 1984; Beaty et al., 1988; Hellinger et al., 1994; Jiang et al., 1998).

In situ trace element analyses of tourmalines have potential use in exploration. Proton microprobe studies of 23 metamorphosed massive sulfide deposits (Griffin et al., 1996) indicate that tourmalines related to massive sulfide and sedex deposits have distinctive trace element signatures that survive metamorphic recrystallization; also, that the base metal proportions of the tourmalines generally match those of the related deposits. The presence of high base metal contents (up to 195 ppm Cu, 2,800 ppm Pb, and 4,160 ppm Zn) in tourmalines from the Kidd Creek, Broken Hill (Australia), and Sazare (Japan) deposits serve to discriminate ore-related tourmalinite from those of barren rocks in these areas (Griffin et al., 1996). However, Griffin et al. (1996) identified high base metal values from tour-

malinites in areas apparently lacking associated base metal sulfides. Griffin et al. (1996) suggested that, rather than considering high individual contents of Cu or Pb or Zn of tourmalinites as exploration guides, the combination of high  $\text{Zn/Fe} \pm \text{Cu} \pm \text{Pb}$  serves as a better guide. They showed that a systematic relationship exists between base metal proportions in tourmalines and metallogeny of the host massive sulfide deposit, regardless of metamorphic grade. This consequently suggests that the analyzed tourmalines retain a strong chemical signature of their original hydrothermal formation. Benefits of this trace element approach may be enhanced in the future through the use of a laser-ablation ICP-MS microprobe (e.g., Jackson et al., 1992) for determining a wider suite of trace elements for a much lower cost (Griffin et al., 1996).

Isotope studies may have some exploration potential in the evaluation of tourmalinites. Oxygen isotope data can document the high formational temperatures ( $>200^\circ\text{C}$ ) of tourmalinites that might preferentially be associated with submarine-hydrothermal feeder zones, as opposed to low-temperature tourmalinites ( $<200^\circ\text{C}$ ) that may only reflect basin dewatering and a lack of associated mineralization (see Slack, 1993b, 1996). Insights into fluid/rock ratios of the tourmalinizing process can also be obtained through oxygen isotope studies. Boron isotope analyses, integrated with oxygen isotope data on the same samples, might further constrain the temperatures and fluid/rock ratios of tourmalinite-forming reactions (Jiang, 1998), and provide evidence of potentially related mineralization.

#### *Zincian spinel- or zincian staurolite-bearing rocks*

Zincian spinel and zincian staurolite that form by desulfidation and deoxidation mechanisms involving sphalerite have been proposed as useful indicators of proximity to metamorphosed massive sulfides (Spry and Scott, 1986a,b). Sandhaus and Craig (1986) also considered gahnite an exploration guide by emphasizing its mechanical and chemical resistance to weathering, and its preservation in the heavy mineral fraction of stream sediment, saprolite float, and gossan. Gandhi (1971) reported the presence of gahnite in soil samples 170 m from the Mandur base metal prospect, India, whereas Bernier et al. (1986) noted its utilization as an indicator mineral to ore in glacial till of the Montauban area, Quebec. Gahnite is so abundant in several localities in Proterozoic rocks of the southern Rocky Mountains (Colorado) that it potentially constitutes an ore mineral (Sheridan and Raymond, 1984), in much the same way that Zn oxides and silicates were ore minerals at the Franklin and Sterling Hill deposits, New Jersey.

Several workers have suggested that the composition of zincian spinel reflects its host environment and that it therefore serves as a useful guide to ore. Ririe and Foster (1984) and Bernier et al. (1987) showed that the Zn content of gahnite increases with proximity to the Zn deposits at Cotopaxi, Colorado, and Montauban, Quebec. Spry and Scott (1986a; Fig. 12) demonstrated that the composition of zincian spinel associated with metamorphosed massive

sulfide deposits (including meta-exhalative gahnite-quartz rocks) can be discriminated from spinels in pegmatites, aluminous metasediments, and marbles. Spinel in marbles are enriched in spinel sensu stricto ( $MgAl_2O_4$ ), aluminous metasediments in hercynite ( $FeAl_2O_4$ ), and massive sulfides and pegmatites in gahnite ( $ZnAl_2O_4$ ). Zincian spinels in the last two geological settings can be discriminated because those in pegmatites generally contain less than 5 mole percent of the spinel molecule, whereas those associated with massive sulfides typically contain between 5 and 20 mole percent spinel. There is an overlap between the compositional fields of zincian spinels in massive sulfide deposits and aluminous metasediment compositions. Zincian spinels with the following range of compositions (55–90 mole %  $ZnAl_2O_4$ , 10–40 mole %  $FeAl_2O_4$ , and 5–20 mole %  $MgAl_2O_4$ ), are considered to be the best guides to ore (Spry and Scott, 1986b).

Spry and Scott (1986a) proposed that the Zn content of staurolite, similar to zincian spinel, might be a useful guide to metamorphosed sulfide ores. Trembath (1986), Huston and Patterson (1995), and Both et al. (1995) supported this concept by showing that staurolite is enriched in Zn with proximity to the Anderson Lake (Manitoba), Dry River South (Queensland), and Angas (South Australia) base metal sulfide deposits, respectively. Huston and Patterson (1995, fig. 5) derived a  $TiO_2$ -ZnO scattergram that supposedly distinguished staurolite associated with massive sulfides from staurolite occurring in other environments. However, their conclusion must be treated cautiously because their results, when combined with data from sources including meta-exhalites and alteration zones, show that staurolite has a wide variation in  $TiO_2$  content regardless of geological environment (Fig. 17). Nevertheless, staurolite in massive sulfide deposits generally contains 4 to 9 wt percent ZnO, whereas staurolite in meta-exhalites and alteration zones contains 0.5 to 5.0 wt percent ZnO and 0 to 7 wt percent ZnO, respectively, thus suggesting that Zn content, rather than Zn combined with Ti, is a better discriminator of proximity to ore. Although staurolite in metasedimentary rocks can have ZnO contents greater than 4 wt percent, examples are few when compared with those genetically related to ore-forming processes. The latter generally occur in rocks metamorphosed to upper amphibolite facies, where Zn content increases the stability of staurolite to higher pressures, or in rocks deficient in quartz.

### Summary

#### General conclusions

The spatial relationships between meta-exhalites, in particular iron formations, and various hydrothermal ore deposits have been known for over 20 years and have long been considered as potential guides to exploration (e.g., Stanton, 1972). However, since the middle 1970s, there have been several hundred documented examples of meta-exhalites spatially associated with hydrothermal ore deposits. Furthermore, the spatial and genetic relationships

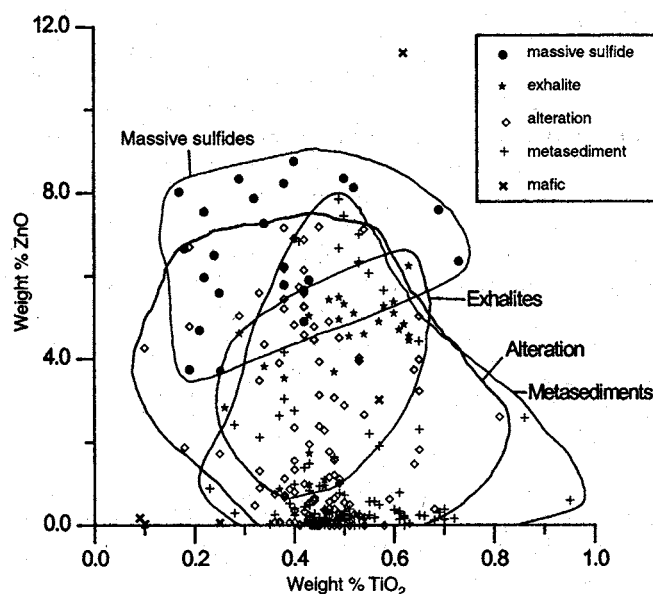


FIG. 17.  $TiO_2$ -ZnO plot for staurolite from different geological settings (metamorphosed massive sulfide deposits, meta-exhalative gahnite-quartz rocks, pegmatites, aluminous metasediments, and marbles). Data sources: Némec (1978), Stoddard (1979), Froese and Moore (1980), Sandhaus (1981), Nesbitt (1982), Bottrill (1983), Hiroi (1983), Purtschellar and Mogesie (1984), Spry (1984), Ward (1984a, b), Miyake (1985), Schumaker (1985), Dutrow et al. (1986), Holdaway et al. (1986), Leopold and Franz (1986), Trembath (1986), Treloar (1987), Tusiku et al. (1987), Bristol and Froese (1989), Froese et al. (1989), Moore and Reid (1989), Zaleski (1989), Bernier (1992), Cook (1993), Goodman (1993), Soto and Azañón (1993), McElhinney (1994), Cesare and Grobety (1995), Huston and Patterson (1995), Rosenberg (1998). Modified after Huston and Patterson (1995).

among coticles, tourmalinites, and hydrothermal ore deposits have gained acceptance, partly reflecting a dramatic increase in the number of geochemical analyses (specifically major and trace element) of meta-exhalites. The use of in situ microbeam techniques (e.g., proton microprobe, laser-ablation ICP-MS microprobe) on certain minerals in meta-exhalites holds great potential as a tool to aid in prospecting for hydrothermal ore deposits, including metamorphosed sulfide ores. Such techniques have usefully documented the trace element signatures of original hydrothermal formation for tourmaline in tourmalinites from metamorphosed massive sulfide (e.g., Griffin et al., 1996). Whether such signatures can be identified from garnet in coticles, gahnite in quartz-gahnite horizons, and zincian staurolite in staurolite-bearing rocks is yet to be determined, but microbeam techniques hold great promise.

Major and trace element (including REE) data demonstrate that iron formations, coticles, and tourmalinites spatially associated with metamorphosed hydrothermal ore deposits contain variable contributions of detrital material and hydrothermal components. The hydrothermal component is generally greater than 70 percent for iron formations, approximately 30 to 70 percent for coticles,

and less than 30 percent for tourmalinites (excluding contributions from B). Of the major constituents of meta-exhalites, Fe, Mn, B, P, and Zn generally have a hydrothermal source, whereas Al and Ti are from detrital clastic material. Silica can have hydrothermal and/or detrital sources. Variability in physicochemical conditions (e.g., T,  $f_{O_2}$ , pH, ionic strength,  $f_{S_2}$ ,  $f_{CO_2}$ ) partly account for the presence or absence of layering in the meta-exhalite, the proximity of the meta-exhalite to the hydrothermal sulfide deposit, and the mineralogy of the exhalite. Other contributing factors to these parameters include detrital input, the amount of hydrothermal input via venting, fluid/rock ratio, bottom current drift, and the degree of basin isolation from clastic sedimentation.

#### Exploration applications

**Iron formations:** Although all of the classical iron formation types of James (1954) are associated with metamorphosed massive sulfide deposits, these deposits are most often spatially associated with sulfide-predominant iron formation. Apart from the presence of individual sulfides, such as pyrite and pyrrhotite, no other mineral in iron formation is particularly diagnostic of the presence of nearby metallic sulfides. This is despite some massive sulfide districts (e.g., the Brunswick belt—Peter and Goodfellow, 1996b) having characteristic suites of minerals in iron formations that have proven to be useful indicators of ore. However, these minerals are not necessarily guides to ore in other districts.

Elevated concentrations of many individual elements (particularly Cu, Pb, or Zn, but also S, Ag, As, Au, Bi, Cd, Hg, In, Sb, Te, Tl, Mo, Se, Co, Ni, F, and Cl) in iron formations, have proven useful as indicators in several districts (e.g., Bathurst, Matagami, Lake Dufault, Løkken, Høydal). However, metal ratios that exhibit increasing proportions of hydrothermal components to clastic components (e.g.,  $Fe^T + Mn/Al$ ,  $Fe^T/Ti$ ,  $Mn/Ti$ ,  $Ba/Ti$ ,  $Ba/Al$ ,  $P/Ti$ ,  $Sr/Ti$ ) are a more consistent indicator of ore. Positive Eu anomalies also serve as good guides to ore because they seemingly reflect decreasing temperatures of the hydrothermal fluid away from the hydrothermal vent(s) and/or changing redox conditions; they therefore potentially reflect proximity to nearby vents and vent-related sulfide mineralization.

Variations in the chemical composition of mineral phases in iron formations do not serve as a panacea in the guide for economic mineralization because individual districts apparently exhibit different trends. Proximity to ore is reflected by changes in chlorite (Fe, Mn, Sr, and Na contents, and Fe/Mn ratio, Fig. 16); stilpnomelane (high Fe and Mn contents, and Fe/Mn ratio); magnetite ( $Fe^{2+}$ ,  $Fe^{3+}$ , and Si contents); siderite (Mn content and Fe/Mn ratio); and sphalerite (high Mn content and Fe/Mn ratio) in the Heath Steele belt, New Brunswick. However, with the exception of increases in the Mn content of various silicates (e.g., garnet, pyroxenoids), which occur with proximity to the Broken Hill (Australia), Gamsberg, and Pegmont deposits, the increases are generally not found elsewhere.

**Coticules:** Although coticules that are dominated by garnet and quartz can be associated with hydrothermal ore deposits, particularly massive sulfide deposits, coticules with a variety of minerals (e.g., apatite, gahnite, tourmaline, biotite, feldspar, apatite) are commonly associated with the largest deposits (e.g., Broken Hill, Australia; Aggeneys; Gamsberg) and appear to be a potential guide to ore. The utilization of trace element contents of coticules as guides for hydrothermal ore deposits remains unclear, partly due to the lack of systematic studies around known deposits, and in turn due to the limited areal extent of coticules (cf. tourmalinite and iron formation). However, the use of positive Eu anomalies as a guide to ore appears to have promise in the same manner as for iron formations.

**Tourmalinites:** Magnesian tourmalines are useful prospecting guides for massive sulfide deposits in most geological environments (e.g., Slack, 1996). However, caution must be exercised when using tourmaline compositions because Fe-rich tourmalines may be associated with some deposits (e.g., Broken Hill, Kidd Creek). Although exploration programs may focus on the distribution of tourmalinites in the field, several stream sediment studies have demonstrated the potential of Mg-rich tourmaline as an exploration guide to massive sulfides, due to its chemical and mechanical stability and its relatively high specific gravity (Pavlidis et al., 1982; Slack, 1982; Robinson et al., 1988; Robinson, 1989).

Great potential also exists for utilizing trace element contents of tourmaline in tourmalinites in the search for metamorphosed massive sulfide deposits. The combination of high  $Zn/Fe \pm Cu \pm Pb$  serves as a guide to these deposits (Griffin et al., 1996).

**Zincian spinel- or zincian staurolite-bearing rocks:** Although zincian spinels and staurolites occur in a wide variety of geological settings, those found in strata-bound horizons, particularly gahnite-quartz horizons, should be considered excellent guides to ore. Zincian spinels with the following range of compositions (55–90 mole %  $ZnAl_2O_4$ , 10–40 mole %  $FeAl_2O_4$ , and 5–20 mole %  $MgAl_2O_4$ ) are considered the best guides to ore (Spry and Scott, 1986b). By analogy, zincian staurolite with greater than 5 wt percent ZnO (or approximately >1 Zn atom in the formula  $(Fe_2, Zn, Mg)Al_{17}(Si, Al)_8O_{44}(OH)_4$ ) is an excellent indicator of close proximity to sulfides. The chosen staurolite formula is based on the composition of zincian staurolite generally found in metamorphosed massive sulfide deposits (e.g., Spry and Scott, 1986b; Huston and Patterson, 1995). The compositions of zincian spinel and staurolite apply to outcrop, stream sediment, saprolite float, gossan, or glacial till, because staurolite and particularly gahnite are mechanically and chemically resistant to weathering.

#### Acknowledgments

The manuscript was substantially improved by the comments of S.H.B. Clark, G. Davidson, R.R. Large, B.G. Lottermoser, B. Marshall, S. Paradis, S.E. Thieben, F.M.

Vokes, and L.G. Woodruff. D.F. Sangster kindly provided photographs Figures 1c to e and is thanked for discussions. D. Huston is also thanked for providing raw data that were used in Figure 17, M.K. de Brodtkorb provided data for coticles from Argentina.

## REFERENCES

- Abraham, K., Mielke, H., and Povondra, P., 1972, On the enrichment of tourmaline in metamorphic sediments of the Arzberg Series, W. Germany (NE Bavaria): *Neues Jahrbuch für Mineralogie Monatshefte*, v. 5, p. 209-219.
- Adamson, R.G., and Teichmann, R.F.H., 1986, The Matchless cupreous pyrite deposit, South West Africa/Namibia, in Anhaesser, C.R., and Maske, S., eds., *Mineral deposits of southern Africa*: Johannesburg, Geological Society of South Africa, v. II, p. 1755-1760.
- Anderson, P., and Guilbert, J.M., 1979, The Precambrian massive sulfide deposits of Arizona—a distinct metallogenic epoch and province: *Nevada Bureau of Mines Report*, v. 33, p. 39-48.
- Annis, M.P., Slack, J.F., and Rolph, A.L., 1983, Stratabound massive sulphide deposits of the Elizabeth mine, Orange County, Vermont, in Sangster, D.F., ed., *Field trip guidebook to stratabound sulphide deposits, Bathurst area, N.B., Canada and west-central New England, U.S.A.*: Canada Geological Survey Miscellaneous Report, v. 36, p. 41-51.
- Appel, P.W.U., and Garde, A.A., 1987, Stratabound scheelite and stratiform tourmalinites in the Archaean Malene supracrustal rocks, southern West Greenland: *Grønlands Geologiske Undersøgelse Bulletin*, no. 156, 26 p.
- Ashley, P.M., Cook, N.D.J., and Fanning, C.M., 1996, Geochemistry and age of metamorphosed felsic igneous rocks with A-type affinities in the Willyama Supergroup, Olary block, South Australia, and implications for mineral exploration: *Lithos*, v. 38, p. 167-184.
- Bandyopadhyay, B.K., Slack, J.F., Palmer, M.R., and Roy, A., 1993, Tourmalinites associated with stratabound massive sulphide deposits in the Proterozoic Sakoli Group, Nagpur district, central India, in Maurice, Y.T., ed., *Proceedings of the Eighth Quadrennial IAGOD Symposium*: Stuttgart, F. Schweizerbart'sche Verlagsbuchhandlung, p. 867-885.
- Banks, D.A., 1985, A fossil hydrothermal worm assemblage from the Tynagh lead-zinc deposit in Ireland: *Nature*, v. 313, p. 128-131.
- Barley, M.E., 1992, A review of Archean volcanic-hosted massive sulfide and sulfate mineralization in Western Australia: *Economic Geology*, v. 87, p. 855-872.
- Barnes, R.G., Stroud, W.J., Brown, R.E., Willis, I.L., and Bradley, G.M., 1983, Zinc, manganese, and iron-rich rocks and various minor rock types: *Geological Survey of New South Wales Records*, v. 21, p. 289-323.
- Barrett, T.J., 1981, Chemistry and mineralogy of Jurassic bedded chert overlying ophiolites in the north Apennines, Italy: *Chemical Geology*, v. 34, p. 289-317.
- 1987, Metalliferous sediments from DSDP Leg 92: The East Pacific Rise transect: *Geochimica et Cosmochimica Acta*, v. 51, p. 2241-2253.
- Barrett, T.J., Wares, R.P., and Fox, J.S., 1988, Two-stage hydrothermal formation of a Lower Proterozoic sediment-hosted massive sulfide deposit, northern Labrador trough, Quebec: *Canadian Mineralogist*, v. 26, p. 871-888.
- Barriga, F.J.A.S., 1983, Hydrothermal metamorphism and ore genesis at Aljustrel, Portugal: Unpublished Ph.D. thesis, London, University of Western Ontario, 368 p.
- Beaty, D.W., Hahn, G.A., and Threlkeld, W.E., 1988, Field, isotopic, and chemical studies of tourmaline-bearing rocks in the Belt-Purcell Supergroup: Genetic constraints and exploration significance for Sullivan type ore deposits: *Canadian Journal of Earth Sciences*, v. 25, p. 392-402.
- Beeson, R., 1990, Broken Hill-type lead-zinc deposits—an overview of their occurrence and geological setting: *Institution of Mining and Metallurgy Transactions*, v. 99, sec. B, p. B163-B175.
- Benvenuti, M., Lattanzi, P., and Tanelli, G., 1989, Tourmalinite-associated Pb-Zn-Ag mineralization at Bottino, Apuane Alps, Italy: *Geologic setting, mineral textures, and sulfide chemistry*: *Economic Geology*, v. 84, p. 1277-1292.
- Bernier, L.R., 1992, Lithogeochemistry and geothermobarometry of mineralized cordierite-orthoamphibole and related rocks at Atik Lake, Manitoba, and Némiscau and Montauban, Québec: Unpublished Ph.D. thesis, Montreal, McGill University, 386 p.
- Bernier, L.R., Pouliot, G., and MacLean, W.H., 1986, Origin of garnite in the north gold zone of the metamorphosed Zn-Pb-Au-Ag-Cu deposit of Montauban-Les Mines, Quebec, Canada [abs.]: *Terra Cognita*, v. 6, p. 524.
- 1987, Geology and metamorphism of the Montauban north gold zone: A metamorphosed polymetallic exhalative deposit, Grenville province, Quebec: *Economic Geology*, v. 82, p. 2076-2090.
- Beukes, N.J., and Klein, C., 1992, Models for iron formation deposition, in Schopf, J.W., and Klein, C., eds., *The Proterozoic biosphere: A multidisciplinary study*: New York, Cambridge University Press, p. 147-151.
- Bjergarkgård, T., and Bjørlykke, A., 1996, Sulfide deposits in Follidal, southern Trondheim region Caledonides, Norway: Source of metals and wall-rock alterations related to host rocks: *Economic Geology*, v. 91, p. 676-696.
- Bodou, S.B., 1996, Genetic implications of the paragenesis and rare-earth element geochemistry at the Cannington Ag-Pb-Zn deposit, Mt. Isa inlier, northwest Queensland, in Pongratz, J., and Davidson, G.J., eds., *New developments in Broken Hill type deposits*: Hobart, Tasmania, Centre for Ore Deposit and Exploration Studies Special Publication 1, p. 133-144.
- 1998, Paragenetic relationships and their implications for ore genesis at the Cannington Ag-Pb-Zn deposit, Mt. Isa inlier, northwest Queensland: *Economic Geology*, v. 93, p. 1463-1488.
- Boldy, J., 1968, Geological observations on the Delbridge massive sulphide deposit: *Canadian Institute of Mining and Metallurgy Bulletin*, v. 61, no. 677, p. 1045-1054.
- Bonatti, E., Kolla, V., Moore, W.S., and Stern, C., 1979, Metallogenesis in marginal basins: Fe-rich basal deposits from the Philippine Sea: *Marine Geology*, v. 32, p. 21-37.
- Boström, K., 1973a, The origin and fate of ferromanganese active ridge sediments: *Stockholm University Contributions to Geology*, v. 27, p. 129-243.
- 1973b, Submarine volcanism as a source for iron: *Earth and Planetary Science Letters*, v. 9, p. 348-354.
- Boström, K., and Peterson, M.N.A., 1966, Precipitates from hydrothermal exhalations on the East Pacific Rise: *Economic Geology*, v. 61, p. 1258-1265.
- Both, R.A., McElhinny, R., and Toteff, S., 1995, The Angas Zn-Pb-Ag deposit in the Kanmantoo Group, South Australia, in Pašava, J., Kříbek, B., and Žák, K., *Mineral deposits: From their origin to their environmental impacts*: Rotterdam, Balkema, p. 847-850.
- Bottrill, R.S., 1983, Zincian staurolite from Broken Hill, New South Wales: *Australian Mineralogist*, v. 44, p. 251-253.
- Bristol, C.C., and Froese, E., 1989, Highly metamorphosed altered rocks associated with the Osborne Lake volcanogenic massive sulfide deposit, Snow Lake area, Manitoba: *Canadian Mineralogist*, v. 27, p. 593-600.
- Brook, D.K., 1974, Relative ages of stratiform sulfide ores and wall rock determined by structural analysis of the Copper Queen mine, Yavapai County, Arizona: Unpublished M.Sc. thesis, Tucson, University of Arizona, 60 p.
- Burke, W.A., Denison, R.F., Hetherington, F.A., Koepnick, R.B., Nelson, H.F., and Otto, J.B., 1982, Variation of seawater  $^{87}\text{Sr}/^{86}\text{Sr}$  throughout Phanerozoic time: *Geology*, v. 10, p. 516-519.
- Carvalho, I.G., Zantop, H., and Torquato, J.R.F., 1982, Geologic setting and genetic interpretation of the Boquira Pb-Zn deposits, Bahia State, Brazil: *Revista Brasileira de Geociências*, v. 12, p. 414-425.
- Cesare, B., and Grobety, B., 1995, Epitaxial replacement of kyanite by staurolite: A TEM study of the microstructures: *American Mineralogist*, v. 80, p. 78-86.
- Cloud, P.F., 1973, Paleocological significance of the banded iron formation: *Economic Geology*, v. 68, p. 1135-1143.
- Coats, J.S., Smith, C.G., Fortey, N.J., Gallagher, M.J., May, F., and McCourt, W.J., 1980, Stratabound barium-zinc mineralization in Dalradian schist near Aberfeldy, Scotland: *Institution of Mining and Metallurgy Transactions*, v. 89, sec. B, p. B110-B122.
- Constantinou, G., and Govett, G.J.S., 1972, Genesis of sulphide deposits, ochre and amber of Cyprus: *Institution of Mining and Metallurgy Transactions*, v. B81, sec. B, p. B34-B46.
- Conway, C.M., 1986, Field guide to Early Proterozoic strata that host massive sulfide deposits at Bagdad, Arizona, in Nations, J.D., Conway, C.M., and Swann, G.A., eds., *Geology of central and northern Arizona: Geo-*

- logical Society of America, Rocky Mountain Section, Guidebook, p. 104-157.
- Cook, N.D.J., and Ashley, P.M., 1992, Meta-evaporite sequence, exhalative chemical sediments and associated rocks in the Proterozoic Willyama Supergroup, South Australia: Implications for metallogenesis: *Precambrian Research*, v. 56, p. 211-226.
- Cook, N.J., 1993, Conditions of metamorphism estimated from alteration lithologies and ore at the Bleikvassli Zn-Pb- (Cu) deposit, Nordland, Norway: *Norsk Geologisk Tidsskrift*, v. 73, p. 226-233.
- Cook, N.J., and Halls, C.J., 1990, Coticules at Sulitjelma, Norway and their possible origin: *Norsk Geologisk Tidsskrift*, v. 70, p. 153-158.
- Cornell, D.H., Thomas, R.J., Bowring, S.A., Armstrong, R.A., Grantham, G.H., 1996, Protolith interpretation in metamorphic terranes: A back-arc environment with Besshi-type base metal potential for the Quha Formation, Natal Province, South Africa: *Precambrian Research*, v. 77, p. 243-271.
- Costa, U.R., Barnett, R.L., and Kerrich, R., 1983, The Matagami Lake mine Archean Zn-Cu sulfide deposit, Quebec: Hydrothermal coprecipitation of talc and sulfides in a sea-floor brine pool—evidence from geochemistry,  $^{18}\text{O}/^{16}\text{O}$ , and mineral chemistry: *Economic Geology*, v. 78, p. 1144-1203.
- Crerar, D.A., Cormick, R.K., and Barnes, H.L., 1980, Geochemistry of manganese: An overview, in Varentsov, I.M., and Grassely, G.Y., eds., *Geology and geochemistry of manganese*: Budapest, Akademiai Kiadó, v. 1, p. 293-334.
- Cruise, M.D., 1996, Replacement origin of Crinkill ironstone: Implications for genetic models of base metal mineralization, central Ireland: *Exploration and Mining Geology*, v. 5, p. 241-249.
- Davidson, A.J., 1977, Petrography and chemistry of the Key tuffite at Bell Allard, Matagami, Quebec: Unpublished M.Sc. thesis, Montreal, McGill University, 131 p.
- de Brodtkorb, M.K., Fernández, R.R., Pezutti, N., and Ametrano, S.J., 1995, Exhalites associated with scheelite deposits, in Pašava, J., Kříbek, B., and Žák, K., *Mineral deposits: From their origin to their environmental impacts*: Rotterdam, Balkema, p. 221-224.
- Deb, M., Tiwary, A., and Palmer, M.R., 1997, Tourmaline in Proterozoic massive sulfide deposits from Rajasthan, India: *Mineralium Deposita*, v. 32, p. 94-99.
- Degens, E.T., and Ross, D.A., eds., 1969, *Hot brines and Recent heavy metal deposits in the Red Sea*: New York, Springer Verlag, 600 p.
- Duhig, N., Stolz, J., Davidson, G.J., and Large, R.R., 1992, Cambrian microbial and silica gel textures in silica iron exhalites from the Mount Windsor volcanic belt, Australia: Their petrography, chemistry and origin: *Economic Geology*, v. 87, p. 764-784.
- Dutrow, B.L., Holdaway, M.J., and Hinton, R.W., 1986, Lithium in staurolite and its petrologic significance: *Contributions to Mineralogy and Petrology*, v. 94, p. 496-506.
- Dymond, J., 1981, Geochemistry of Nazca plate surface sediments: An evaluation of hydrothermal, biogenic, detrital, and hydrogenous sources: *Geological Society of America Memoir*, v. 154, p. 133-173.
- Dymond, J., Corliss, J.B., Heath, G.R., Field, C.W., Dasch, E.J., and Veeh, H.H., 1973, Origin of metalliferous sediments from the Pacific Ocean: *Geological Society of America Bulletin*, v. 84, p. 3355-3372.
- Eeson, B.P., 1971, The constitution of the main banded iron formation at Broken Hill, and its spatial variation: Unpublished B.Sc. Honours thesis, Armidale, New South Wales, University of New England.
- Elderfield, H., Hawkesworth, C.J., Greaves, M.J., and Calvert, S.E., 1981, Rare earth element geochemistry of oceanic ferromanganese nodules: *Earth and Planetary Science Letters*, v. 55, p. 163-170.
- Elliot, S.M., 1979, Geochemistry of the rocks associated with Broken Hill-type deposits in the Broken Hill block, Australia: Unpublished Ph.D. thesis, Broken Hill, University of New South Wales.
- Embley, R.W., Chadwick, W., Perfit, M.R., and Baker, E.T., 1991, Geology of the northern Cleft segment, Juan de Fuca ridge: Recent lava flows, sea-floor spreading, and the formation of megaplumes: *Geology*, v. 19, p. 771-775.
- Ethier, V.G., and Campbell, F.A., 1977, Tourmaline concentrations in Proterozoic sediments of the southern Cordillera of Canada and their economic significance: *Canadian Journal of Earth Sciences*, v. 14, p. 2348-2363.
- Fernández, R.R., Pezutti, N., de Brodtkorb, M.K., and Paar, Y.W., 1994, Cuarzitas spessartíticas (coticules) del yacimiento scheelítico "La Higuera", Provincia de San Luis: *II Reunión de Mineralogía y Metalogía Publicación del Instituto de Recursos Minerales Universidad Nacional de La Plata*, v. 3, p. 89-100 (in Spanish).
- Fernández Fernández, A., and Moro Benito, M.C., 1992, Las turmalinitas estratiformes Ordovícicas de latado en el flanco s del sinforme de Alcañices (Zamora): *Estudios Geológicos*, v. 48, p. 31-41 (in Spanish).
- Franklin, J.M., Lydon, J.W., and Sangster, D.F., 1981, Volcanic-associated massive sulfide deposits: *Economic Geology 75th Anniversary Volume*, p. 485-627.
- French, B.M., 1968, Progressive contact metamorphism of the Biwabik iron formation, Mesabi Range, Minnesota: *Minnesota Geological Survey Bulletin*, v. 45, 103 p.
- 1973, Mineral assemblages in diagenetic and low-grade metamorphic iron formation: *Economic Geology*, v. 68, p. 1063-1074.
- Friesen, R.G., Pierce, G.A., and Weeks, R.M., 1982, Geology of the Geco base metal deposit, in Hutchinson, R.W., Spence, C.D., and Franklin, J.M., eds., *Precambrian sulphide deposits*: Geological Association of Canada Special Paper 25, p. 343-364.
- Froese, E., and Moore, J.M., 1980, Metamorphism in the Snow Lake area, Manitoba: *Canada Geological Survey Paper 78-27*, 16 p.
- Froese, E., Lemkow, D.R., and Fedikow, M.A.F., 1989, Metamorphism of the host rocks to the North Cook Lake massive sulphide type copper deposit, Snow Lake area (NTS 63K/16): Manitoba Energy and Mines, Minerals Division, Report of Field Activities, p. 139-144.
- Frost, B.R., 1979, Metamorphism of iron formation. Parageneses in the system Fe-Si-C-O-H: *Economic Geology*, v. 24, p. 775-785.
- Gair, J.E., and Slack, J.F., 1984, Deformation, geochemistry, and origin of massive sulfide deposits, Gossan Lead district, Virginia: *Economic Geology*, v. 79, p. 1483-1520.
- Gandhi, S.M., 1971, On the ferroan gahnite of Mamandur, Madras State, India: *Mineralogical Magazine*, v. 38, p. 528-529.
- Gardiner, W.W., and Venugopal, D.V., 1992, Spessartine-quartz rock (coticule) occurrences in New Brunswick, Canada, and their use in exploration for massive sulphide, tin-tungsten and gold deposits: *Institution of Mining and Metallurgy Transactions*, v. 101, sec. B, p. B147-157.
- Garrels, R.M., and Christ, C.L., 1965, *Solutions, minerals, and equilibria*: New York, Harper and Row, 450 p.
- Goodfellow, W.D., 1984, Geochemistry of rocks hosting the Howards Pass (XY) strata-bound Zn-Pb deposit, Selwyn basin, Yukon Territory, Canada, in Janelidze, T.V., and Tvalchrelidze, A.G., eds., *Proceedings of the Sixth Quadrennial IAGOD Symposium*: Stuttgart, E. Schweizerbart'sche Verlagsbuchhandlung, p. 91-112.
- Goodfellow, W.D., Lydon, J.W., and Turner, R., 1993, Geology and genesis of stratiform sediment-hosted (SEDEX) Zn-Pb-Ag sulphide deposits, in Kirkham, R.V., Sinclair, W.D., Thorpe, R.L., and Duke, J.M., eds., *Mineral deposit modeling*: Geological Association of Canada Special Paper 40, p. 201-251.
- Goodman, S., 1993, Survival of zincian staurolite to upper amphibolite facies metamorphic grade: *Mineralogical Magazine*, v. 57, p. 736-739.
- Graf, J.L., 1975, Rare earth elements as hydrothermal tracers during the formation of massive sulfide deposits and associated iron formations in New Brunswick: Unpublished Ph.D. thesis, New Haven, Yale University, 226 p.
- 1977, Rare earth elements as hydrothermal tracers during the formation of massive sulfide deposits in volcanic rocks: *Economic Geology*, v. 72, p. 527-548.
- 1978, Rare earth elements, iron formations and seawater: *Geochimica et Cosmochimica Acta*, v. 42, p. 1845-1850.
- Green, G.R., Solomon, M., and Walshe, J.L., 1981, The formation of the volcanic-hosted massive sulfide deposit at Rosebery, Tasmania: *Economic Geology*, v. 76, p. 304-338.
- Gregory, P.W., Hartley, J.S., and Wills, K.J.A., 1990, Thalanga zinc-lead-copper-silver deposit, in Hughes, F.E., ed., *Geology of the mineral deposits of Australia and Papua New Guinea*: Australasian Institute of Mining and Metallurgy Monograph 14, p. 1527-1538.
- Grenne, T., 1986, Ophiolite-hosted Cu-Zn deposits at Løkken and Høydal, Trondheim nappe complex, upper allochthon, in Stephens, M.B., ed., *Stratabound sulphide deposits in the central Scandinavian Caledonides*: Sveriges Geologiska Undersökning, no. 60, p. 55-68.
- Grenne, T., and Slack, J.F., 1997, Jaspers from the Løkken ophiolite, Norway: Geochemistry and relationship to massive sulphide deposition [abs.]: F.M. Vokes Symposium on the Formation and Metamorphism of Massive Sulfides, Trondheim, Norway, March 17-19, 1997, Abstracts Volume, p. 9.

- Grenne, T., and Vokes, F.M., 1990, Sea-floor sulfides at the Høydal volcanogenic deposit, central Norwegian Caledonides: *Economic Geology*, v. 85, p. 344-359.
- Griffin, W.L., Slack, J.F., Ramsden, A.R., Win, T.T., and Ryan, C.G., 1996, Trace elements in tourmalines from massive sulfide deposits and tourmalinites: Geochemical controls and exploration applications: *Economic Geology*, v. 91, p. 657-675.
- Grim, R.E., and Kulbrick, G., 1961, Montmorillonite. High-temperature reactions and classification: *American Mineralogist*, v. 46, p. 1329-1369.
- Gross, G.A., 1980, A classification of iron formation based on depositional environments: *Canadian Mineralogist*, v. 18, p. 215-222.
- 1993, Element distribution patterns as metallogenic indicators in siliceous metalliferous sediments: *Resource Geology Special Issue*, v. 17, p. 96-107.
- Haase, C.S., 1982, Phase equilibria in metamorphosed iron formations: Qualitative T-X( $\text{CO}_2$ ) petrologic grids: *American Journal of Science*, v. 282, p. 1623-1654.
- Halls, C., Reinsbakken, A., Ferriday, I., Haugen, A., and Rankin, A., 1977, Geological setting of the Skorovass orebody within the allochthonous stratigraphy of the Gjersvik nappe, central Norway, in *Volcanic processes in ore genesis: Institution of Mining and Metallurgy-Geological Society of London Special Paper 7*, p. 128-151.
- Hamilton, J.M., Bishop, D.T., Morris, H.C., and Owens, O.E., 1982, Geology of the Sullivan orebody, Kimberley, B.C., Canada, in *Hutchinson, R.W., Spence, C.D., and Franklin, J.M., eds., Precambrian sulphide deposits: Geological Association of Canada Special Paper 25*, p. 597-665.
- Haydon, R.C., and McConachy, G.W., 1987, The stratigraphic setting of Pb-Zn-Ag mineralization at Broken Hill: *Economic Geology*, v. 82, p. 826-856.
- Hedström, P., Simeonov, A., and Malmström, L., 1989, The Zinkgruvan ore deposit, south-central Sweden: A Proterozoic, proximal Zn-Pb-Ag deposit in distal volcanic facies: *Economic Geology*, v. 84, p. 1235-1261.
- Hellingwerf, R.H., Gatedal, K., Gallagher, V., and Baker, J.H., 1994, Tourmaline in the central Swedish ore district: *Mineralium Deposita*, v. 29, p. 189-205.
- Hendricks, R.L., Reisbick, F.B., Mahaffey, E.J., Roberts, D.B., and Peterson, M.N.A., 1969, Chemical composition of sediments and interstitial brines from the Atlantis II, Discovery and Chain Deeps, in *Degens, E.T., and Ross, D.A., eds., Hot brines and Recent heavy metal deposits in the Red Sea: New York, Springer-Verlag*, p. 407-440.
- Herzig, P.M., Hannington, M.D., Scott, S.D., Malotis, G., Rona, P.A., and Thompson, G., 1991, Gold-rich sea-floor gossans in the Troodos ophiolite and on the Mid-Atlantic Ridge: *Economic Geology*, v. 86, p. 1747-1755.
- Hiroi, Y., 1983, Progressive metamorphism of the Unazuki pelitic schists in the Hida terrane, central Japan: *Contributions to Mineralogy and Petrology*, v. 82, p. 334-350.
- Hitzman, M., Earls, G., Shearley, E., and Kelly, J., Cruise, M., and Sevastopulo, G., 1995, Ironstones (iron oxide-silica) in the Irish Zn-Pb deposits and regional iron oxide-(silica) alteration of the Waulsortian Limestone in southern Ireland, in *Anderson, K., Ashton, J., Earls, G., Hitzman, M., and Tear, S., eds., Irish carbonate-hosted Zn-Pb deposits: Society of Economic Geologists-Irish Association of Economic Geologists, SEG Guidebook Series*, v. 21, p. 261-273.
- Hoffmann, D., 1993, Aspects of the geology, geochemistry and metamorphism of the lower orebody, Broken Hill deposit, Aggeneys: Unpublished M.Sc. thesis, University of Cape Town, Cape Town, 211 p.
- 1994, Geochemistry and genesis of manganiferous silicate-rich iron formation bands in the Broken Hill deposit, Aggeneys, South Africa: *Exploration and Mining Geology*, v. 3, p. 407-417.
- Hogdahl, O.T., Melson, S., and Bowen, V.T., 1968, Neutron activation analysis of lanthanide elements in seawater, in *Gould, R.F., ed., Trace inorganics in water: Advances in Chemistry Series*, v. 73, p. 308-325.
- Holdaway, M.J., Dutrow, B.L., and Shore, P., 1986, A model for the crystal chemistry of staurolite: *American Mineralogist*, v. 71, p. 1142-1159.
- Holland, H.D., 1984, The chemical evolution of the atmosphere and oceans: Princeton, Princeton University Press, 582 p.
- Huston, D.L., and Patterson, D.J., 1995, Zincian staurolite in the Dry River South volcanic-hosted massive sulfide deposit, northern Queensland, Australia: An assessment of its usefulness in exploration: *Applied Geochemistry*, v. 10, p. 329-336.
- Imai, H., 1978, Geology and genesis of the Okuki mine, Ehime Prefecture, and other related cupriferous pyrite deposits in southwest Japan, in *Imai, H., ed., Geological studies of the mineral deposits in Japan and east Asia: Tokyo, University of Tokyo Press*, p. 234-256.
- Immega, I.P., and Klein, C., 1976, Mineralogy and petrology of some metamorphic Precambrian iron formations in southwestern Montana: *American Mineralogist*, v. 61, p. 1117-1144.
- Isley, A.E., 1995, Hydrothermal plumes and the delivery of iron to banded iron formation: *Journal of Geology*, v. 103, p. 169-185.
- Jackson, S.E., Longerich, H.P., Dunning, G.R., and Fryer, B.J., 1992, The application of laser-ablation microprobe-inductively coupled plasma-mass spectrometry (LAM-ICP-MS) to in situ trace-element determinations in minerals: *Canadian Mineralogist*, v. 30, p. 1049-1064.
- Jacobsen, S.B., and Pimentel-Klose, M.R., 1988, A Nd isotopic study of the Hamersley and Michipicoten banded iron formations: The source of REE and Fe in Archean oceans: *Earth and Planetary Science Letters*, v. 87, p. 29-44.
- James, H.L., 1954, Sedimentary facies of iron formation: *Economic Geology*, v. 49, p. 235-293.
- James, H.L., and Howland, A.C., 1955, Mineral facies in iron- and silica-rich rocks [abs.]: *Geological Society of America Bulletin*, v. 66, p. 1580.
- Jedwab, J., and Boulègue, J., 1986, Les spinelles de fer et de fer-zinc trouvés dans les trappes à sédiments amarrés près d'événements hydrothermaux océaniques: *Bulletin Société française de Minéralogie*, v. 109, p. 635-642 (in French).
- Jiang, S.-Y., 1998, Stable and radiogenic isotope studies of tourmaline: An overview, in *Novák, M., ed., Tourmaline special issue: Journal of the Czech Geological Survey*, v. 43, p. 75-90.
- Jiang, S.-Y., Palmer, M.R., Li, Y.-H., and Xue, C.-J., 1995, Chemical compositions of tourmaline in the Yindongzi-Tongmugou Pb-Zn deposits, Qinling, China: *Mineralium Deposita*, v. 30, p. 225-234.
- Jiang, S.-Y., Palmer, M.R., Slack, J.F., and Shaw, D.R., 1998, Paragenesis and chemistry of multistage tourmaline formation in the Sullivan Pb-Zn-Ag deposit, British Columbia: *Economic Geology*, v. 92, p. 47-67.
- Jones, E.M., Rice, C.M., and Tweedie, J.R., 1987, Lower Proterozoic stratiform sulphide deposits in Loch Maree Group, Cairloch, northwest Scotland: *Institution of Mining and Metallurgy Transactions*, v. 96, sec. B, p. B128-B140.
- Kalogeropoulos, S.I., 1982, Chemical sediments in the hanging wall of volcanogenic massive sulfide deposits: Unpublished Ph.D. thesis, Toronto, University of Toronto, 248 p.
- Kalogeropoulos, S.I., and Scott, S.D., 1983, Mineralogy and geochemistry of tuffaceous exhalites (tetsusekiei) of the Fukazawa mine, Hokuroku district, Japan: *Economic Geology Monograph 5*, p. 412-432.
- 1989, Mineralogy and geochemistry of an Archean tuffaceous exhalite: The Main Contact tuff, Millenbach mine area, Noranda, Quebec: *Canadian Journal of Earth Sciences*, v. 26, p. 88-105.
- Kanehira, K., and Tatsumi, T., 1970, Bedded cupriferous iron sulfide deposits in Japan, a review, in *Tatsumi, T., ed., Volcanism and ore genesis: Tokyo, University of Tokyo Press*, p. 51-76.
- Killick, A.M., 1982, The cupreous pyrite deposits associated with the Matchless Member, South West Africa/Namibia: *Proceedings of the 12th Congress of the Council of Mining and Metallurgical Institutions, South African Institute of Mining and Metallurgy*, v. 1, p. 163-171.
- 1983, Sulphide mineralization at Gorob and its genetic relationship to the Matchless Member, Damara Sequence, SWA/Namibia: *Special Publications of the Geological Society of South Africa*, v. 11, p. 381-384.
- Klein, C., 1983, Diagenesis and metamorphism of Precambrian banded iron formations, in *Trendall, A.F., and Morris, R.C., eds., Iron formation: Facts and problems: Amsterdam, Elsevier*, p. 417-469.
- Kretz, R., 1983, Symbols for rock-forming minerals: *American Mineralogist*, v. 68, p. 277-279.
- Ialou, C., Thompson, G., Arnold, M., Brichet, F., Druffel, E., and Rona, P., 1990, Geochronology of TAG and Snakepit hydrothermal fields, Mid-Atlantic Ridge: Witness to a long and complex hydrothermal history: *Earth and Planetary Science Letters*, v. 97, p. 113-128.
- Large, R.R., 1992, Australian volcanic-hosted massive sulfide deposits: Features, styles, and genetic models: *Economic Geology*, v. 87, p. 471-510.
- Large, R., Bodon, S., Davidson, G., and Cooke, D., 1996, The chemistry of BHT ore formation—one of the keys to understanding the differences between SEDEX and BHT deposits, in *Pongratz, J., and Davidson, G.J., eds., New developments in Broken Hill type deposits: Hobart, Tasmania, Centre for Ore Deposit and Exploration Studies, University of Tasmania, Special Publication no. 1*, p. 105-111.

- Leistel, J.M., Marcoux, E., and Deschamps, Y., 1998, Chert in the Iberian pyrite belt: *Mineralium Deposita*, v. 33, p. 59–81.
- Leopold, L., and Franz, G., 1986, Zink-staurolite aus metasedimenten der eklogitzone, Tauern/Osterreich: *Fortschritte der Mineralogie*, v. 64, p. 96 (in German).
- Liaghat, S., and MacLean, W.H., 1992, The Key tuffite, Matagami mining district: Origin of the tuff components and mass changes: *Exploration and Mining Geology*, v. 1, p. 197–207.
- Lipson, R.D., 1990, Litho-geochemistry and origin of metasediments hosting the Broken Hill deposit, Aggeneys, South Africa, and implications for ore genesis: Unpublished Ph.D. thesis, Cape Town, University of Cape Town, 245 p.
- Lipson, R.D., and McCarthy, T.S., 1977, Geochemical correlation between some rock-types of the Namaqualand granite-gneiss complex: *Geological Society of South Africa Transactions*, v. 80, p. 177–181.
- London, D., Morgan, G.B., VI, and Wolf, M.B., 1996, Boron in granitic rocks and their contact aureoles: *Reviews in Mineralogy*, v. 33, p. 299–330.
- Lottermoser, B.G., 1988, Rare earth element composition of garnets from the Broken Hill Pb-Zn-Ag orebodies, Australia: *Neues Jahrbuch für Mineralogie Monatshefte*, v. H9, p. 423–431.
- 1989, Rare earth element study of exhalites within the Willyama Supergroup, Broken Hill block, Australia: *Mineralium Deposita*, v. 24, p. 92–99.
- 1991, Trace element composition of exhalites associated with the Broken Hill sulfide deposit, Australia: *Economic Geology*, v. 86, p. 870–877.
- Lottermoser, B.G., and Ashley, P.M., 1995, Exhalites within the Proterozoic Willyama Supergroup, Olary block, South Australia, in Pašava, J., Kříbek, B., and Žák, K., eds., *Mineral deposits: From their origin to their environmental impacts*: Rotterdam, Balkema, p. 237–240.
- 1996, Geochemistry and exploration significance of ironstones and barite-rich rocks in the Proterozoic Willyama Supergroup, Olary block, South Australia: *Journal of Geochemical Exploration*, v. 57, p. 57–73.
- Main, J.V., Mason, D.O., and Tuckwell, K.D., 1983, The characteristics and interpretation of whole rock geochemical data, Willyama Supergroup, New South Wales—trends towards ore: *Australasian Institute of Mining and Metallurgy Symposium Series 12*, p. 115–131.
- Mao, J., 1995, Tourmalinite from northern Guangxi, China: *Mineralium Deposita*, v. 30, p. 235–245.
- Marchig, V., 1978, Brown clays from the central Pacific—metalliferous sediments or not?: *Geologisches Jahrbuch*, v. D30, p. 3–25.
- Marcoux, E., 1998, Lead isotope systematics of the giant massive sulphide deposits in the Iberian pyrite belt: *Mineralium Deposita*, v. 33, p. 45–58.
- McArdle, P., and Kennan, P.S., 1988, Controls on the occurrence and distribution of tungsten and lithium deposits on the southeast margin of the Leinster granite, Ireland, in Boissonnas, J., Omenetto, P., eds., *Mineral deposits in the European community*: Berlin, Springer-Verlag, p. 199–209.
- McArdle, P., Fitzell, M., Oosterom, M.G., O'Conner, P.J., and Kennan, P.S., 1989, Tourmalinite as a potential host rock for gold in the Caledonides of southeast Ireland: *Mineralium Deposita*, v. 24, p. 154–159.
- McElhinney, R., 1994, Style and genesis of base metal sulphide mineralisation of Angas prospect—Strathalbyn area, South Australia: Unpublished B.S. Honours thesis, Adelaide, University of Adelaide, 33 p.
- Mills, R.A., and Elderfield, H., 1995, Rare earth element geochemistry of hydrothermal deposits from the active TAG mound, 26 degrees N Mid-Atlantic Ridge: *Geochimica et Cosmochimica Acta*, v. 59, p. 3511–3524.
- Mitra, A., Elderfield, H., and Greaves, M.J., 1994, Rare earth elements in submarine hydrothermal fluids and plumes from the Mid-Atlantic Ridge: *Marine Chemistry*, v. 46, p. 217–235.
- Miyake, A., 1985, Zn-rich staurolite from the Uvete area, central Kenya: *Mineralogical Magazine*, v. 49, p. 573–578.
- Miyano, T., and Klein, C., 1986, Fluid behavior and phase relations in the system Fe-Mg-Si-C-O-H: Application to high grade metamorphism of iron formations: *American Journal of Science*, v. 286, p. 540–575.
- Moore, J.M., 1989, A comparative study of metamorphosed supracrustal rocks from the western Namaqualand metamorphic complex: *Precambrian Research Unit, University of Cape Town, Bulletin* 37, 370 p.
- Moore, J.M., and Reid, A.M., 1989, A Pan-African zircon staurolite imprint on Namaqua quartz-gahnite-sillimanite assemblages: *Mineralogical Magazine*, v. 53, p. 63–70.
- Morris, R.C., 1993, Genetic modelling for banded-iron formation of the Hamersley Group, Pilbara craton, Western Australia: *Precambrian Research*, v. 60, p. 243–286.
- Mottl, M.J., and McConachy, T.F., 1990, Chemical processes in buoyant hydrothermal plumes on the East Pacific Rise near 21°N: *Geochimica et Cosmochimica Acta*, v. 54, p. 1911–1927.
- Munha, J., Barriga, F.J.A.S., and Kerrich, R., 1986, High <sup>18</sup>O ore-forming fluids in volcanic-hosted base metal massive sulfide deposits: *Geologic, <sup>18</sup>O/<sup>16</sup>O, and D/H evidence from the Iberian pyrite belt; Crandon, Wisconsin; and Blue Hill, Maine: Economic Geology*, v. 81, p. 530–552.
- Némec, V.D., 1978, Zink im staurolith: *Chemie der Erde*, v. 37, p. 307–314 (in German).
- Nesbitt, B.E., 1982, Metamorphic sulfide-silicate equilibria in massive sulfide deposits at Ducktown, Tennessee: *Economic Geology*, v. 77, p. 364–378.
- Nesbitt, B.E., Longstaffe, F.J., Shaw, D.R., and Muehlenbachs, K., 1984, Oxygen isotope geochemistry of the Sullivan massive sulfide deposit, Kimberley, British Columbia: *Economic Geology*, v. 79, p. 933–946.
- Nicholson, P.M., 1980, The geology and economic significance of the Golden Dyke dome, Northern Territory, in Ferguson, J., and Goleby, A.B., eds., *Uranium in the Pine Creek geosyncline*: Vienna, International Atomic Energy Agency, p. 319–334.
- Nie, F.J., 1993, Genesis of the Bieluwutu volcanogenic copper deposit, south-central Inner Mongolia, People's Republic of China: *International Geology Review*, v. 35, p. 805–824.
- Nilsen, O., 1978, Caledonian sulphide deposits and minor iron formation from the southern Trondheim region, Norway: *Norges Geologiske Undersøkelse Bulletin*, v. 340, p. 35–85.
- Ohmoto, H., 1972, Systematics of sulfur and carbon isotopes in hydrothermal ore deposits: *Economic Geology*, v. 67, p. 551–579.
- Ohmoto, H., and Lasaga, A., 1982, Kinetics of reactions between aqueous sulfates and sulfides in hydrothermal systems: *Geochimica et Cosmochimica Acta*, v. 46, p. 1727–1745.
- Palmer, M.R., 1985, Rare earth elements in foraminifera tests: *Earth and Planetary Science Letters*, v. 73, p. 285–298.
- Palmer, M.R., and Slack, J.F., 1989, Boron isotopic composition of tourmaline from massive sulfide deposits and tourmalinites: *Contributions to Mineralogy and Petrology*, v. 103, p. 434–451.
- Parák, T., 1991, Volcanic sedimentary rock-related metallogenesis in the Kiruna-Skellefte belt of northern Sweden: *Economic Geology Monograph* 8, p. 20–50.
- Parr, J.M., 1992, Rare-earth element distribution in exhalites associated with Broken Hill-type mineralisation at the Pinnacles deposit, New South Wales: *Chemical Geology*, v. 100, p. 73–91.
- Parr, J.M., and Plimer, I.R., 1993, Models for Broken Hill-type lead-zinc-silver deposits, in Kirkham, R.V., Sinclair, W.D., Thorpe, R.I., and Duke, J.M., eds., *Mineral deposit modeling*: Geological Association of Canada Special Paper 40, p. 253–288.
- Pavlidis, L., Gair, J.E., and Cranford, S.L., 1982, Central Virginia volcanic-plutonic belt as a host for massive sulfide deposits: *Economic Geology*, v. 77, p. 233–272.
- Pertold, Z., Chrt, J., Budil, V., Burda, J., Burdová, B., Kříbek, B., Pertoldová, J., and Gaskarth, B., 1994, The Tisová Cu-deposit: A Besshi-type mineralization in the Krušné hory Mts., Bohemian Massif, Czech Republic, in von Gehlen, K., and Klemm, D.D., eds., *Mineral deposits of the Erzgebirge/Krušné hory (Germany/Czech Republic)*: Monograph Series on Mineral Deposits, v. 31, p. 71–95.
- Peter, J.M., and Goodfellow, W.D., 1993, Bulk and stable sulphur and carbon isotope geochemistry of hydrothermal sediments associated with the Brunswick no. 12 deposit, northern New Brunswick, in Abbott, S.A., ed., *Current research: New Brunswick Department of Natural Resources and Energy, Mineral Resources Information Circular* 93-1, p. 154–169.
- 1994, Hydrothermal sediment geochemistry in the exploration for concealed massive sulphide mineralization in the Brunswick belt, Bathurst, New Brunswick: Unpublished report for Brunswick Mining and Smelting Company Limited and Noranda Exploration Company Limited, 269 p.
- 1995, Progress report on Geological Survey of Canada-Noranda industrial partners program (IPP) on development of new geochemical exploration techniques for deeply buried volcanogenic massive sulphide deposits in northeastern New Brunswick: Unpublished report for the Geological Survey of Canada, 246 p.

- 1996a, Mineralogy, bulk and rare earth element geochemistry of massive sulphide-associated hydrothermal sediments of the Brunswick horizon, Bathurst mining camp, New Brunswick: Canadian Journal of Earth Science, v. 33, p. 252–283.
- 1996b, Final report on Geological Survey of Canada-Noranda industrial partners program (IPP) on development of new geochemical exploration techniques for deeply buried volcanogenic massive sulphide deposits in northeastern New Brunswick: Unpublished report for the Geological Survey of Canada, 569 p.
- 1997, The importance of hydrothermal sediments (iron formation) in the exploration for concealed massive sulphide deposits in the Bathurst mining camp, northern Appalachians, New Brunswick, Canada [abs.]: F.M. Vokes Symposium on the Formation and Metamorphism of Massive Sulphides, Trondheim, Norway, March 17–19, 1997, Abstracts Volume, p. 19.
- Peter, J.M., and Scott, S.D., 1998, Windy Craggy, northwestern British Columbia: The world's largest Besshi-type deposit: Reviews in Economic Geology, v. 8, p. 261–296.
- Piper, D.Z., and Graef, P.A., 1974, Gold and rare-earth elements in sediments from the East Pacific Rise: Marine Geology, v. 17, p. 287–297.
- Plimer, I.R., 1984, The role of fluorine in submarine exhalative systems with special reference to Broken Hill, Australia: Mineralium Deposita, v. 19, p. 19–25.
- 1986, Tourmalinites from the Golden Dyke dome, northern Australia: Mineralium Deposita, v. 21, p. 263–270.
- 1987, The association of tourmalinite with stratiform scheelite deposits: Mineralium Deposita, v. 22, p. 282–291.
- 1988a, Broken Hill, Australia and Bergslagen, Sweden—why God and mammon bless the antipodes!: Geologie en Mijnbouw, v. 67, p. 265–278.
- 1988b, Tourmalinites associated with Australian Proterozoic submarine exhalative ores, in Friedrich, G.H., and Herzig, P.M., eds., Base metal sulfide deposits in sedimentary and volcanic environments: Berlin, Springer-Verlag, p. 255–283.
- Purtschellar, F., and Mogesie, A., 1984, Staurolite in garnet amphibolite from Solden, Ortztal old crystalline basement, Austria: Tscherma's Mineralogische und Petrographische Mitteilungen, v. 32, p. 223–233.
- Raith, J.G., 1988, Tourmaline rocks associated with stratabound scheelite mineralization in the Austroalpine crystalline complex, Austria: Mineralogy and Petrology, v. 39, p. 265–288.
- Rehtjärvi, P., Äikäs, O., and Mäkelä, M., 1979, A Middle Precambrian uranium- and apatite-bearing horizon associated with the Vihanti zinc ore deposit, western Finland: Economic Geology, v. 74, p. 1102–1117.
- Renard, A., 1878, Sur la structure et la composition minéralogique du coticule et sur ses rapports avec le phyllade oligistifère: Mémoires couronnés de l'Académie Royale Belgique, v. 41, 42 p. (in French).
- Richards, S.M., 1966a, The banded iron formations at Broken Hill, Australia, and their relationship to the lead-zinc orebodies, Part 1: Economic Geology, v. 61, p. 72–96.
- 1966b, The banded iron formations at Broken Hill, Australia, and their relationship to the lead-zinc orebodies, Part 2: Economic Geology, v. 61, p. 257–274.
- Ridler, R.H., 1971, Analysis of Archean volcanic basins in the Canadian shield using the exhalite concept [abs.]: Bulletin of the Canadian Institute of Mining and Metallurgy, v. 64, p. 20.
- Ririe, G.T., and Foster, C.T., 1984, Zinc ratios in gahnite associated with massive sulfide deposits [abs.]: Geological Society of America Abstracts with Programs, v. 16, p. 635.
- Riviere, M., Rautureau, M., Besson, G., Steinberg, M., and Amour, M., 1985, Complémentarité des rayons X et de la microscopie électronique pour la détermination des diverses phases d'une argile zincifère: Clay Minerals, v. 20, p. 53–67 (in French).
- Robertson, A. H. F., and Hudson, J. D., 1973, Cyprus umbers: Chemical precipitates on a Tethyan ocean ridge: Earth and Planetary Science Letters, v. 18, p. 93–101.
- Robinson, G.D., 1989, Stream sediment tourmaline geochemistry in massive sulfide exploration: An example from Virginia, U.S.A.: Journal of Geochemical Exploration, v. 34, p. 173–188.
- Robinson, G.D., Healey, K., and Kelly, V.C., 1988, Use of tourmaline in stream sediments to detect submarine exhalative deposits: Examples from central Virginia, U.S.: Applied Geochemistry, v. 3, p. 225–230.
- Rock, N.M.S., 1988, The need for standardization of normalized multi-element diagrams in geochemistry: A comment: Geochemical Journal, v. 21, p. 75–84.
- Rosenberg, J.I., 1998, The effects of metamorphism on the Bleikvassli Zn-Pb (Cu) deposit, Nordland, Norway: Unpublished M.S. thesis, Ames, Iowa State University, 299 p.
- Rozendaal, A., 1980, The Gamsberg zinc deposit, South Africa: A banded stratiform base metal sulfide ore deposit, in Ridge, J.D., ed., Proceedings of the Fifth Quadrennial IAGOD Symposium: Stuttgart, Germany, E. Schweizerbart'sche Verlagsbuchhandlung, v. I, p. 619–718.
- 1986, The Gamsberg zinc deposit, Namaqualand district, in Anhaeusser, C.R., and Maske, S., eds., Mineral deposits of South Africa: Johannesburg, Geological Society of South Africa, v. II, p. 1477–1488.
- Rozendaal, A., and Stumpfl, E.F., 1984, Mineral chemistry and genesis of Gamsberg zinc deposit, South Africa: Institution of Mining and Metallurgy Transactions, v. 93, sec. B, p. B161–B175.
- Sakrisson, H.C., 1967, Chemical studies of the host rocks of the Lake Du-fault mines, Quebec: Unpublished Ph.D. thesis, Montreal, McGill University, 138 p.
- Sand, K., 1986, A study of Paleozoic iron formations in the central Norwegian Caledonides [abs.]: Norges Tekniske Høgskole, Trondheim, Norway, Geological Institute Report, v. 23b, p. 23.
- Sandhaus, D.J., 1981, Gahnite in metamorphosed volcanogenic massive sulfides of the Mineral district, Virginia: Unpublished M.S. thesis, Blacksburg, Virginia Polytechnic Institute and State University, 167 p.
- Sandhaus, D.J., and Craig, J.R., 1986, Gahnite in metamorphosed stratiform massive sulfide deposits of the Mineral district, Virginia, U.S.A.: Tscherma's Mineralogische und Petrographische Mitteilungen, v. 35, p. 77–98.
- Sawyer, E.W., 1986, The influence of source rock type, chemical weathering and sorting on the geochemistry of clastic sediments from the Quetico metasedimentary belt, Superior province, Canada: Chemical Geology, v. 55, p. 77–95.
- Schreyer, W., Bernhard, H.-J., and Medenbach, O., 1992, Petrologic evidence for a rhodochrosite precursor of spessartine in coticles of the Venn-Stavelot massif, Belgium: Mineralogical Magazine, v. 56, p. 527–532.
- Schumaker, R., 1985, Zincian staurolite in Glenn Doll, Scotland: Mineralogical Magazine, v. 49, p. 561–571.
- Scott, S.D., Kalogeropoulos, S.I., Shegelski, R.J., and Siriunas, J.M., 1983, Tuffaceous exhalites as exploration guides for volcanogenic massive sulphide deposits, in Parslow, G.R., ed., Geochemical exploration 1982: Journal of Geochemical Exploration, v. 19, p. 500–502.
- Seal, R.R., Slack, J.F., and Shaw, D.R., 2000, Oxygen and hydrogen isotope systematics of tourmalinites and associated rocks from the Sullivan mine, B.C., and elsewhere in the Belt and Purcell supergroups, in Lydon, J.W., Höy, T., Slack, J.F., and Knapp, M.E., eds., Geological environment of the Sullivan deposit, British Columbia: Geological Association of Canada Special Volume, in press.
- Segnit, E.R., 1961, Petrology of the zinc lode, N.B.H.C., Broken Hill: Australasian Institute of Mining and Metallurgy Proceedings, v. 199, p. 87–112.
- Serdychenko, D.P., 1977, Archean tourmaline-bearing and other metasedimentary gneisses of the Azov region, as related to their paleogeographic environment of formation: Akademiia Nauk SSSR Doklady, v. 227, p. 90–93.
- Shaw, H.F., and Wasserburg, G.J., 1985, Sm-Nd in marine carbonates and phosphates: Implications for Nd isotopes in seawater and crustal ages: Geochimica et Cosmochimica Acta, v. 49, p. 503–518.
- Sheridan, D.M., and Raymond, W., 1984, Precambrian deposits of zinc-copper-lead sulfides and zinc spinel (gahnite) in Colorado: U.S. Geological Survey Bulletin 1550, 31 p.
- Shimizu, H., and Masuda, A., 1977, Cerium in chert as an indicator of marine environment of its formation: Nature, v. 266, p. 346–348.
- Siriunas, J.M., 1979, Primary trace element dispersion in the stratigraphic horizon containing an Archean massive sulphide ore body; Wilroy Mines Ltd. no. 4 zone, Manitouwadge, Ontario: Unpublished M.Sc. thesis, Toronto, University of Toronto, 87 p.
- Skauli, H., 1990, The Bleikvassli zinc-lead deposit, Nordland, north Norway; petrography, petrochemistry and depositional environment: Intern Skriftserie 55, Geological Institute, University of Oslo, 355 p.
- Slack, J.F., 1982, Tourmaline in Appalachian-Caledonian massive sulphide deposits and its exploration significance: Institution of Mining and Metallurgy Transactions, v. 91, sec. B, p. B81–B89.

- 1993a, Descriptive and grade-tonnage models for Besshi-type massive sulphide deposits, in Kirkham, R.V., Sinclair, W.D., Thorpe, R.I., and Duke, J.M., eds., *Mineral deposit modeling: Geological Association of Canada Special Paper 40*, p. 343–371.
- 1993b, Models for tourmalinite formation in the Middle Proterozoic Belt and Purcell supergroups (Rocky Mountains) and their exploration significance: *Geological Survey of Canada, Current Research Paper 93-1E*, p. 33–40.
- 1994, Geochemical constraints on the evolution of the Connecticut valley trough, east-central Vermont [abs.]: *Geological Society of America Abstracts with Programs*, v. 26, p. 73.
- 1996, Tourmaline associations with hydrothermal ore deposits: *Reviews in Mineralogy*, v. 33, p. 559–643.
- Slack, J.F., and Coad, P.R., 1989, Multiple hydrothermal and metamorphic events in the Kidd Creek volcanogenic massive sulphide deposit, Timmins, Ontario: Evidence from tourmalines and chlorites: *Canadian Journal of Earth Sciences*, v. 26, p. 694–715.
- Slack, J.F., and Stevens, B.P.J., 1994, Clastic metasediments of the Early Proterozoic Broken Hill Group, New South Wales, Australia: *Geochemistry, provenance, and metallogenic significance: Geochimica et Cosmochimica Acta*, v. 58, p. 3633–3652.
- Slack, J.F., Herriman, N., Barnes, R.G., and Plimer, I.R., 1984, Stratiform tourmalinites in metamorphic terranes and their geologic significance: *Geology*, v. 12, p. 713–716.
- Slack, J.F., Palmer, M.R., and Stevens, B.P.J., 1989, Boron isotope evidence for the involvement of non-marine evaporites in the origin of the Broken Hill ore deposits: *Nature*, v. 342, p. 913–916.
- Slack, J.F., Offield, T.W., Shanks, W.C., III, and Woodruff, L.G., 1993a, Besshi-type massive sulfide deposits of the Vermont copper belt: *Society of Economic Geologists, Field Trip Guidebook Series*, v. 17, p. 32–73.
- Slack, J.F., Palmer, M.R., Stevens, B.P.J., and Barnes, R.G., 1993b, Origin and significance of tourmaline-rich rocks in the Broken Hill district, Australia: *Economic Geology*, v. 88, p. 505–541.
- Slack, J.F., Passchier, C.W., and Zhang, J.S., 1996, Metasomatic tourmalinite formation along basement-cover décollements, Orobic Alps, Italy: *Schweizerische Mineralogische und Petrographische Mitteilungen*, v. 76, p. 193–207.
- Slack, J.F., Ramsden, A.R., Griffin, W.L., Win, T.T., French, D.H., and Ryan, C.G., 1999, Trace elements in tourmaline from the Kidd Creek massive sulfide deposit and vicinity, Timmins, Ontario—a proton microprobe study: *Economic Geology Monograph 10*, p. 415–430.
- Slack, J.F., Shaw, D.R., Leitch, C.H.B., and Turner, R.J.W., 2000, Tourmalinites and cotécules from the Sullivan Pb-Zn-Ag deposit and vicinity, British Columbia: *Geology, geochemistry, and genesis*, in Lydon, J.W., Höy, T., Slack, J.F., and Knapp, M.E., eds., *Geological environment of the Sullivan deposit, British Columbia: Geological Association of Canada Special Volume*, in press.
- Slack, J.F., Turner, R.J.W., and Ware, P.L.G., 1998, Boron-rich mud volcanoes of the Black Sea region: Modern analogues to ancient sea-floor tourmalinites associated with Sullivan-type Pb-Zn deposits?: *Geology*, v. 26, p. 439–442.
- Soto, J.I., and Azañón, J.M., 1993, The breakdown of Zn-rich staurolite in a metabasite from the Betic Cordillera (SE Spain): *Mineralogical Magazine*, v. 57, p. 530–533.
- Spry, P.G., 1978, The geochemistry of garnet-rich lithologies associated with the Broken Hill orebody, N.S.W., Australia: Unpublished M.S. thesis, Adelaide, University of Adelaide, 129 p.
- 1984, The synthesis, stability, origin, and exploration significance of zincian spinels: Unpublished Ph.D. thesis, Toronto, University of Toronto, 234 p.
- 1988, Manganese anomalies as a guide in the exploration for metamorphosed massive sulfide deposits: The Aggeney example [abs.]: *Geological Society of America Abstracts with Programs*, v. 20, no. 7, p. A300.
- 1990, Geochemistry and origin of cotécules (spessartine-quartz rocks) associated with metamorphosed massive sulfide deposits, in Spry, P.G., and Bryndzia, L.T., eds., *Regional metamorphism of ore deposits and genetic implications: Utrecht, VSP*, p. 49–75.
- 2000, Sulfidation and oxidation haloes as guides in the exploration for metamorphosed massive sulfide ores: *Reviews in Economic Geology*, v. 11, p. 149–162.
- Spry, P.G., and Scott, S.D., 1986a, The stability of zincian spinels in sulfide systems and their potential as exploration guides for metamorphosed massive sulfide deposits: *Economic Geology*, v. 81, p. 1146–1163.
- 1986b, Zincian spinel and staurolite as guides to ore in the Appalachians and Scandinavian Caledonides: *Canadian Mineralogist*, v. 24, p. 147–163.
- Spry, P.G., and Wonder, J.D., 1989, Manganese-rich rocks associated with the Broken Hill lead-zinc-silver deposit, New South Wales, Australia: *Canadian Mineralogist*, v. 27, p. 275–292.
- Stanton, R.L., 1972, A preliminary account of chemical relationships between sulfide lode and “banded iron formation” at Broken Hill, New South Wales: *Economic Geology*, v. 67, p. 1128–1145.
- 1976a, Petrochemical studies of the ore environment at Broken Hill, New South Wales: 1. Constitution of ‘banded iron formations’: *Institution of Mining and Metallurgy Transactions*, v. 85, sec. B, p. B33–B46.
- 1976b, Petrochemical studies of the ore environment at Broken Hill, New South Wales: 2. Regional metamorphism of banded iron formations and their immediate associates: *Institution of Mining and Metallurgy Transactions*, v. 85, sec. B, p. B118–B131.
- 1976c, Petrochemical studies of the ore environment at Broken Hill, New South Wales: 3. Banded iron formations and sulphide orebodies: Constitutional and genetic ties: *Institution of Mining and Metallurgy Transactions*, v. 85, sec. B, p. B132–B141.
- 1976d, Petrochemical studies of the ore environment at Broken Hill, New South Wales: 4. Environmental synthesis: *Institution of Mining and Metallurgy Transactions*, v. 85, sec. B, p. B221–B233.
- 1976e, Speculations on the chemical metasediments of Broken Hill, New South Wales, Australia [abs.]: *Institution of Mining and Metallurgy Transactions*, v. 85, sec. B, p. B477–B480.
- Stanton, R.L., and Vaughan, J.P., 1979, Facies of ore formation: A preliminary account of the Pegmont deposit as an example of potential relations between small “iron formations” and stratiform sulphide ores: *Australasian Institute of Mining and Metallurgy Proceedings*, v. 270, p. 25–38.
- Stanton, R.L., and Williams, K.L., 1978, Garnet compositions at Broken Hill, New South Wales, as indicators of metamorphic processes: *Journal of Petrology*, v. 19, p. 514–529.
- Stillwell, F., 1959, Petrology of the Broken Hill lode and its bearing on ore genesis: *Australasian Institute of Mining and Metallurgy Proceedings*, v. 190, p. 1–84.
- Stoddard, E.F., 1979, Zinc-rich hercynite in high-grade metamorphic rocks: A product of the dehydration of staurolite: *American Mineralogist*, v. 64, p. 736–741.
- Stumpf, E.F., 1979, Manganese haloes surrounding metamorphic stratabound base metal deposits: *Mineralium Deposita*, v. 14, p. 207–217.
- Sverjensky, D.A., 1984, Europium redox equilibria in aqueous solution: *Earth and Planetary Science Letters*, v. 67, p. 70–78.
- Taylor, B.E., and Slack, J.F., 1984, Tourmalines from Appalachian-Caledonian massive sulfide deposits: Textural, chemical, and isotopic relationships: *Economic Geology*, v. 79, p. 1703–1726.
- Taylor, B.E., Palmer, M.R., and Slack, J.F., 1999, Mineralizing fluids in the Kidd Creek massive sulfide deposit, Ontario: Evidence from oxygen, hydrogen, and boron isotopes in tourmaline: *Economic Geology Monograph 10*, p. 389–414.
- Taylor, G.F., and Scott, K.M., 1982, Evaluation of gossans in relation to lead-zinc mineralisation of the Mount Isa inlier, Queensland: *BMR Journal of Australian Geology and Geophysics*, v. 7, p. 159–180.
- Theye, T., Schreyer, W., and Franselot, A.-M., 1996, Low-temperature, low-pressure metamorphism of Mn-rich rocks in the Liègne syncline, Venn-Stavelot massif (Belgian Ardennes), and the role of carpholite: *Journal of Petrology*, v. 37, p. 767–783.
- Treloar, P.J., 1987, The Cr-minerals of Outokumpu—their chemistry and significance: *Journal of Petrology*, v. 28, p. 867–886.
- Trembath, G.D., 1986, The compositional variation of staurolite in the area of Anderson Lake, Snow Lake, Manitoba, Canada. Unpublished M.S. thesis, Winnipeg, University of Manitoba, 187 p.
- Troop, D.G., 1984, The petrology and geochemistry of Ordovician banded iron formations and associated rocks at the Flat Landing Brook massive sulphide deposit, northern New Brunswick: Unpublished M.Sc. thesis, Toronto, University of Toronto, 218 p.
- Tuisku, P., Ruostesuo, P., and Hakkinen, A.-M., 1987, The metamorphic behaviour and paragenetic significance of zinc in amphibolite facies, staurolite-bearing mica schists, Puolankajarvi Formation, central Finland: *Geochimica et Cosmochimica Acta*, v. 51, p. 1639–1650.

- Turner, R.J.W., Höy, T., Leitch, C.H.B., Anderson, D., and Ransom, P., 1993, Guide to the geologic setting of the Middle Proterozoic Sullivan sediment-hosted Pb-Zn deposit, southeastern British Columbia, in Link, P.K., ed., *Geologic guidebook to the Belt-Purcell Supergroup, Glacier National Park and vicinity, Montana, and adjacent Canada*: Spokane, Washington, Belt Association, Incorporated, p. 53-94.
- van Staal, C.R., Fyffe, L.R., Langton, J.P., and McCutcheon, S.R., 1992, The Ordovician Tetagouche Group, Bathurst camp, northern New Brunswick, Canada: History, tectonic setting, and distribution of massive-sulfide deposits: *Exploration and Mining Geology*, v. 1, p. 93-103.
- Vaughan, J.P., and Stanton, R.L., 1986, Sedimentary and metamorphic factors in the development of the Pegmont stratiform Pb-Zn deposit, Queensland, Australia: *Institution of Mining and Metallurgy Transactions*, v. 95, sec. B, p. B94-B121.
- Von Damm, K.L., 1990, Sea floor hydrothermal activity: Black smoker chemistry and chimneys: *Annual Review of Earth and Planetary Sciences*, v. 18, p. 173-204.
- Ward, C.M., 1984a, Magnesium staurolite and green chromium staurolite from Fiordland, New Zealand: *American Mineralogist*, v. 69, p. 541-545.
- 1984b, Titanium and the color of staurolite: *American Mineralogist*, v. 69, p. 531-540.
- Wiggins, T.R., 1990, Highly metamorphosed ferromanganese sediments in the vicinity of the Broken Hill orebody: *Proceedings of the Pacific Rim 90 Congress, Gold Coast, Queensland*: Australasian Institute of Mining and Metallurgy, p. 563-569.
- Williams, P.J., 1994, Iron mobility during synmetamorphic alteration in the Selwyn Range area, NW Queensland: Implications for the origin of ironstone-hosted Au-Cu deposits: *Mineralium Deposita*, v. 29, p. 250-260.
- Williams, P.J., and Manby, G.M., 1987, Syngenetic sulfides and Fe-Mn metasediments in middle to upper Paleozoic sequences of Karnten, southern Austria: *Economic Geology*, v. 82, p. 1070-1076.
- Williams, P.J., and Kennan, P.S., 1983, Stable isotope studies of sulphide mineralization on the Leinster granite margin and some observations on its relationship to cotecule and tourmalinite in the aureole: *Mineralium Deposita*, v. 18, p. 335-337.
- Wilner, A., 1992, Tourmalinites from the stratiform peraluminous metamorphic suite of the central Namaqualand mobile belt (South Africa): *Mineralium Deposita*, v. 27, p. 304-313.
- Wonder, J.D., Spry, P.G., and Windom, K.E., 1988, Geochemistry and origin of manganese-rich rocks related to iron formation and sulfide deposits, western Georgia: *Economic Geology*, v. 83, p. 1070-1081.
- Zaleski, E., 1989, Metamorphism, structure and petrogenesis of the Linda volcanogenic massive sulphide deposit, Snow Lake, Manitoba, Canada: Unpublished Ph.D. thesis, Winnipeg, University of Manitoba, 344 p.
- Zaleski, E., and Peterson, V.L., 1995, Depositional setting and deformation of massive sulfide deposits, iron formation, and associated alteration in the Manitowadge greenstone belt, Superior province, Ontario: *Economic Geology*, v. 90, p. 2244-2261.
- Zaleski, E., Froese, E., and Gordon, T.M., 1991, Metamorphic petrology of Fe-Zn-Mg-Al alteration at the Linda volcanogenic massive sulfide deposit, Snow Lake, Manitoba: *Canadian Mineralogist*, v. 29, p. 995-1017.
- Zhang, J.S., Passchier, C.W., Slack, J.F., Fliervoet, T.F., and de Boorder, H., 1994, Cryptocrystalline Permian tourmalinites of possible metasomatic origin in the Orobic Alps, northern Italy: *Economic Geology*, v. 89, p. 391-396.